Advancements in Robust Fault Reconstruction Using Sliding Mode Observers

Ng Kok Yew

B. Eng (Electrical and Computer Systems) (Hons)
Monash University

A thesis submitted in fulfillment of the requirements for the degree of
Doctor of Philosophy

Faculty of Engineering
Monash University

April 2009

Contents

ABSTRACT

With the massive growth of technologies used in the industry, more is expected from the control systems. Issues such as safety, efficiency and economical operation of the systems and the equipment are of utmost importance as these systems are expected to perform complicated and complex tasks. Hence, there is an essential need for fault detection and isolation.

This thesis describes the developments and advancements in the use of sliding mode observers for the purpose of robust fault reconstruction. Existing work has shown that the effect of the disturbances onto the fault reconstruction was minimised in an $\mathcal{L}_2$ sense; but complete disturbance decoupling was not guaranteed.

The first contribution of this thesis is the investigation of the conditions that enable actuator (input) faults to be reconstructed independently of the disturbances. The conditions are found in terms of the original system matrices. Then, the next contribution is the extension of those results to the case of sensor (output) faults. Following that, using the results of the first contribution, a scheme was developed using cascaded observers to enable disturbance decoupled fault reconstruction for a more general class of systems. Finally, this thesis presents a method to reconstruct faults in cases where the first Markov matrix is rank deficient. The efficacy of these schemes is demonstrated by simulation examples.

STATEMENT OF AUTHORSHIP

The thesis contains no material which has been accepted for the award of any other degree or diploma in any university or other institution. I affirm that, to the best of my knowledge, the thesis contains no material previously published or written by another person, except where due reference is made in the text of the thesis.

Signed: .....

Ng Kok Yew

April 2009

Acknowledgements

I would like to thank the following for their help and support, in one way or another, in the writing of this thesis

1. My supervisor, Dr Tan Chee Pin, for his unending support, encouragement and guidance, as well as his unselfishness to share knowledge and being there at all times when needed.

2. Fellow academic and administration staff in School of Engineering, Monash University Sunway Campus for their support and community spirit, in particular Prof. Serge Demidenko, Prof. Ian Prince, Prof. Man Zhihong, Prof. Teoh Kok Soo, Dr Rini Akmeliawati, Dr Royan Ong, Dr Martin King, Dr Ooi Yong Wee, Mr Tan Ying Oon, Ms Lim Jen Nee, Ms Penny Tan, Ms Eliz Tan, Ms Deborah Cheah, Ms Tong Siew Peng, Ms Teh See Lim and Ms Nicole Woon.

3. Fellow postgraduates at Monash University Sunway Campus, Boon How, Jason, Darwin, Allen, Alpha, Yoges and Oon-Ee for providing a cohesive and fun environment to work in. Good luck to you guys.

4. My sister, Kei Yan for her support and her antics to keep me de-stressed :-)

5. My best friends, Yuan Wu, Choon Seng, Choon Meng and Henry for keeping me company whenever I felt demotivated, for their support and friendship, and times of fun and laughter.

6. Last, but **definitely not the least**, my parents, Mr and Mrs Ng Yoon Choy who encouraged and motivated me to undertake this research study, for their unconditional love and affection as well as their constant reminder for me to rest well, and always ensuring that my only concern was my education. Without them, all this work would not have been possible.

Ng Kok Yew

April 2009

LIST OF PUBLICATIONS

Journal Papers Accepted/Published

1. K.Y. Ng, C.P. Tan, C. Edwards & Y.C. Kuang. New results in robust actuator fault reconstruction for linear uncertain systems using sliding mode observers, *International Journal of Robust and Nonlinear Control*, 17:1294–1319, 2007.

Journal Papers Submitted

1. K.Y. Ng, C.P. Tan, Z. Man & R. Akmeliawati. New results in disturbance decoupled fault reconstruction in linear uncertain systems using two sliding mode observers in cascade, *International Journal of Control, Automation and Systems*, 2008.

2. K.Y. Ng, C.P. Tan, R. Akmeliawati & C. Edwards. Disturbance decoupled fault reconstruction using sliding mode observers, *Asian Journal of Control*, 2008.

Conference Papers Accepted/Published

1. K.Y. Ng, C.P. Tan, Y.C. Kuang & C. Edwards. New result in robust actuator fault reconstruction with application to an aircraft, *16th IEEE International Conference on Control Applications. Part of IEEE Multi-conference on Systems and Control, Singapore*, p 801–806, October 2007.

2. K.Y. Ng, C.P. Tan, R. Akmeliawati & C. Edwards. Disturbance decoupled fault reconstruction using sliding mode observers, *Proceedings of the 17th World Congress The International Federation of Automatic Control Seoul, Korea*, v 17, p 7215–7220, July 2008.

3. K.Y. Ng & C.P. Tan. New results in disturbance decoupled fault reconstruction in linear uncertain systems using two sliding mode observers in cascade, *7th IFAC Symposium on Fault Detection, Supervision and Safety of Technical Processes, SAFEPROCESS, Barcelona, Spain*, July 2009.

Chapter 1

Research Motive and Overview of Thesis

With the massive growth of technologies in this fast-paced modern society, more is expected from the control systems where these systems are expected to perform more complicated and complex tasks. Jobs which previously could not be performed by humans can now be carried out by these control systems. For example, scientists can now carry out researches to explore places under extreme conditions (i.e. craters of active volcanoes or the core of a hurricane) [136, 153, 102] which were out of humans' reach all this while, thanks to these control systems. On the other hand, in the manufacturing sector these control systems are used to perform tasks previously done by human operators for their high productivity as well as their ability to commit less errors and not restrained by fatigue and illness compared to their human counterparts [79, 191]. Furthermore, these systems do not succumb to emotions and therefore, are able to carry out the tasks more efficiently. As a result, the cost of manufacturing can be drastically cut down and the time taken from the design level to the manufactured output level can be greatly reduced.

However, no matter how productive and efficient these control systems are, they are still prone to malfunctions and errors. There are many causes which can contribute to these malfunctions and errors. They could be external factors that physically damage the components or sensors of the systems (i.e. physical damages to a robot which operates under harsh weathers near a volcano [136]), or they could just be ordinary wear and tear of system parts which cause degradation in the overall performance of the systems (i.e. internal parts of a manufacturing machine which has not been serviced for a long duration of time [149, 181]). A *fault* is said to have occurred whenever these systems start to behave abnormally and are

not able to perform the tasks well [16].

If these faults are allowed to be left undetected and unattended to in the system for an extended amount of time, it can bring about negative consequences such as damage to the system itself, causing injuries or loss of precious human lives, economic losses and also some unhealthy effects onto the environment. Early detection of faults will not only prevent the above consequences from happening, but will also help to enhance the productivity, efficiency and reliability of the system. Therefore, there is an essential need for an effective *fault detection and isolation* (FDI) scheme. The main purpose of this FDI scheme is to generate an alarm whenever a fault occurs in the system (detection), and then to determine the location of the fault in the system (isolation). As a result, early preventive and counter measures can be taken to eliminate or at least to minimise the effects of the fault.

Generally, this thesis focusses on the dealing with *additive faults*. These faults can either occur at the actuators (inputs) or the sensors (outputs) of the system, as depicted in Figure 1.1 below. From Figure 1.1, actuator faults act directly onto the system and hence will influence the process as a whole by affecting the system variables, whereby the input into the system $G(s)$ is now expressed as $u + f_i$ (control inputs plus the additive actuator faults). An example of an actuator fault is the damage to the collective pitch control of an aircraft, resulting in great difficulty in controlling the pitch rate and pitch angle of the aircraft [177] or the loss of control effectiveness of the motors in a winding machine [160].

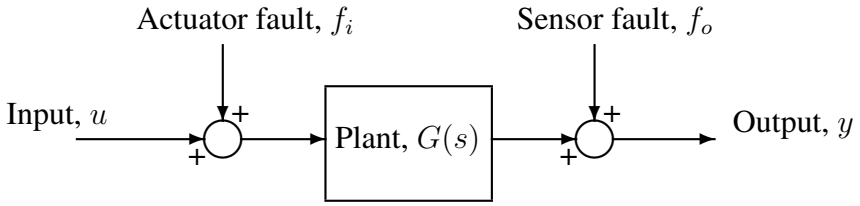

Figure 1.1: Schematic showing additive actuator and sensor faults onto the system

As for sensor faults, they act onto the sensors that measure variables of the system. Basically, sensor faults do not affect the process of open loop systems, such as the one shown in Figure 1.1. However, in closed loop systems where the output is used to generate the control signal, sensor faults will indirectly affect the operations of the systems [58, 183], as shown in Figure 1.2. The cause of these sensor faults might be due to wear and tear of sensors leading to

inaccurate measurements, or total failure of the sensors, yielding zero measurements.

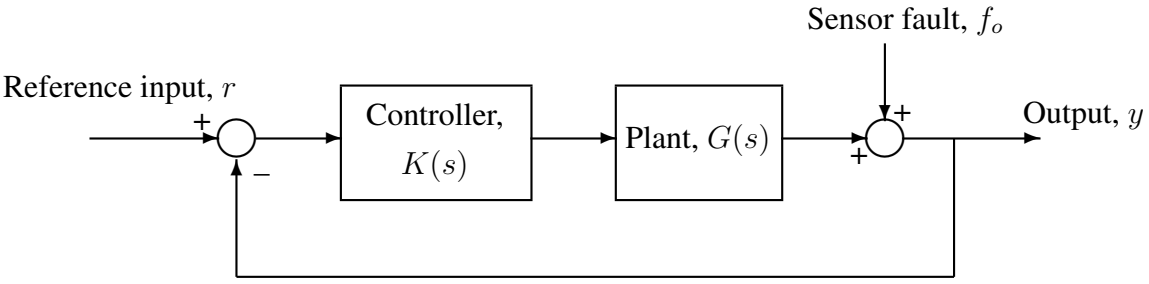

Figure 1.2: Schematic showing how sensor fault affects a closed-loop system

Faults can be further classified into two groups: *abrupt* (fast changing) faults and *incipient* (slow changing) faults. In the case of an abrupt fault, its effect onto the system is easily noticeable. As a result, there will be a sudden change in the system behaviour and this might cause the system to fail. For example, it could be a sudden offset in the value measured by a sensor (or even a total failure of the sensor), contributing to inaccurate or zero readings of measurements. Conversely, an incipient fault will not cause the system to exhibit a sudden change in its performance as its effects are more subtle, or even negligible. The most that it could do is to degrade the performance of the system as it may be due to normal operation wear and tear of components of the system. However, if left undetected for a long period of time, incipient faults can cause catastrophic damages just like abrupt faults [221] do. Therefore, it is crucial for the FDI scheme to be able to detect both abrupt and incipient faults as soon as possible.

As for this thesis, it will discuss and present work related to the use of sliding mode observer in the area of fault detection and isolation. The next section of this chapter outlines the overview of this thesis and the contribution of each chapter to this research area.

1.1 Structure of Thesis

Chapter 2 - This chapter discusses about the concept of *fault detection and isolation* (FDI), giving the reader an overview of the research area and presents the existing work that has been done by other researchers. Other that that, the notion of *robust* FDI schemes will also be mentioned, especially on the importance to distinguish the effect

of the uncertainty/disturbance from the fault. The concept and importance of *fault reconstruction* will also be presented.

Chapter 3 - This chapter presents the study of the sliding mode observer that will be used as the basis for the fault reconstruction schemes proposed in the later chapters in this thesis. This chapter will also provide an overview of the developments in the design of the sliding mode observer over the years as well as its characteristics in rejecting disturbances.

Chapter 4 - This chapter investigates the conditions that guarantee disturbance decoupled fault reconstruction (DDFR) for actuator faults using the sliding mode observer. The presence of disturbance/uncertainty may corrupt the performance of the fault reconstruction due to the mismatches between the model about which the observer is designed and the real system. The observer is designed using pole-placement method and is an improvement over previous method which only could minimise the effect of the disturbance/uncertainty onto the fault reconstruction in an $\mathcal{L}_2$ sense. The conditions that guarantee DDFR are presented in terms of the original system matrices. The work in this chapter has been submitted to an international journal [138] for review and has been published as a conference paper [139].

Chapter 5 - This chapter continues on the study in Chapter 4 where the DDFR scheme is extended such that it can be applied to the case of sensor fault as well. Using the technique in [177], certain signals are filtered in order to obtain a fictitious system where the sensor fault is now treated as an 'actuator' fault of which the method in Chapter 4 can then be used to reconstruct the fault while being completely robust towards the effect of the disturbance/uncertainty. The conditions that guarantee DDFR are investigated and presented in terms of the original system matrices.

Chapter 6 - This chapter addresses the case when the DDFR scheme in Chapter 4 is not feasible and proposes that by using multiple sliding mode observers in cascade mode, it can be shown that signal from an observer are found to be the output of a 'fictitious' system that is driven by faults and disturbances and these signals are then fed into

the next observer arranged in cascade form. This process is repeated until a fictitious system is able to successfully robustly reconstruct the fault. The scheme proposed in this chapter can be applied to a wider class of system compared to the method in Chapter 4 or any other single observer methods and a systematic routine to check for the feasibility of the design method will also be presented. The preliminary ideas in this chapter has been accepted as a conference paper [137] and submitted as a journal paper [142].

Chapter 7 - This chapter presents a robust fault reconstruction method for a class of systems of which the first Markov parameter is not full rank, thus relaxing the conditions required by some existing work (in previous chapters, the first Markov parameter is full rank). This new method uses two sliding mode observers arranged in cascade where the equivalent output error injection in the first observer is processed to yield the measurable output of a 'fictitious' system that is of relative degree one. As a result, a second sliding mode observer can be implemented for the purpose of fault reconstruction. The work in this chapter has been published as a journal paper [140] as well as a conference paper [141].

Chapter 8 - In this chapter, conclusions are made and future research ideas are outlined.

Appendix A - Attached to this thesis is a CD-ROM containing all .mat and .m files that are needed to run the simulations discussed in this thesis using the Matlab software. The description of each individual file and their contents are given.

Appendix B - The attached CD-ROM.

Chapter 2

An Overview of Fault Detection and Isolation

In this chapter, the concept of FDI and the different methodologies available that have been developed over the years will be presented. Basically, there are two main methods for FDI: *physical redundancy* and *analytical redundancy*, and the various methods of each of the two FDI redundancies as well as their contributions to this area of research will be discussed further in the remaining of this chapter.

2.1 Physical redundancy method

In physical or hardware redundancy FDI schemes, the sensitivity of the hardware sensors are set or tweaked or additional sensors are installed such that they are able to detect faults in the system and to generate an alarm to warn about the situation. As a result, preventive measures can then be taken. Since this thesis deals only with a class of model based FDI schemes (analytical redundancy method), only the commonly used hardware based methods will be briefly highlighted.

2.1.1 Limit checking sensors for FDI

In physical FDI schemes using limit checking sensors, the actual measurements of the system are compared with the preset limits. If these measurements exceed their limits, then a fault is deemed to have occurred. Normally, there will be two levels of preset limits: exceeding first one will issue a warning while exceeding the second one will sound the alarm. Work using this method can be found in Gertler [77].

2.1.2 Installing special sensors for FDI

Unlike the previous method where the measurements are compared with their threshold limits, this method makes use of sensors with built-in limits checking ability to determine abnormalities or any other unusual values while measurements are being taken. An example of such design and implementation of self-check checkers which are fault-secure has been presented by Sogomonyan & Gossel [166]. Furthermore, some of these sensors are specially made to be sensitive to certain conditions, i.e. vibration, heat or sound, depending on the applications, and this is extremely useful for FDI if the types of faults that might corrupt the operation of the system are known or foreseen. Cristalli *et al.* [31] have presented the implementations of accelerometer and laser vibrometer to detect faults in the universal motors used in washing machines.

2.1.3 FDI using multiple sensors

In this method of FDI, additional parallel connected hardware sensors are installed onto the system so that there will be more than one sensor to make the same measurement. Whenever a fault occurs in the system, some of these sensors will produce different results compared to others and therefore, by comparing their respective values the fault can be detected and identified. Alternatively, this method is also known as the *voting systems*, as noted by Gertler [77], Reibman & Nolte [156], Visinky *et al.* [192] and Willsky [202]. Hereford [87] developed an evolvable hardware whereby whenever a fault is detected in the system via the three sensors, the circuit will reprogram itself as a means of preventive measure. Reibman & Nolte [156] have also shown how a redundant system with a general voting rule where multiple identical processors are used to determine a failure in signal detection. Meanwhile, Stroud & Tannehill [170] explored the combination of the built-in self-test method (similar to the limit checking sensor mentioned in Chapter 2.1.1) with the majority voting circuits to provide a better result than using only either one of them.

2.1.4 FDI using frequency analysis

Some systems (such as washing machines) operate at a specified frequency spectrum under normal operating conditions. Therefore, a fault is said to have occurred if the sensor detects frequencies that do not fall within the typical operating frequency spectrum. Furthermore, some of these faults have their own unique frequencies characteristics and therefore this method can also be used for fault isolation as well. Lee & White [114] have demonstrated how a signal processing and analysis tool can be used to detect impulsive acoustic and vibration signals caused by irregular impacting within the rotating machinery of a car engine or an industrial gearbox.

2.2 Analytical redundancy method

In the case of analytical redundancy method, the knowledge of the input-output relationship of the system is used to design the FDI scheme. One of the main advantages of the analytical redundancy over the physical redundancy is that all the computation and processing of the FDI scheme can be carried out without the need for the installation of physical instrumentations onto the plant. All that is needed for the functionality of the FDI scheme is a mathematical model of the system under observation. This is extremely useful for systems where it is difficult or almost infeasible for additional sensors to be installed onto the systems due to the existence of some physical limitations or some other constraints such as cost or weight related issues. For example, it is almost impossible to install tachometers to measure the angular velocity of the rods of a double inverted pendulum due to its hardware constraints. Therefore, the cost needed for hardware installation and maintenance work can be ultimately reduced as all the computations can be done using the computer. Furthermore, this will also reduce the overall weight of the system and as a result, the FDI scheme can be applied onto systems where weight and size are the main concerns for operation, such as unmanned aircrafts.

One of the popular analytical methods for FDI is the *model-based approach* where the inputs and outputs of the system are analyzed to generate a *residual signal* [16, 65]. Ideally

speaking, the residual should be zero under fault-free conditions and it should be nonzero if and only if there is a fault in the system. Therefore, the FDI scheme has to be designed so that the residual will provide information on the condition of the system based on the two circumstances above.

To ensure that the FDI scheme is performing well, a good mathematical model describing the input-output relationship of the system is required. Figure 2.1 shows the schematic diagram of a model based residual generator where it can be seen that the accuracy of the mathematical model detailing the input-output relationship of the system is essential in order to generate an accurate residual signal.

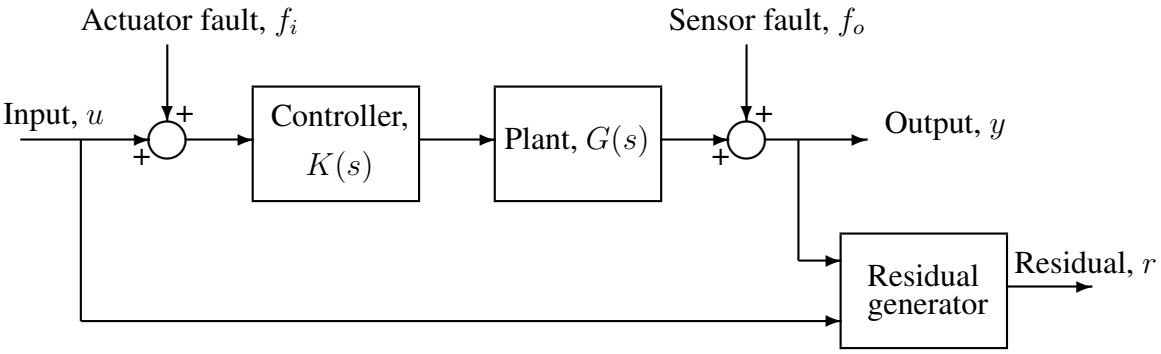

Figure 2.1: Schematic of a model-based residual generator

Other than that, the FDI scheme is also usually designed such that the residual will exhibit a fixed-direction in the residual space whenever the presence of certain faults is detected by the FDI scheme [49, 201]. The direction of the residual indicates the location of the fault in the system and as a result, good fault isolation can then be achieved.

2.2.1 Failure sensitive or fault detection filter

The most basic type of model based FDI scheme is the *fault detection filter* (FDF) scheme. Other model based FDI schemes which will be described in this section are a subset of the FDF scheme. The FDF was first introduced by Beard [8] and Jones [96] and was later further developed by Massoumnia [131]. Chen *et al.* [19], Jikuya *et al.* [95], Laurence & Speyer [113] and Liberatore *et al.* [117] then applied the FDF onto practical systems. Liberatore *et al.* [117] has also presented the general theory of the FDF scheme. Furthermore, there have

been some improvements to the FDF scheme to perform fault isolation as well, as has been presented by Young & Jae [218] while Park & Rizzoni [145] embraced the eigenstructure assignment algorithm to design the FDF.

2.2.2 Multiple hypothesis approach for FDI

Another method for model based FDI is the class of multiple hypothesis fault detection filter, as discussed in Ono [144]. This method serves to locate the faulty parameter from the deviations of the identified system models. One of the advantages of using this method is that it can apply to not only single fault but to multiple faults as well. Generally, fault diagnosis using this method consists of the detection of fault, the discrimination of the faulty parameter and the evaluation of its variations. So, the system model is identified online continuously and if any of the system parameters varies from its normal value, it will be detected by the deviations of the default system model. After the fault is detected, the system switches to offline operating mode and runs the fault identification. Ono [144] has shown on how the FDI scheme will then discriminate the faulty parameter from the normal one and estimates the deviation by the multiple hypothesis tests. Examples of this scheme have been presented in Basseville & Nikiforov [6], Bogh [10] and Jung *et al.* [99].

2.2.3 Nonlinear identity observer approach for FDI

This method for FDI is different from others as it uses nonlinear observers instead of linear observers. This approach was first introduced by Hengy & Frank [86] and it has been demonstrated that the introduction of the nonlinearities of the system into the design of the observers improves the efficiency of fault isolation. This is so because nonlinear observers are able to capture the nonlinear characteristics of the system compared to linear observers which are only able to capture the linear characteristics of the system. Thus, nonlinear observers are able to estimate the parameters of the system more accurately. Examples of this approach have been presented in Adjallah [1], Alcorta-Garcia *et al.* [3, 97], Ashton *et al.* [4], Frank [65] as well as Martinez-Guerra [129].

2.2.4 Parity space approach for FDI

The parity space approach is another class of model based FDI scheme. Some early contributions of this approach can be found in Deckert *et al.* [39] and Willsky [28, 121]. Using this method, the mathematical equations of the system are continuously checked for consistency (parity) by using the actual measurements of the system. This can be done by multiplying the system data with a *parity vector*. Whenever the predefined error bounds are surpassed, the system is said to behave in a way that it should not and a fault is deemed to have happened. As a result, a residual signal will be generated to indicate the presence of the fault. Therefore, the parity is designed such that the residual will be zero during fault-free conditions and nonzero whenever a fault occurs in the system. Extensive work of the parity space approach for FDI can be found in Delmaire *et al.* [40], Ding *et al.* [48], Kabore [100], Kratz *et al.* [108], Massoumnia & Vander Velde [132] and Patton & Chen [146].

Further developments have also been carried out onto the parity space approach. For example, Hamelin *et al.* [82] proposed a new method for residual generation while Patton & Chen [147] presented the concept of the parity space approach for FDI based on eigenstructure assignment. Kim & Lee [104] on the other hand, proposed a new parity space approach for general systems which utilised efficient numerical algorithm.

2.2.5 Stochastic and statistical FDI

Another method for model based FDI is the stochastic and statistical methods. It is also called the *generalised likelihood ratio approach*, as mentioned by Li & Kadirkamanathan [116, 115], Litkouhi & Boustany [120] and Willsky & Jones [203]. These methods test the residual for its statistical properties such as zero-mean Gaussian white noise and covariance. When a fault occurs, the statistical properties of the residual will deviate from their normal operation conditions and therefore, an alarm will be sounded to indicate the presence of the fault. Examples of these methods in FDI were shown in Chowdhury [30], Fouladirad & Nikiforov [64], Larson *et al.* [112] and Simani *et al.* [164].

Throughout the years, various improvements have been made to the statistical FDI scheme.

Chowdhury [30] used a neural technique to implement the statistical tool to detect the fault while Li & Kadirkamanathan [116, 115] combined the likelihood ratio test with particle filtering (also known as Monte-Carlo filtering) so that the FDI scheme can handle any nonlinearities characteristics in the system and noise measurements of any probability distribution.

2.2.6 Sliding mode observer for FDI

The sliding mode observer (SMO) is a type of nonlinear observer introduced by Utkin [188] that is becoming very popular of late for FDI. As the name of this observer suggests, this method adopts a *sliding motion* for the state estimation error of the system where finite-time convergence is attained. As long as the state estimation error is forced to slide onto and remain on a certain hyperplane, then the observer is said to be in a *sliding mode* [53]. In earlier work such as those by [23], whenever there is a fault in the system, the observer will stop sliding and the residual will generate the alarm. However, in later work such as Edwards *et al.* [55], the observer will remain sliding although there is a fault in the system.. Slotine *et al.* [165] produced one of the earliest work on SMO and it was followed suit by Husain *et al.* [91], Krishna *et al.* [110, 109], Sreedhar *et al.* [168], Thein & Misawa [186] and Venkataramanan [190]. In the later years, further developments and applications of the SMO were demonstrated by Edwards *et al.* [55], Goh *et al.* [78], Kim *et al.* [105] and Tan *et al.* [177, 176, 175, 173].

In addition to that, the concept of the SMO has also been improved throughout the years. For example, Yang & Saif [210], Furuhashi *et al.* [72] and Jiang *et al.* [94, 93] incorporated adaptive observers into the SMO design to enhance the estimation of the states of the systems while Yeu & Kawaji [217, 216] designed the SMO to be used on descriptor systems. Ma *et al.* [126, 199] designed the nonlinear observer using a neural network in order to capture the nonlinear characteristics of the faults. As for Akhenak *et al.* [2], they used multiple models and observers in their design of the SMO for FDI. Meanwhile, Xiong & Saif [207] addressed the case where it is not necessary for all state variables to be estimated by the observer in order for the SMO to be designed.

Lately, there have been some developments in the area of research involving higher order

SMOs. It is a relatively new area of research that has been progressing well and has shown great potentials for the purpose of FDI. The higher order SMO uses a continuous term to generate the equivalent output error injection signal for tracking purposes. Compared to the method of using an ordinary SMO which uses a discontinuous term for the same objective, no smoothing is needed for the higher order SMO. However, its structure is more suitable to be used on single input single output systems as opposed to low order SMOs. Some of the research work in this area are shown in Fridman *et al.* [163, 70, 162, 51, 71, 69].

The work in this thesis is developed based on the SMO by Edwards & Spurgeon [52] as the existence Necessary and Sufficient conditions for its feasibility has been presented and that it can be easily implemented onto multi-variable systems. Therefore, the theoretical concepts and mathematical workings involved in the design process of the particular SMO will be discussed in more details in Section 3.

2.3 The need for robustness in FDI

In model based FDI schemes, the observers are designed based on the idealised assumption that the models are the exact replicas of the systems under consideration. However, this is only true in theoretical work and in software simulations as an accurate and complete mathematical description of the system is never available in practice. For some applications, the parameters or mathematical structure of the dynamic of the system is not fully known, or may only be known over a limited range of the operation of the plant. In these circumstances, the observer could only be designed by analyzing the input and output signals of the system. Therefore, there will be a *model-reality mismatch* between the actual system and the model used for FDI, as noted by Patton & Chen [149].

Moreover, the task of modelling the system and its disturbances will become more difficult as the complexity of the dynamic system increases due to the presence of various noise and modelling errors or uncertainties. And to make things worse, they appear to be the same as multiplicative faults and can only be distinguished from the ordinary faults based on the time analysis of the problem. Therefore, these uncertainties/disturbances can actually corrupt the

functionality of the FDI scheme whereby the residual could be nonzero when there is no fault, resulting in false alarms, or worse, the residual is zero when there is a fault, thus masking the effect of the fault on the system.

Therefore, there is a need for a *robust* FDI scheme to tackle this problem. The main objective of the robust FDI scheme would be to separate the residuals from the effects of the uncertain signals and perturbations. As a result, the detection of the faults can be maximised and the effect of the modelling errors and disturbances on the FDI procedure can be minimised or eliminated, if best. Hence, this will produce residuals that are sensitive only to faults but insensitive towards the uncertainties/disturbances.

There have been many developments of the robust FDI schemes throughout the years and the following subsections will briefly describe some of the commonly used robust FDI schemes.

2.3.1 Robust FDI schemes using the unknown input observer

One of the methods to perform robust FDI is through the use of the *unknown input observer* (UIO). The basic principle of the UIO is to decouple disturbances and uncertainties from the state estimation error, as shown by Dassanayake & Balas [35]. One of the earliest works done for robust FDI using unknown input observer was by Kudva *et al.* [111]. Other subsequent developments that had been carried out include Dassanayake & Balas [35], Frank [65] and Yang & Wilde [209].

In addition to that, the UIO concept has also been developed substantially and integrated with other design approaches. Guan & Saif [80] proposed a simple and yet elegant approach for designing a reduced-order of the UIO with pole-placement capability by rewriting the equations of the system to eliminate the unknown inputs part and then partitioning them into two interconnected subsystems. Other than that, Tsui [187] introduced a new design method for the UIO which can completely unify the regular UIO and the static output feedback of which he claimed, are two basic feedback structures of modern control theory which have never been unified before this new design approach. Koenig & Mammar [106] extended the linear UIO design to a nonlinear UIO for FDI of nonlinear systems. Kawaji & Sawada [103]

managed to apply the UIO design onto descriptor systems while Hayar *et al.* [83] used the frequential approach to design the UIO. Some of the practical applications of the UIO were presented in Dassanayake & Balas [35] and Gaddouna & Ouladsine [73].

2.3.2 Robust FDI using eigenstructure assignment

Another method to perform robust FDI is through the eigenstructure assignment of the observer. Patton *et al.* first demonstrated the eigenstructure assignment approach in [152] and was then further developed and applied in [148, 151]. The design of the observer using eigenstructure assignment method is usually applied to existing non-robust FDI schemes such as FDF or other observer-based methods. For this FDI scheme, the eigenvectors of the observer are assigned to be orthogonal to the disturbances of the system. As a result, the residual can be made to be robust against the disturbances as shown in Patton & Chen [150].

Other works using this approach have been shown in Zhang *et al.* [225], Choi *et al.* [27, 26], Shen *et al.* [161], Xiong & Saif [205], Jorgensen *et al.* [98] and Fantuzzi *et al.* [61].

2.3.3 Robust FDI using adaptive observer

Another method to perform robust FDI is through the means of adaptive observers. The early works on adaptive observers can be found in Carroll & Lindorff [14], Luders & Narendra [124, 123, 122] and Bastin & Gevers [7].

The advantage of using the adaptive observer is that it is able to compensate for the decrease in the sensitivity of the FDI scheme to detect incipient faults when the robustness of the FDI scheme is enhanced. Therefore, the adaptive observer can successfully estimate the states as well as both the slowly and abruptly varying uncertainties of a system. Furthermore, the adaptive observer can be applied on-line so that the model of the system can be updated continuously and thus, the robustness of the FDI scheme towards the disturbances in the system can be enhanced.

Some of the later works and developments on the adaptive observers were demonstrated in Ding *et al.* [45, 68], Wang & Daley [196], Saif *et al.* [211, 24, 204], Jiang *et al.* [94,

169], Kallesoe *et al.* [101] and Zhang [224]. Ding *et al.* [45] used a recursive algorithm to estimate the coefficients of the orthogonal expansions of the system states. Chen *et al.* in [24] constructed a variable structure adaptive observer based on the inputs and outputs of the observed system such that the observer managed to diagnose faults using a learning method. Other than that, Kallesoe *et al.* [101] had successfully applied the adaptive observer scheme onto an induction motor system. Wu & Saif [204] investigated the use of neural network in the design of the adaptive observer for fault detection in satellite attitude control systems.

2.3.4 Robust FDI using frequency domain approach

Robust FDI using frequency domain approach was first introduced by Viswanadham *et al.* [193]. This method constructs the output observer using the input-output relationship which is described by the transfer function of the system in the frequency domain. From there, the effect of the uncertainty on the residual can be minimised and the effect of the fault on the residual can be maximised using the $\mathcal{H}_\infty$ theory. Furthermore, this method allows the involvement of the frequency specifications as an additional criterion for better fault detection and discrimination as discussed in Frank & Ding [68].

Ding & Frank have contributed much on the development and extension of the frequency domain approach through their works in [44, 47, 46, 66, 67] and also some discussions by Marquez & Diduch *et al.* [128] and Hamelin & Sauter [81, 159].

2.3.5 Robust FDI using parity equation approach

Robust FDI methods have also been designed using the parity equation approach. The method was first proposed by Chow & Willsky [28] and Lou *et al.* [121] later developed the method to achieve better robustness against the disturbances. Lou *et al.* in [121] designed the parity vector using the least-squares optimization technique to minimise the effect of the disturbances onto the residual. Zhang & Patton [222] meanwhile designed the parity vector using the theory of generalised eigenstructure. Magrabi & Gibbens [127] combined the parity equation method with the filter innovations method to design the FDI scheme. Puig

& Quevedo [154] applied the knowledge of fuzzy set theory to design the parameters of the model used in their FDI scheme. Other than that, Ye *et al.* [213] introduced a stationary wavelet waveform into the residual signal of which they claimed to be able to enhance the performance of the FDI scheme as well as to reduce the occurrence of false alarms and also a faster response time towards faults. In addition to that, Zhang *et al.* had in [223] explored the relationship between the parity space and $\mathcal{H}_2$ approaches towards robust fault detection.

2.3.6 Robust FDI using fuzzy logic

One of the methods that has gained much popularity over the recent years for the purpose of robust FDI is fuzzy logic. While the methods discussed before this classify the condition of the system into either 0 (fault-free) or 1 (faulty), the fuzzy logic method provides a more accurate qualitative nature of the system under observation to more than just binary values of 0 and 1. To human beings, the system under consideration can be categorised as one of the following: almost certainly faulty, likely to be faulty, unlikely to be faulty and almost certainly not faulty. Therefore, fuzzy logic is able to perform robust FDI which resembles that of human expert systems using the "if-then" rule, as shown in Molnar [135]. The designer of the algorithm will then program the FDI scheme which suits the system most.

The advantage of using the fuzzy logic is that it is able to compute the algorithm fast enough for on-line robust FDI since there is no need for a design of the mathematical model of the system. However, the characteristics of the system have to be clearly understood since the algorithm is programmed based on the data provided by the input and output of the system.

Existing works on robust FDI methods using fuzzy logic can be found in Deng & Tang [41], Linkens & Shieh [119], Chow & Goode [29], Huang *et al.* [90], Miquel *et al.* [38, 37], Linder [118], Boudaoud & Mason [11], Curry *et al.* [32], Mendonca *et al.* [134] and Dash *et al.* [34].

2.3.7 Robust FDI using neural network

Another artificial intelligence technique for robust FDI scheme is through the implementation of neural network. Generally, there are many algorithms available in the literature to design the FDI scheme using the neural network method as presented in Takahashi *et al.* [171], He *et al.* [84], Xu & Chan [208], Song & Yin [167], Yang *et al.* [212], Yen & Ho [215], Deng & He [42] and Yee & Chow [214].

Under this method, the neural network FDI scheme is trained to recognise faults in the system. Normally, the FDI scheme is trained to generate an alarm indicating the presence of fault if there are abrupt changes of amplitude and phase or the presence of transient components in the system. To detect the faults, either current or voltage signals can be used but current signals are more sensitive towards fault inception. This is so because Vazquez *et al.* [189] has shown that amplitude and phase changes are greater for current signals than for voltage signals. Therefore, it can be seen that this method relies heavily on the reliability of the FDI scheme rather than on the known information of the system. Thus, the amount of training and the quality of training is crucial to determine the effectiveness of the performance of the FDI scheme as has been demonstrated by Molnar [135].

The advantage of using this method is that a well-trained neural network FDI scheme is able to handle a vast variety of linear and nonlinear faults, multiple faults, noise as well as disturbances in the system. Its disadvantage is that without proper training, the FDI modelling process is defective and as a result, this will corrupt the performance of the FDI scheme and will defeat the purpose of FDI.

2.4 Fault reconstruction

Besides detecting and isolating the faults, sometimes it is also important for the faults that occur in the system to be known. As a result, an estimate of the fault of the system can be provided for further analysis and diagnosis. Thus, this leads to the idea of *fault reconstruction*, as suggested by the work done by Chen *et al.* [20] and Edwards *et al.* [53, 55, 54, 173, 175, 177, 176] and is different from the majority of the FDI schemes

that have been discussed so far as it goes beyond detecting and isolating. This approach is very useful for incipient faults and slow drifts, which are well known to be very difficult to detect. In general, fault reconstruction is a subclass of of FDI and that it is able to provide the nature and magnitude of the faults so that appropriate corrective measures can be taken.

In the work by Chen *et al.* [20, 21], the fault reconstruction process uses the residual generated by the FDI to estimate the magnitude of the fault. The transfer matrix from the faults to the residual is derived in terms of the eigenvalues of the fault detection filter and the invariant zeros of the faults. And for each fault, the fault reconstruction process is obtained by applying a projector to the transfer matrix and taking the inverse of it. According to Chen & Speyer [21], in order for a well-conditioned fault reconstruction process, the invariant zeros of the fault have to be stable. Furthermore, to reconstruct a sensor fault, the system has to be detectable with respect to the other sensors.

Meanwhile, Rajaraman *et al.* [155] proposed a methodology which does not require historical operational data and/or a priori fault information in order to achieve accurate fault reconstruction, where it used a two-step procedure to achieve the desired result: parameter estimator and a fault isolation and identification filter. Parameter estimation within the observer is performed by using the unknown parameters as augmented states of the system, and robustness towards uncertainty is ensured by application of a variation of Kharitonov's stability theory [9] to the observer design. As for the fault reconstruction filter, it is based upon a linearization, which has to be repeatedly computed whenever a fault is to be identified. However, the computation for the fault diagnosis is still based on the generation of the residual signal.

Other than that, Tan & Habib [182, 183] have also produced much work on fault reconstruction. For the fault reconstruction scheme in [182], Tan & Habib adapted the work on unknown input observer by Hou & Muller [89] and improved it so that the fault reconstruction scheme is robust to system uncertainties. The fault reconstruction scheme is designed using the Bounded Real Lemma [13] and an inverted pendulum system injected with sensor fault was used to verify its performance. The fault reconstruction scheme managed to reconstruct the fault very well even though a reference position signal was applied to the cart of

the inverted pendulum. In [183], Tan & Habib worked on a fault reconstruction scheme for the same system, but in this case the scheme utilised a linear observer, designed using right eigenstructure assignment to null the effect of the nonlinearities on the fault reconstruction. Early work on right eigenstructure assignment by Patton & Chen [151, 150] was for fault detection only, Tan & Habib [185] then extended on this early work for fault reconstruction.

Fault reconstruction can also be achieved using the sliding mode observer. Hermans & Zarrop [88] designed a sliding mode observer such that the sliding motion is destroyed in the presence of faults but not when uncertainties are present. Edwards *et al.* [55] used the observer from [52] to reconstruct the faults using the so-called 'equivalent output estimation error injection' concept. In their work, whenever sliding motion has taken place, it is found that the 'equivalent output error injection' (similar to the equivalent control [188]) is a scaling of the fault. As a result, by scaling the 'equivalent output error injection', an accurate reconstruction of the fault can be achieved. Tan & Edwards [173] then built on the work in [55] so that the sliding mode observer can be used to reconstruct sensor faults. Here the equivalent output estimation error injection from the first observer is filtered to form a fictitious system in which the sensor faults appear as actuator faults. Then, a second observer is used to reconstruct the actuator faults. However, [55] and [173] did not consider robustness. From their work in [176], the fault reconstruction scheme is designed such that it is able to reconstruct *simultaneous* actuator and sensor faults. In this newer work, the system output is appropriately filtered to yield an 'augmented fictitious system' with 'actuator faults' comprising the actual system actuator faults and sensor faults. The new actuator faults are then reconstructed and the fault reconstruction scheme is able to accurately classify the fault as an actuator fault or a sensor fault, without having to make any a-priori assumptions. While the earlier work mentioned dealt with additive faults acting onto the system, Tan & Edwards [178] built on those work and presented a method to reconstruct multiplicative faults. Faults such as the failure of a component in a system where the results are 'internal' can be classified as multiplicative (or parametric) faults. In a multiplicative scenario the fault signals appear multiplied by (functions of) the states and/or inputs as shown in Garcia *et al.* [75, 76]. The work described in this paper is associated with a reasonably general class of systems

and is not tied in to a specific system. Tan & Edwards [174, 177] then described a new design method for the observer gains such that the $\mathcal{L}_2$ gain between the uncertainty and the fault reconstruction is minimised while maintaining sliding motion all the time.

Besides that, fault reconstruction can also serve as a foundation to the design of a fault tolerant control (FTC) system. With the implementation of a FTC system, the system is able to perform well (similar to a *fault-free* scenario) albeit there is fault acting onto the system. As a result, a reliable and effective FTC scheme can help to cut cost as well as to prevent catastrophic damage and it is not necessary for the system to be shut down immediately for repair or maintenance works to be carried out. Some of the examples of different FTC schemes and the theories behind them are available in Chen & Jiang [22], Diao & Passino [43], Eryurek & Upadhyaya [60], Jamouli *et al.* [92], Marx *et al.* [130], Noura *et al.* [143], Wang & Wang [198], Yu *et al.* [219], Zhang *et al.* [220] and Zidani *et al.* [227].

The principle of fault reconstruction for actuator fault using the sliding mode observer is the FDI approach that will be explored in this thesis.

2.5 Conclusion and Direction of Research Thesis

This chapter has presented an introduction and has also described the importance of FDI schemes as well as a literature review on the many FDI schemes available. As have been shown in the literature review, the availability and accuracy of the model of the system is crucial for a reliable FDI scheme. For methods which are using linear observers to model the system, the FDI schemes cannot be implemented on very complex systems. This is so because linear models are idealised replicates of the systems under consideration and as a result, the complete characteristics of the systems could not be captured. That explains the limited applications of linear model-based FDI schemes. Therefore, the design of FDI schemes using nonlinear observers such as the sliding mode observer and the adaptive observers and artificial intelligence-based FDI schemes such as the fuzzy logic and neural network are getting more popular as they have a wider range of applications.

Other than that, this chapter has also demonstrated the effect of disturbances and modelling

uncertainties onto the efficiency of the FDI schemes and thus, the need for a robust FDI scheme to minimise or even to eliminate the effects of the disturbances onto the residual generation. An overview of the various robust FDI schemes available in the literature has also been presented. Robustness is still an enormous and on-going challenge in FDI.

Chapter 3

Robust Fault Reconstruction Using Sliding Mode Observers

3.1 Introduction

In general control systems, not all the states are measurable (the ones that can be measured are the outputs of the systems), and yet they are needed for the design of the controller. As a result, an observer is often used so that the measurable control inputs and outputs of the system under observation are fed into a dynamic system to generate the estimate of the states. In essence, the observer is designed based on the known properties of the system under observation. The first observer that was designed was a linear observer by Luenberger [125] where the estimates of the states from the observer would converge exponentially to the actual states of the system. However, the Luenberger observer [125] was not able to estimate the states of the system in the presence of disturbances or parameter uncertainties, which represent components that do not fit into the framework of the model of the system. Under these circumstances, the estimates of the states are corrupted by the disturbances and thus, would not converge to the actual states.

Then, Utkin [188] introduced the sliding mode observer, which utilises a nonlinear discontinuous term and the estimated outputs converge to the actual outputs of the system *in finite time*. This results in a reduced order sliding motion where the rest of the estimated non-output states would converge exponentially to the actual non-output states. In addition, it was found that the performance of the sliding mode observer is not affected by the presence of disturbances. During sliding motion, the equivalent output error injection, which is a low

frequency version of the nonlinear discontinuous term, is able to track the disturbances and thus, it can be extended and used for the purpose of fault reconstruction.

Walcott & Zak [194, 195] then improved on the Utkin observer [188] by including a linear gain into the design of their observer such that the error system is quadratically stable despite the presence of uncertainties. Also it was found that a linear gain will increase the sliding patch. They also proposed a method to design the observer using a structural constraint. Overall, their design method was quite alluring. However, their method needed a symbolic manipulation package due to the tedious calculations involved, especially for larger and more complicated systems. Edwards & Spurgeon [52] then further improved on the observer by Walcott & Zak [194, 195]. In their design, they formulated a more systematic design method as opposed to the one by Walcott & Zak [194, 195] where a symbolic manipulation package was needed. In addition to that, Edwards & Spurgeon [52] also designed their observer such that the sliding surface was defined to be the output estimation error whereas the sliding surface was only a subset of the output estimation error in the design shown by Walcott & Zak [194, 195].

Then, Edwards *et al.* in their work in [52, 54, 55], presented and used a method to design the sliding mode observer that differs from other sliding mode observer schemes, i.e. by Chen & Saif [23], Sreedhar *et al.* [168] and Yang & Saif [210], in that the sliding motion is maintained at all times, even during the presence of faults in the system. It has been argued in Edwards *et al.* [55] that if a so-called equivalent output error injection signal which is essential to maintain the sliding motion is introduced in the design of the siding mode observer, the faults could then be reconstructed. Their work is attractive in that the Necessary and Sufficient conditions are known (in terms of the original system matrices) for the scheme to work. So the designer can know at the outset whether the method is applicable to their system. However, the robustness towards uncertainties was not considered. As a result, in order for the fault reconstruction to be robust towards uncertainties, Tan & Edwards [177] presented a method to design the Edwards-Spurgeon observer [52] such that the $\mathcal{L}_2$ gain from the disturbance to the fault reconstruction is minimised.

Generally, the use of sliding mode observer for the purpose of FDI (for both robust and non-

robust considerations) has prospered over the past 15 years or so. Sreedhar *et al.* [168] has produced work with simulations for actuator, sensor as well as process faults. Their work argued that Watanabe & Himmelblau [200] presented an observer-based FDI scheme that is minimally sensitive to certain uncertainties in the system. The simulation presented by Sreedhar *et al.* [168] shows that their sliding mode observer is robust towards system uncertainty compared to the linear observer approach which is not robust and is easily corrupted by the modelling errors and potential false alarms could be generated.

Yang & Saif [210] then later developed an FDI scheme which uses an adaptive sliding observer for threshold setting where this established threshold affects the sensitivity of the fault detection. In their work, they proposed that the use of time-varying threshold is highly desired. They designed their observer for a class of nonlinear system with slowly varying parameters and stressed that an observer designed using the exact linearisation is not robust towards disturbance and may generate false alarms. Their design method is similar to the one by Walcott & Zak [194] but with an added advantage whereby Yang & Saif [210] added the uncertain parameter estimation into the FDI process. They also introduced the use of unknow parameter terms which were previously put into the B input matrix.

Later in 2001, Chen & Saif [23] proposed the use of second order dynamics for the sliding surface so that the FDI scheme can filter the unwanted high frequencies due to the unmodelled dynamics of the system. Their second order sliding mode observer was designed with references being made to Chang [15] and Elmali *et al.* [59]. The key issues addressed in Chen & Saif [23] were on the choice for the observer gain which depends on the measure of uncertainties and disturbances where a big gain will suppress the faults while a small gain cannot guarantee the sliding of the output estimation error. The selection approach they used for the threshold (switching gain) is similar to Yang & Saif [210].

In the same year, some of the work produced have also been proven with some practical experimentations. For example, Goh *et al.* [78] addressed the key issue of minimising the number of sensors required for the purpose of FDI in real-life applications. Their method was tested on a laboratory-based power generator set (Genset) where the perturbation in the component parameters were recovered by manipulating the equivalent input injection signal.

Kim *et al.* [105] and McGookin [133] have both tested their FDI schemes onto a power-train control system and a submarine respectively.

Xiong & Saif [207] compared the use of sliding mode observer for FDI with the unknown input observer and it was found that the sliding mode observer approach can be designed under less restrictive conditions. Their work mainly addressed the issues of whereby some of the previous work are based on the principle that all state variables need to be estimated by the observer and that some existing methods do not consider robustness at all. Their effort has proved that the detection of large and abrupt faults are possible for general class of nonlinear systems and that the sliding mode observer could deal with incipient faults much better than the unknown input observer.

Yeu & Kawaji, meanwhile, in [216] developed a FDI scheme for descriptor systems with complicated structure of differential-algebraic equations with actuator faults. Their work includes robustness, and the simplicity of the design that uses discontinuity functions with error trajectories which moves on a specified hyperspace and then aims to construct the residual signal. The FDI results published were a little different from the actual ones but the reconstructed faults were accurate.

Later in 2002, Ma *et al.* [126] used the sliding mode observer approach for FDI on nonlinear systems with uncertainties of unknown bounds. In their proposed method, in order to capture the nonlinear characteristics of the faults, an online nonlinear estimator is designed using neural networks. Yeu & Kawaji [217], in the same year had also presented a FDI scheme with fault reconstruction for descriptor systems with both actuator and sensor faults. In this work, they developed a design of the sliding mode observer which is independent to the influence of each fault based on the general full order observer for the system. They proved the stability of the state reconstruction error system using the Lyapunov method, where the feedforward injection map and compensation signal are both defined and the sufficient conditions to ensure the stability of the error reconstruction system and the existence of the sliding mode are derived.

Akhenak *et al.* [2] demonstrated the design of a sliding mode multiple observer on a multiple

model, which allows the estimation of the state vector of a nonlinear dynamical system and subsequently remain on a pre-defined surface in the state space. Mainly their method focuses on the design of the nonlinear observer for state estimation of linear systems which are subjected to unknown inputs.

Floquet *et al.* [63] then presented on a method which focuses on the design of a fault detection filter when the conditions for existence of a solution to the nonlinear fundamental problem of residual generation are not satisfied (when the fault cannot be decoupled from the unknown input). The design for their sliding mode observer was based on the approach used in Barbot *et al.* [5] and Boukhobza *et al.* [12]. The conditions are given for the existence of a fault decoupled and an observable subsystem which is affected by the disturbance. In addition to that, the case of loss of observability in nonlinear systems with respect to faults and singular inputs has also been introduced.

As for Wang *et al.* in [199], they have presented a FDI scheme which uses a radial basis function neural network to approximate the faults. Their main focus is on the sliding mode observer for FDI based on nonlinear systems with uncertainties whereby the estimation error is kept within sliding boundary size during fault-free scenario. The main purpose of their radial basis function neural network is to capture the nonlinear characteristics of the faults present in the system.

This chapter will describe the observer formulated by Edwards & Spurgeon [53] for fault reconstruction and also the method used by Tan & Edwards [177] to design the sliding mode observer such that the $\mathcal{L}_2$ gain from the disturbance onto the fault reconstruction will be minimised and it will be demonstrated with an example. This sliding mode observer design method will then be used as the basis for the rest of the work in this thesis.

3.2 Problem Statement and Preliminaries

Consider the following uncertain dynamic system

$$\dot{x} = Ax + Mf + Q\xi \tag{3.1}$$

$$y = Cx \tag{3.2}$$

where $x \in \mathbb{R}^n, y \in \mathbb{R}^p, f \in \mathbb{R}^q$ and $\xi \in \mathbb{R}^h$ represent the states, outputs, unknown faults and unknown disturbances respectively. It is also assumed that $n \geq p > q$ where the matrices C, M and Q are full rank. The function $f : \mathbb{R}_+ \times \mathbb{R}_m \rightarrow \mathbb{R}^q$ is unknown but bounded such that

$$||f|| \leq \alpha \tag{3.3}$$

where $\alpha : \mathbb{R}_+ \times \mathbb{R}^m \rightarrow \mathbb{R}^+$ is a known function. The signal f models the actuator fault within the system. Therefore, $f = 0$ signifies a fault free condition. As for the signal $\xi \in \mathbb{R}^h$, it encapsulates the unknown uncertainties that exist in the system where it is assumed to be unknown but bounded within $||\xi|| < \beta$ where the positive scalar β is known.

3.2.1 Canonical Form for Sliding Mode Observer Design

Edwards & Spurgeon [52] have proven that if $p > q$ and if the following conditions hold

A1. $rank(CM) = q$

A2. (A, M, C) is minimum phase

then there exists a coordinate transformation such that the system (A, M, C, Q) can be written the following structure

$$A = \begin{bmatrix} A_1 & A_2 \\ A_3 & A_4 \end{bmatrix}, \quad M = \begin{bmatrix} 0 \\ M_2 \end{bmatrix}, \quad Q = \begin{bmatrix} Q_1 \\ Q_2 \end{bmatrix} \begin{matrix} \updownarrow n-p \\ \updownarrow p \end{matrix}, \quad C = \begin{bmatrix} 0 & T \end{bmatrix} \tag{3.4}$$

where $T \in \mathbb{R}^{p \times p}$ is orthogonal. Partition A_3 as follows

$$A_3 = \begin{bmatrix} A_{31} \\ A_{32} \end{bmatrix} \begin{matrix} \updownarrow p-q \\ \updownarrow q \end{matrix} \tag{3.5}$$

By construction, the pair (A_1, A_{31}) is detectable and the unobservable modes of (A_1, A_{31}) are the invariant zeros of (A, M, C) as noted in Edwards & Spurgeon [52]. Also, the matrix M_2 can be further partitioned to be

$$M_2 = \begin{bmatrix} 0 \\ M_o \end{bmatrix} \begin{matrix} \updownarrow p-q \\ \updownarrow q \end{matrix} \tag{3.6}$$

where $M_o \in \mathbb{R}^{q \times q}$ is square and invertible and the matrix Q has no particular structure.

3.2.2 The Sliding Mode Observer

Edwards & Spurgeon [52] propose a state observer for the system (3.1) - (3.2)

$$\dot{\hat{x}} = A\hat{x} - G_l e_y + G_n \nu \tag{3.7}$$

$$\hat{y} = C\hat{x} \tag{3.8}$$

where ν is a nonlinear discontinuous output error injection vector defined by

$$\nu = -\rho \frac{e_y}{||e_y||} \quad \text{if } e_y \neq 0 \tag{3.9}$$

where $e_y = \hat{y} - y$. As for the scalar function ρ, it is the upper bound of the magnitude of the fault signal plus the uncertainty and will be formally defined later.

The gain matrices G_l, G_n are to be determined. However, G_n in the coordinate system in

(3.4) is assumed to have the structure

$$G_n = \begin{bmatrix} -LT^T \\ T^T \end{bmatrix} P_o^{-1} \tag{3.10}$$

where $P_o \in \mathbb{R}^{p\times p}$ is a symmetric positive definite (s.p.d.) matrix which will be formally discussed later in this chapter and

$$L = \begin{bmatrix} L^o & 0 \end{bmatrix} \in \mathbb{R}^{(n-p)\times p} \tag{3.11}$$

with $L^o \in \mathbb{R}^{(n-p)\times(p-q)}$.

Proposition 3.1 *If there exists a s.p.d. Lyapunov matrix P such that $P(A - G_lC) + (A - G_lC)^T P < 0$ is satisfied, where*

$$P = \begin{bmatrix} P_1 & P_1L \\ L^TP_1 & P_2 + L^TP_1L \end{bmatrix} > 0 \tag{3.12}$$

with $P_1 \in \mathbb{R}^{(n-p)\times(n-p)}$, $P_2 \in \mathbb{R}^{p\times p}$ and P_o from (3.9) is defined as

$$P_o = TP_2T^T \tag{3.13}$$

then the state estimation error system is ultimately bounded.

Proof

Substituting from (3.1) and (3.7), the state estimation error system can be expressed as

$$\dot{e} = (A - G_lC)e + G_n\nu - Mf - Q\xi \tag{3.14}$$

Define positive scalars

$$\mu_o = -\lambda_{max}(P(A - G_lC) + (A - G_lC)^T P) \tag{3.15}$$

and

$$\mu_1 = ||PQ||$$

Suppose the scalar gain function in (3.9) satisfies

$$\rho \geq ||P_o CM||\alpha + \eta_o \tag{3.16}$$

where η_o is a positive scalar.

According to Koshkouei & Zinober [107], define a Lyapunov function $V(e) = e^T Pe$. The derivative along the estimation error state trajectory is

$$\dot{V} = e^T(P(A - G_l C) + (A - G_l C)^T P)e - 2e^T PMf - 2e^T PQ\xi + 2e^T PG_n \nu \tag{3.17}$$

From (3.15), applying the Rayleigh's inequality to the first term of (3.17) yields

$$e^T(P(A - G_l C) + (A - G_l C)^T P)e < -\mu_o ||e||^2$$

The Cauchy-Schwartz inequality is then applied to the third term of the same equation. As a result, (3.17) can be re-written as

$$\dot{V} \leq -\mu_o ||e||^2 - 2e^T PMf + 2||e||\mu_1 \beta + 2e^T PG_n \nu \tag{3.18}$$

From (3.4), (3.12) and (3.13), it can be established that $PM = C^T P_o CM$ and $PG_n = C^T$. Hence (3.18) can be written as

$$\begin{aligned} \dot{V} &\leq -\mu_o ||e||^2 + 2||e||\mu_1 \beta - 2e^T C^T P_o CMf + 2e^T C^T \nu & (3.19) \\ &= -\mu_o ||e||^2 + 2||e||\mu_1 \beta - 2e_y^T P_o CMf + 2e_y^T \nu & (3.20) \end{aligned}$$

From Cauchy-Schwartz inequality, and the bound on ρ from (3.16),

$$\begin{aligned} \dot{V} &\leq -\mu_o||e||^2 + 2||e||\mu_1\beta - 2||e_y||(\rho - ||P_oCM||\,||f||) && (3.21)\\ &\leq ||e||(-\mu_o||e|| + 2\mu_1\beta) && (3.22) \end{aligned}$$

which proves that the magnitude of the error $||e||$ is ultimately bounded. ■

Proposition 3.1 will now be used to prove the main result of this section, namely that for an appropriate choice of ρ a sliding motion can be induced. Introduce a change of coordinates as proposed in Edwards & Spurgeon [53, 52] using $T_L : e \mapsto e_L$ where

$$T_L = \begin{bmatrix} I_{n-p} & L \\ 0 & T \end{bmatrix} \tag{3.23}$$

where L has been defined in (3.11). The system (A, M, C) in this new coordinates can be written as

$$\tilde{A} = \begin{bmatrix} \tilde{A}_1 & \tilde{A}_2 \\ \tilde{A}_3 & \tilde{A}_4 \end{bmatrix}, \quad \tilde{M} = \begin{bmatrix} 0 \\ \tilde{M}_2 \end{bmatrix}, \quad \tilde{C} = \begin{bmatrix} 0 & I_p \end{bmatrix} \tag{3.24}$$

where $\tilde{A}_1 = A_1 + L^o A_{31}$ and $\tilde{M}_2 = TM_2$. The nonlinear gain matrix G_n from (3.10) will then become

$$\tilde{G}_n = \begin{bmatrix} 0 \\ P_o^{-1} \end{bmatrix} \tag{3.25}$$

and the Lyapunov matrix will have the form

$$\tilde{P} = (T_L^{-1})^T P (T_L^{-1}) = \begin{bmatrix} P_1 & 0 \\ 0 & P_o \end{bmatrix} \tag{3.26}$$

Remark 3.1 *The fact that $\tilde{P}$ is a block diagonal Lyapunov matrix for $\tilde{A} - \tilde{G}_l\tilde{C}$ implies that $\tilde{A}_1$ is stable and as a result, the sliding motion is stable.* ♯

The state estimation error in the new coordinate system is

$$\dot{e}_L = \tilde{A}_o e_L + \tilde{G}_n \nu - \tilde{M} f - T_L \tilde{Q} \xi \tag{3.27}$$

where $\tilde{A}_o = \tilde{A} - \tilde{G}_l \tilde{C}$. Partitioning the state estimation error conformably with (3.24) produces

$$\dot{e}_1 = \tilde{A}_1 e_1 + (\tilde{A}_2 - \tilde{G}_{l,1}) e_y - (Q_1 + L Q_2) \xi \tag{3.28}$$

$$\dot{e}_y = \tilde{A}_3 e_1 + (\tilde{A}_4 - \tilde{G}_{l,2}) e_y + P_o^{-1} \nu - \tilde{M}_2 f - T Q_2 \xi \tag{3.29}$$

where $Q_1, Q_2, \tilde{G}_{l,1}$ and $\tilde{G}_{l,2}$ represent the partitions of Q and $\tilde{G}_l$ respectively.

Proposition 3.2 *If the gain function ρ from (3.9) satisfies*

$$\rho \geq 2||P_o \tilde{A}_3|| \mu_1 \beta / \mu_o + ||P_o Q_2|| \beta + ||P_o \tilde{M}_2|| \alpha + \eta_o \tag{3.30}$$

where η_o is a positive scalar, then an ideal sliding motion takes place on $\mathcal{S} = \{e : Ce = 0\}$ in finite time.

Proof

Consider the Lyapunov function $V_s = e_y^T P_o e_y$. The derivative along the trajectory can be written as

$$\begin{aligned} \dot{V}_s = {} & e_y^T (P_o (\tilde{A}_4 - \tilde{G}_{l,2}) + (\tilde{A}_4 - \tilde{G}_{l,2})^T P_o) e_y + 2 e_y^T P_o \tilde{A}_3 e_1 - 2 e_y^T P_o \tilde{M}_2 f \\ & - 2 e_y^T P_o T Q_2 \xi + 2 e_y^T \nu \end{aligned}$$

The term $(P_o(\tilde{A}_4 - \tilde{G}_{l,2}) + (\tilde{A}_4 - \tilde{G}_{l,2})^T P_o) < 0$ because $\tilde{P}$ from (3.26) is a block diagonal Lyapunov matrix for $(\tilde{A} - \tilde{G}_l \tilde{C})$. Therefore, it follows that

$$\begin{aligned} \dot{V}_s &\leq 2 e_y^T P_o \tilde{A}_3 e_1 - 2 e_y^T P_o \tilde{M}_2 f - 2 e_y^T P_o T Q_2 \xi - 2\rho ||e_y|| \\ &\leq -2||e_y|| (\rho - ||P_o \tilde{A}_3 e_1|| - ||P_o \tilde{M} f|| - ||P_o T Q_2 \xi||) \end{aligned}$$

From Proposition 3.1, it has been shown that in finite time $e \in \Omega_\varepsilon$ which implies $||e_1|| < \frac{2\mu_1\beta}{\mu_o} + \varepsilon$. Therefore, from the definition of ρ in (3.30),

$$\dot{V}_s \leq -2\eta_o||e_y|| \leq -2\eta_o\eta\sqrt{V_s} \tag{3.31}$$

where $\eta := \sqrt{\lambda_{min}(P_o^{-1})}$. Inequality (3.31) shows that the reachability condition has been achieved and hence proves that the output estimation error $e_y = \hat{y} - y$ will reach zero in finite time and a sliding motion takes place. ■

Remark 3.2 *Since $\tilde{M}_2 = CM$, it follows that the definition of ρ in (3.30) is consistent with the assumption on its magnitude in (3.16).* ♯

Note that the signal e_1 does not go towards zero due to the unmatched disturbance Q ($rank(CQ) \leq rank(Q)$) which appears in the dynamics of e_1. Instead, the important property here is that e_y converges to 0 in finite time. Furthermore, G_n is not designed to be matched to Q, i.e. $rank \begin{bmatrix} G_n & Q \end{bmatrix} > rank(G_n)$.

3.3 Robust Actuator Fault Reconstruction

In this section, the sliding mode observer described in Section 3.2.2 will be analysed with regard to its ability to reconstruct the fault f in the presence of the disturbance ξ. Throughout the analysis, it is assumed that $p > q$. In the case when $p = q$, the sliding motion is completely determined by the invariant zeros of (A, M, C) and the design freedom L^o does not exist. The situation $p > q$ allows some design freedom which can be appropriately exploited.

Assuming the sliding mode observer described in Section 3.2.2 has been designed and that a stable sliding motion has been achieved, then $e_y = \dot{e}_y = 0$ and (3.28) - (3.29) can be written as

$$\dot{e}_1 = \tilde{A}_1 e_1 - (Q_1 + LQ_2)\xi \tag{3.32}$$

$$0 = \tilde{A}_3 e_1 + P_o^{-1}\nu_{eq} - \tilde{M}_2 f - TQ_2\xi \tag{3.33}$$

where ν_{eq} is the equivalent output error injection term required to maintain sliding motion as has been discussed in Utkin [188]. In (3.32) - (3.33), the vector signal of ξ will be treated as an unknown exogenous signal.

The equivalent output error injection ν_{eq} can be approximated to any degree of accuracy by replacing (3.9) with

$$\nu = -\rho \frac{e_y}{||e_y|| + \delta} \tag{3.34}$$

where δ is a small positive constant. In this situation, the error trajectories do not slide perfectly on the surface of $\mathcal{S}$, but within a small boundary layer around it. For more details see Section 1.4 in Edwards & Spurgeon [53]. In practice, the scalar δ needs to be chosen small enough so that the boundary layer is negligible, but not too small that it causes difficulties in solving the differential equation. Note that the signal ν in (3.34) can be computed online.

In the case when $\xi \neq 0$, the attempted reconstruction of the fault f will be corrupted by the exogenous disturbance signal ξ. The objective is to exploit all degrees of freedom to minimise the effect of the exogenous signal ξ on the fault reconstruction. Define

$$W := \left[\begin{array}{cc} W_1 & M_o^{-1} \end{array} \right] \tag{3.35}$$

where $W_1 \in \mathbb{R}^{q \times (p-q)}$ is a design freedom, and M_o has been defined in (3.6). Define a fault reconstruction signal to be

$$\hat{f} = W T^T P_o^{-1} \nu_{eq} \tag{3.36}$$

Rewriting (3.32) - (3.33) in terms of the coordinates in (3.4), and re-arranging produces

$$\dot{e}_1 = (A_1 + LA_3)e_1 - (Q_1 + LQ_2)\xi \tag{3.37}$$

$$T^T P_o^{-1} \nu_{eq} = -A_3 e_1 + M_2 f + Q_2 \xi \tag{3.38}$$

Multiplying (3.38) by WT^T yields

$$\hat{f} = -WA_3 e_1 + f + WQ_2 \xi \tag{3.39}$$

Introduce a fault estimation error signal $e_f := \hat{f} - f$ and thus,

$$e_f = -WA_3e_1 + WQ_2\xi \tag{3.40}$$

The objective now is to minimise the effect of ξ on the fault reconstruction (i.e. minimise e_f). From (3.37) and (3.39), by using the Bounded Real Lemma presented in Gahinet *et al.* [25, 74], the $\mathcal{H}_\infty$ norm from the exogenous signal ξ to e_f will not exceed γ if the following inequality holds

$$\begin{bmatrix} \hat{P}(A_1 + LA_3) + (A_1 + LA_3)^T\hat{P} & -\hat{P}(Q_1 + LQ_2) & -(WA_3)^T \\ -(Q_1 + LQ_2)^T\hat{P} & -\gamma I & (WQ_2)^T \\ -WA_3 & WQ_2 & -\gamma I \end{bmatrix} < 0 \tag{3.41}$$

where γ is a positive scalar and $\hat{P} \in \mathbb{R}^{(n-p)\times(n-p)}$ is s.p.d. The objective is therefore to find $\hat{P}, L$ and W in order to minimise γ subject to the inequality (3.41) and $\hat{P} > 0$. However, this must be done in conjunction with satisfying the requirements of obtaining a suitable sliding mode observer (namely, to design G_l) as expressed in Proposition 3.2.

Expressing P from (3.12) to be

$$P = \begin{bmatrix} P_{11} & P_{12} \\ P_{12}^T & P_{22} \end{bmatrix} > 0 \tag{3.42}$$

where $P_{11} \in \mathbb{R}^{(n-p)\times(n-p)}$, $P_{22} \in \mathbb{R}^{p\times p}$ and $P_{12} := \begin{bmatrix} P_{121} & 0 \end{bmatrix}$ with $P_{121} \in \mathbb{R}^{(n-p)\times(p-q)}$. It can be seen that there is a one-to-one correspondence between the variables $(P_{11}, P_{121}, P_{22})$ and (P_1, L^o, P_2) since

$$P_1 = P_{11} \tag{3.43}$$

$$L^o = P_{11}^{-1}P_{121} \tag{3.44}$$

$$P_2 = P_{22} - P_{12}^TP_{11}^{-1}P_{12} \tag{3.45}$$

Choosing $\hat{P} = P_{11}$ and using the switch variables in (3.44), inequality (3.41) can be written as

$$\begin{bmatrix} P_{11}A_1 + A_1^T P_{11} + P_{12}A_3 + A_3^T P_{12} & -(P_{11}Q_1 + P_{12}Q_2) & -(WA_3)^T \\ -(P_{11}Q_1 + P_{12}Q_2)^T & -\gamma I & (WQ_2)^T \\ -WA_3 & WQ_2 & -\gamma I \end{bmatrix} < 0 \tag{3.46}$$

which is affine with respect to the variables P_{11}, P_{12}, W_1 and γ.

Remark 3.3

- *For square systems (when $p = q$), it can be seen that L^o from (3.11) and W_1 from (3.35) do not exist. Hence there is no freedom associated with the design of the sliding motion and also to the scaling of the equivalent output error injection ν_{eq}.*

- *As for the case where the actuator faults and uncertainty enter the system through the same channel $(Q = M)$, it follows that $Q_1 = 0, LQ_2 = 0$ and $WQ_2 = I_q$, resulting in the reconstruction in (3.39) reducing to*

$$\hat{f} = f + \xi$$

  for any choice of L.

- *By assumption $||\xi|| < \beta$ and as a result of the optimisation $||\hat{G}(s)||_\infty < \gamma$, it can then be seen that from (3.39), $\gamma\beta \geq ||\hat{G}(s)\xi||$ is small compared to the magnitude of the fault and thus, $\hat{f}$ will represent a good estimate of f in an $\mathcal{L}_2$ sense.* ♯

3.4 Designing The Sliding Mode Observer

This section will present a method shown by Tan & Edwards [177] to design the sliding mode observer gains in (3.7) - (3.10) to 'induce' inequality (3.46). Specifically it is proposed

that the linear gain G_l from (3.7) be chosen to satisfy

$$\begin{bmatrix} P(A-G_lC)+(A-G_lC)^TP & P(G_lD-B_d) & E^T \\ (G_lD-B_d)^TP & -\gamma_o I & H^T \\ E & H & -\gamma_o I \end{bmatrix} < 0 \tag{3.47}$$

where P has the structure given in (3.42). The matrices $B_d \in \mathbb{R}^{n\times(p+k)}$, $D \in \mathbb{R}^{p\times(p+k)}$, $H \in \mathbb{R}^{q\times(p+k)}$ and $E \in \mathbb{R}^{q\times n}$ are effectively design matrices and their formal interpretations will be discussed later. The matrix B_d will depend on the structure of the uncertainty, while D is an *a priori* user-defined constant matrix used to tune the performance of the observer. The matrices E and H will depend on the LMI variable W_1 from (3.35), while the term γ_o represents a strictly positive scalar.

If a feasible solution to the LMIs (3.42) and (3.47) exists then the requirements of Proposition 3.2 will be fulfilled since (3.47) implies $P(A-G_lC)+(A-G_lC)^TP<0$. Therefore, the choice of G_l, the gain matrix L from (3.42) which follows once P is specified, G_n from (3.10) and P_o from (3.13) constitute towards the sliding mode observer design.

- The matrix

$$B_d = \begin{bmatrix} 0 & Q \end{bmatrix} \tag{3.48}$$

  where Q is the uncertainty distribution matrix defined in (3.1).

- The matrix

$$D = \begin{bmatrix} D_1 & 0 \end{bmatrix} \tag{3.49}$$

  where $D_1 \in \mathbb{R}^{p\times p}$ is nonsingular. This is regarded as a user design parameter to tune the performance of the linear part of the sliding mode observer.

- The matrix

$$H = \begin{bmatrix} 0 & H_2 \end{bmatrix} \tag{3.50}$$

  where $H_2 \in \mathbb{R}^{q\times k}$ which itself will be chosen to depend on W_1.

Proposition 3.3 *Under assumptions (3.48) - (3.50), inequality (3.47) is feasible if and only if*

$$\begin{bmatrix} PA + A^T P - \gamma_o C^T (DD^T)^{-1} C & -PB_d & E^T \\ -B_d^T P & -\gamma_o I & H^T \\ E & H & -\gamma_o I \end{bmatrix} < 0 \tag{3.51}$$

in which case

$$G_l = \gamma_o P^{-1} C^T (DD^T)^{-1} \tag{3.52}$$

is an appropriate choice of G_l in (3.47).

Proof

Define $Y := PG_l$, inequality (3.47) can be written as

$$\begin{bmatrix} PA + A^T P - YC - (YC)^T & E^T & YD - PB_d \\ E & -\gamma_o I & H \\ (YD - PB_d)^T & H^T & -\gamma_o I \end{bmatrix} < 0 \tag{3.53}$$

Taking the Schur's Complement implies that for $\gamma_o > 0$, inequality (3.53) becomes

$$\begin{bmatrix} PA + A^T P - YC - (YC)^T + \bar{Y} & E^T + \frac{1}{\gamma_o}(YD - PB_d)H^T \\ E + \frac{1}{\gamma_o} H(YD - PB_d)^T & -\gamma_o I + \frac{1}{\gamma_o} HH^T \end{bmatrix} < 0 \tag{3.54}$$

where $\bar{Y} = \frac{1}{\gamma_o}(YD - PB_d)(YD - PB_d)^T$.

From the assumptions on the structure of D and H in (3.49) and (3.50), $DH^T = 0$ and hence (3.54) simplifies to be

$$\begin{bmatrix} PA + A^T P - YC - (YC)^T + \bar{Y} & E^T - \frac{1}{\gamma_o} PB_d H^T \\ E - \frac{1}{\gamma_o} HB_d^T P & -\gamma_o I + \frac{1}{\gamma_o} HH^T \end{bmatrix} < 0 \tag{3.55}$$

From the assumption on the structure of D and B_d in (3.49) and (3.48), $DB_d^T = 0$, and the

term

$$\bar{Y} = \frac{1}{\gamma_o} Y D D^T Y^T + \frac{1}{\gamma_o} P B_d B_d^T P \tag{3.56}$$

A 'completing the square' argument yields

$$-YC - (YC)^T + \bar{Y} = -\gamma_o C^T (DD^T)^{-1} C + \frac{1}{\gamma_o} P B_d B_d^T P + \Delta(Y) \tag{3.57}$$

where

$$\Delta(Y) := \frac{1}{\gamma_o} (Y D D^T - \gamma_o C^T)(DD^T)^{-1} (Y D D^T - \gamma_o C^T)^T \tag{3.58}$$

The inequality (3.56) is equivalent to

$$\begin{bmatrix} PA + A^T P - \gamma_o C^T (DD^T)^{-1} C \\ + \frac{1}{\gamma_o} P B_d B_d^T P + \Delta(Y) & E^T - \frac{1}{\gamma_o} P B_d H^T \\ E - \frac{1}{\gamma_o} H B_d^T P & -\gamma_o I + \frac{1}{\gamma_o} H H^T \end{bmatrix} < 0 \tag{3.59}$$

A necessary and sufficient condition for (3.59) to hold is that

$$\begin{bmatrix} PA + A^T P - \gamma_o C^T (DD^T)^{-1} C + \frac{1}{\gamma_o} P B_d B_d^T P & E^T - \frac{1}{\gamma_o} P B_d H^T \\ E - \frac{1}{\gamma_o} H B_d^T P & -\gamma_o I + \frac{1}{\gamma_o} H H^T \end{bmatrix} < 0 \tag{3.60}$$

and the sufficiency follows that from the choice $Y = \gamma_o C^T (DD^T)^{-1}$ which makes $\Delta(Y)$ from (3.58) identically zero.

Using the Schur's Complement once again, a necessary and sufficient condition for inequality (3.60) to hold is

$$\begin{bmatrix} PA + A^T P - \gamma_o C^T (DD^T)^{-1} C & -P B_d & E^T \\ -B_d^T P & -\gamma_o I & H^T \\ E & H & -\gamma_o I \end{bmatrix} < 0 \tag{3.61}$$

and the proposition has been proven. ■

The idea is now to relate inequality (3.51) to the inequality associated with the corruption of the fault estimation signal (3.46). Define

$$PA + A^T P = \begin{bmatrix} X_1 & X_2 \\ X_3 & X_4 \end{bmatrix} \tag{3.62}$$

where $X_1 \in \mathbb{R}^{(n-p)\times(n-p)}$, inequality (3.51) can be written as

$$\begin{bmatrix} X_1 & X_2 & 0 & -(P_{11}Q_1 + P_{12}Q_2) & E_1^T \\ X_2^T & X_4 - \gamma_o T^T (D_1 D_1^T)^{-1} T & 0 & -(P_{12}^T Q_1 + P_{22}Q_2) & E_2^T \\ 0 & 0 & -\gamma_o I & 0 & 0 \\ -(P_{11}Q_1 + P_{12}Q_2)^T & -(P_{12}^T Q_1 + P_{22}Q_2)^T & 0 & -\gamma_o I & H_2^T \\ E_1 & E_2 & 0 & H_2 & -\gamma_o I \end{bmatrix} < 0$$

A necessary condition for the inequality above to hold is that

$$\begin{bmatrix} X_1 & -(P_{11}Q_1 + P_{12}Q_2) & E^T \\ -(P_{11}Q_1 + P_{12}Q_2)^T & -\gamma_o I & H_2^T \\ E_1 & H_2 & -\gamma_o I \end{bmatrix} < 0 \tag{3.63}$$

Choosing $E_1 = -WA_3$ and $H_2 = WQ_2$ will yield the same inequality as (3.46).

The design method can now be summarised whereby γ is minimised with respect to the variables P and W_1 subject to

$$\begin{bmatrix} PA + A^T P - \gamma_o C^T (DD^T)^{-1} C & -PB_d & E^T \\ -B_d^T P & -\gamma_o I & H^T \\ E & H & -\gamma_o I \end{bmatrix} < 0 \tag{3.64}$$

and inequalities (3.46) and (3.42), where γ_o is an a priori user-defined positive scalar.

Standard LMI software, such as the one discussed in Gahinet *et al.* [74] can be used to synthesise numerically γ, P and W_1. Once P has been obtained, L^o can be determined from

(3.44). The gain G_l can be determined from (3.52), G_n from (3.10) and P_o from (3.13).

Remark 3.4 *Let γ_{min} be the minimum value of γ that satisfies (3.46). Since (3.46) is a sub-block of (3.51), $\gamma_{min} \leq \gamma_o$ always hold. The feasibility of the design method above depends on the design parameters γ_o and D_1. Basically, a higher value of γ_o and a 'small' D_1 will increase the feasibility, but will increase the magnitude of the linear gain G_l in (3.52) which could prove problematic in practical situations. These relationships provide the designer with a systematic way of tuning the observer design.* ♯

3.5 An Example

The robust FDI scheme in this chapter will now be demonstrated with a crane system taken from the work in Edwards [50]. The system states, control inputs and outputs are

$$x = \begin{bmatrix} \text{angular displacement of pendulum} \\ \text{angular velocity of pendulum} \\ \text{displacement of cart} \\ \text{velocity of cart} \end{bmatrix}, \quad u = \begin{bmatrix} \text{servo-powered dc motor} \\ \text{pulley system} \end{bmatrix}$$

$$y = \begin{bmatrix} \text{angular displacement of pendulum} \\ \text{displacement of cart} \\ \text{velocity of cart} \end{bmatrix}$$

In the notation of (3.1) - (3.2), the state, input and output distribution matrices are

$$A = \begin{bmatrix} 0 & 1.0000 & 0 & 0 \\ -32.4200 & -0.1480 & 0 & 11.5500 \\ 0 & 0 & 0 & 1.0000 \\ 0.8600 & 0.3000 & 0 & -3.1230 \end{bmatrix}, \quad B = \begin{bmatrix} 0 \\ 12.3540 \\ 0 \\ -9.1150 \end{bmatrix}$$

$$C = \begin{bmatrix} 1 & 0 & 0 & 0 \\ 0 & 0 & 1 & 0 \\ 0 & 0 & 0 & 1 \end{bmatrix}$$

Assume also that the input is potentially faulty. Hence, $M = B$.

Suppose that the matrix A is imprecisely known and that there exists parametric uncertainty. The state equation becomes

$$\dot{x} = (A + \Delta A)x + Bu + Mf \tag{3.65}$$

where ΔA is the discrepancy between the known matrix A and its actual value. Suppose the actual value of the system matrix is given by

$$A + \Delta A = \begin{bmatrix} 0 & 1.0000 & 0 & 0 \\ -32.6240 & -0.1480 & 0 & 11.6540 \\ 0 & 0 & 0 & 1.0000 \\ 0.9820 & 0.2790 & 0 & -3.1230 \end{bmatrix}$$

By inspection, only rows 2 and 4 in matrix A have uncertainties, and the other rows are certain due to the nature of the state equations. Writing (3.65) in the framework of (3.1) - (3.2) yields

$$\Delta A = Q\xi = \underbrace{\begin{bmatrix} 0 & 0 \\ 1 & 0 \\ 0 & 0 \\ 0 & 1 \end{bmatrix}}_{Q} \underbrace{\begin{bmatrix} -0.2040 & 0 & 0 & 0.1040 \\ 0.1220 & -0.0210 & 0 & 0 \end{bmatrix}}_{\xi} x$$

It can be verified that CM is full rank and (A, M, C) is minimum phase. As a result, the method discussed in this chapter is applicable.

3.5.1 Simulation Results

The sliding mode observer was designed using the method described in Section 3.4. The design parameters were specified to be $D_1 = I_3$ and $\gamma_o = 1$, which could be obtained from (3.49) and (3.51) respectively. The LMI optimisation routine discussed at the end of Section 3.4 yielded $\gamma = 0.1146$. The associated gains for the observer in (3.7) are

$$G_l = G_n = \begin{bmatrix} 8.3178 & -0.0215 & 2.2905 \\ 21.4986 & -1.5855 & 5.4800 \\ -0.0215 & 0.5847 & 0.0237 \\ 2.2905 & 0.0237 & 0.8999 \end{bmatrix}$$

and the matrix W from (3.35) and L from (3.11) are given by

$$W = \begin{bmatrix} 0.0299 & 0 & -0.1097 \end{bmatrix}, \quad L = \begin{bmatrix} 2.9513 & -2.5480 & 0 \end{bmatrix}$$

As for the Lyapunov matrix from (3.9), it was found to be

$$P_o = \begin{bmatrix} 0.4039 & 0.0566 & -1.0295 \\ 0.0566 & 1.7199 & -0.1892 \\ -1.0295 & -0.1892 & 3.7368 \end{bmatrix}$$

and

$$E_2 = \begin{bmatrix} 0.1268 & 0.0259 & -0.4645 \end{bmatrix}$$

The scalar function ρ from (3.9) was chosen to be 80, and $\delta = 0.001$. Figure 3.1 shows the plot of the output estimation error and the small magnitude of the signal e_y shows that sliding motion has taken place. As for Figure 3.2, it shows the sliding mode observer successfully reconstructed the fault, rejecting the effect of the uncertainty, which is shown in Figure 3.3. This result corresponds to the small value of γ obtained. It can be seen that the disturbance ξ is not small with a magnitude of about 0.05. However, its effect onto the fault reconstruction is negligible.

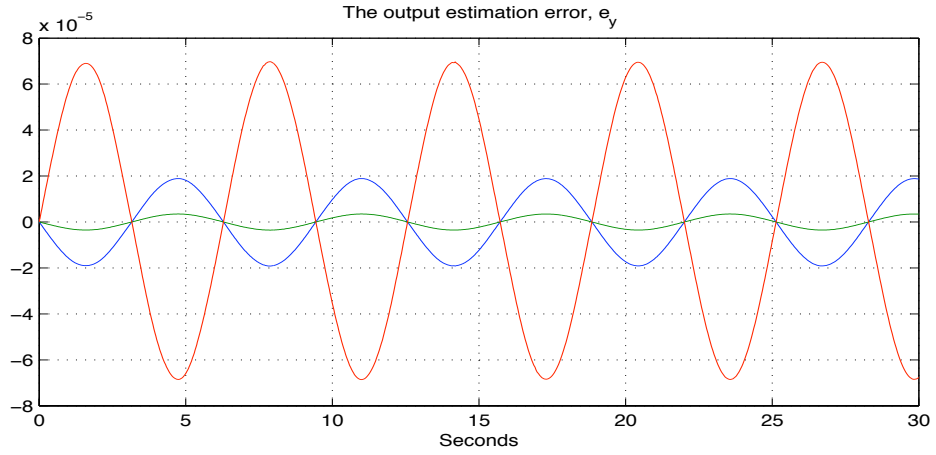

Figure 3.1: The output estimation error e_y.

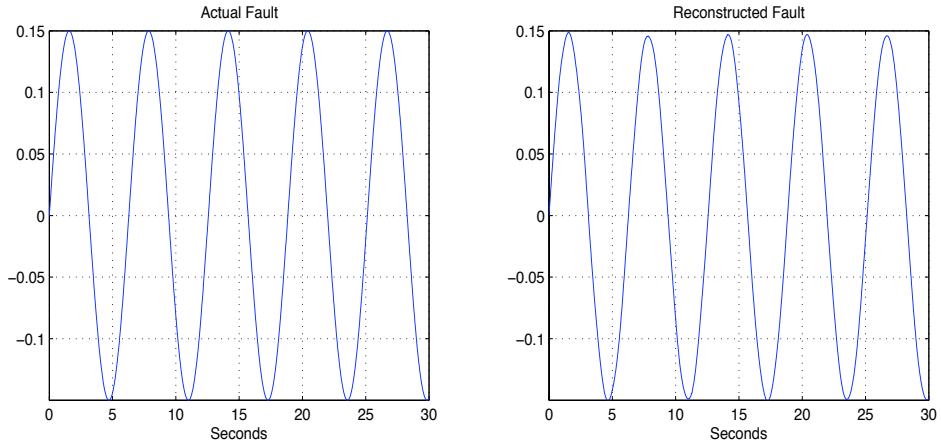

Figure 3.2: The left subfigure is the fault, the right subfigure shows the fault reconstruction.

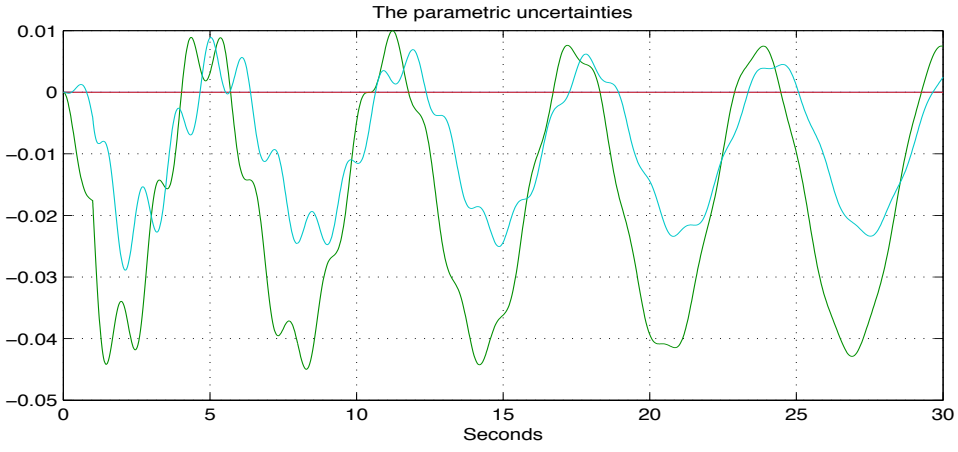

Figure 3.3: The presence of uncertainties in the modelling of the system.

3.6 Conclusion

This chapter has presented a scheme to design the sliding mode observer by Tan & Edwards [177] which minimises the effect of the system uncertainties on the fault reconstruction using standard LMI software such as the one shown in Gahinet [74]. The design method is systematic and the effects of the design parameters are known. This method will be used for the rest of the thesis. The method discussed in this chapter was demonstrated with a crane model and the method provided good fault reconstruction despite the presence of uncertainties.

Chapter 4

Disturbance Decoupled Fault Reconstruction

4.1 Introduction

It has been mentioned in Section 3.1 that Edwards *et al.* [55] used a sliding mode observer from Edwards & Spurgeon [52] to reconstruct faults, but there was no explicit consideration of the disturbances and therefore the fault reconstruction was not robust towards the uncertainties. Tan & Edwards [177] then built on the work by Edwards *et al.* [55] and presented a design algorithm for the sliding mode observer to minimise the $\mathcal{L}_2$ gain from the disturbances to the fault reconstruction. However, this method does not guarantee total decoupling from the disturbances, as the effects of the uncertainties on the fault reconstruction were only minimised.

Then, Saif & Guan [158] designed a method which combined the faults and disturbances to form a new 'fault' vector and used an unknown input observer to reconstruct the new 'fault', which includes the disturbances. Although this method has successfully decoupled the disturbances from the fault reconstruction, it requires very stringent conditions to be fulfilled, and is conservative because the disturbances do not need to be reconstructed, only to be rejected or decoupled. Edwards & Tan [56] later compared the fault reconstruction performances of the work by Edwards *et al.* [55] and also Saif & Guan [158], and found that it was not necessary to reconstruct the disturbances in order to generate a disturbance decoupled fault reconstruction. A counter example was presented by Edwards & Tan [56] to demonstrate this, but the conditions for disturbance decoupling were not formally investigated.

This chapter extends the work in Edwards & Tan [56], and its main contribution is the investigation of conditions that guarantee the disturbance decoupled fault reconstruction (DDFR). It is found that the conditions that guarantee DDFR are less stringent than those shown by Saif & Guan [158], which proves that disturbance reconstruction is not necessary for disturbance decoupled fault reconstruction. In addition, the conditions found in this chapter are easily testable in terms of the original system matrices, hence making it possible to immediately determine whether disturbance decoupled fault reconstruction is feasible. A model of an aircraft system taken from the FDI literature will be used to demonstrate the findings in this chapter.

The method proposed in this chapter has been submitted as a journal paper [138] and has been published as a conference paper [139].

4.2 Preliminaries and Problem Statement

Consider the following system

$$\dot{x} = Ax + Mf + Q\xi \tag{4.1}$$

$$y = Cx \tag{4.2}$$

where $x \in \mathbb{R}^n$, $y \in \mathbb{R}^p$, $f \in \mathbb{R}^q$ and $\xi \in \mathbb{R}^h$ are the states, outputs, unknown faults and unknown disturbances respectively. The signal ξ represents the mismatches between the model and the actual plant as has been discussed in Chen & Patton [16]. Assume that $p > q$.

The objective is to reconstruct f, while rejecting the effects of ξ, hence achieving *disturbance decoupled fault reconstruction* (DDFR). As described in Chapter 3, Tan & Edwards [177] proposed a scheme which minimised the effect of ξ on the fault reconstruction if and only if the following are satisfied

B1. $rank(CM) = rank(M)$

B2. (A, M, C) is minimum phase

The method shown by Tan & Edwards [177] however, does not fully reject ξ but only minimises its effect. Saif & Guan [158] totally reject the effects of ξ (and achieved DDFR) by combining ξ and f to form an augmented 'fault' vector $\bar{f} := \begin{bmatrix} \xi \\ f \end{bmatrix}$ and then designed a fault reconstruction scheme to reconstruct $\bar{f}$. One of the necessary conditions for their scheme is

$$rank\left(C\begin{bmatrix} M & Q \end{bmatrix}\right) = rank\begin{bmatrix} M & Q \end{bmatrix} \tag{4.3}$$

Since only the reconstruction of f is required, reconstructing $\bar{f}$ is unnecessary and hence is conservative. This chapter investigates the conditions that guarantee DDFR with less stringent requirements than (4.3). Firstly, define $k := rank(CQ)$ where $k \leq h$. Then assume B1 holds as well as the following condition

$$rank\left(C\begin{bmatrix} M & Q \end{bmatrix}\right) = rank(CM) + rank(CQ) \tag{4.4}$$

Notice that (4.4) implies $p \geq q + k$. The implication of this assumption will be discussed later in this chapter.

Proposition 4.1 *If B1 and (4.4) hold then there exist appropriately dimensioned nonsingular linear transformations $x \mapsto T_2 x$ and $\xi \mapsto T_1^{-1}\xi$ such that (A, M, C, Q) will be transformed to have the structure*

$$A = \overset{\overset{n-p}{\longleftrightarrow}\ \overset{p}{\longleftrightarrow}}{\begin{bmatrix} A_1 & A_2 \\ A_3 & A_4 \end{bmatrix}}, \quad M = \overset{\overset{q}{\longleftrightarrow}}{\begin{bmatrix} 0 \\ M_2 \end{bmatrix}}, \quad Q = \overset{\overset{h}{\longleftrightarrow}}{\begin{bmatrix} Q_1 \\ Q_2 \end{bmatrix}} \begin{matrix} \updownarrow n-p \\ \updownarrow p \end{matrix}, \quad C = \overset{\overset{n-p}{\longleftrightarrow}\ \overset{p}{\longleftrightarrow}}{\begin{bmatrix} 0 & C_2 \end{bmatrix}} \updownarrow p \tag{4.5}$$

and M_2, Q_1 and Q_2 can be further partitioned as

$$M_2 = \begin{bmatrix} 0 \\ M_o \end{bmatrix} \begin{matrix} \updownarrow p-q \\ \updownarrow q \end{matrix}, \; Q_1 = \begin{bmatrix} 0 & 0 \\ \bar{Q}_1 & 0 \end{bmatrix} \begin{matrix} \updownarrow n-p-h+k \\ \updownarrow h-k \end{matrix}, \; Q_2 = \begin{bmatrix} 0 & 0 \\ 0 & \bar{Q}_2 \\ 0 & 0 \end{bmatrix} \begin{matrix} \updownarrow p-q-k \\ \updownarrow k \\ \updownarrow q \end{matrix} \tag{4.6}$$

where $M_o, C_2, \bar{Q}_1$ and $\bar{Q}_2$ are square and invertible.

Proof

From the work in Edwards & Spurgeon [52], since CM is full rank, then there exists a change of coordinates such that (A, M, C, Q) can be written as

$$\tilde{A} = \begin{bmatrix} \tilde{A}_1 & \tilde{A}_2 \\ \tilde{A}_3 & \tilde{A}_4 \end{bmatrix}, \quad \tilde{M} = \begin{bmatrix} 0 \\ \tilde{M}_2 \end{bmatrix}, \quad \tilde{Q} = \begin{bmatrix} \tilde{Q}_1 \\ \tilde{Q}_2 \end{bmatrix} \begin{matrix} \updownarrow n-p \\ \updownarrow p \end{matrix}, \quad \tilde{C} = \begin{bmatrix} 0 & T \end{bmatrix} \tag{4.7}$$

and $\tilde{M}_2 \in \mathbb{R}^{p \times q}$ can be further partitioned as

$$\tilde{M}_2 = \begin{bmatrix} 0 \\ M_o \end{bmatrix} \tag{4.8}$$

The matrices $\tilde{Q}_1, \tilde{Q}_2$ have no particular structure and $M_o \in \mathbb{R}^{q \times q}$ is invertible whilst $T \in \mathbb{R}^{p \times p}$ is orthogonal.

Since $rank(CQ) = k$ and T is orthogonal, then using $\tilde{C}$ and $\tilde{Q}$ in (4.7), it can be shown that $rank(\tilde{Q}_2) = k$ and there exists an orthogonal matrix $T_1 \in \mathbb{R}^{h \times h}$ (for $\tilde{Q}$) such that

$$\begin{bmatrix} \tilde{Q}_1 \\ \tilde{Q}_2 \end{bmatrix} T_1 = \begin{matrix} \overset{h-k}{\longleftrightarrow} & \overset{k}{\longleftrightarrow} \\ \end{matrix} \begin{bmatrix} \tilde{Q}_{11} & \tilde{Q}_{12} \\ 0 & \tilde{Q}_{22} \end{bmatrix} \begin{matrix} \updownarrow n-p \\ \updownarrow p \end{matrix} \tag{4.9}$$

where $rank(\tilde{Q}_{22}) = k$ since $rank(\tilde{Q}_2) = k$. It then follows that $rank(\tilde{Q}_{11}) = h - k$.

Apply the partitions in (4.7) to (4.4). Since T is orthogonal, using (4.8) causes (4.4) to result in

$$rank\left(\begin{bmatrix} \tilde{M}_2 & 0 & \tilde{Q}_{22} \end{bmatrix}\right) = rank\left(\begin{bmatrix} 0 & \tilde{Q}_{221} \\ M_o & \tilde{Q}_{222} \end{bmatrix}\right) = q + k \tag{4.10}$$

where $\tilde{Q}_{221}$ and $\tilde{Q}_{222}$ are appropriate partitions of $\tilde{Q}_{22}$. Since M_o is square and invertible with rank q, equation (4.10) implies that $\tilde{Q}_{221} \in \mathbb{R}^{(p-q) \times k}$ has full column rank of k which

means there exists a matrix $\tilde{Q}_{221}^{\dagger}$ such that $\tilde{Q}_{221}^{\dagger}\tilde{Q}_{221} = I_k$. Then let T_{21} and T_{22} be orthogonal matrices such that

$$T_{21}\tilde{Q}_{11} = \begin{matrix} \overset{h-k}{\longleftrightarrow} \\ \begin{bmatrix} 0 \\ \bar{Q}_1 \end{bmatrix} \end{matrix} \begin{matrix} \updownarrow n-p-h+k \\ \updownarrow h-k \end{matrix}, \quad T_{22}\tilde{Q}_{221} = \begin{matrix} \overset{k}{\longleftrightarrow} \\ \begin{bmatrix} 0 \\ \bar{Q}_2 \end{bmatrix} \end{matrix} \begin{matrix} \updownarrow p-q-k \\ \updownarrow k \end{matrix} \tag{4.11}$$

and define the following transformation matrix

$$T_2 := \begin{bmatrix} T_{21} & -T_{21}\tilde{Q}_{12}\tilde{Q}_{221}^{\dagger} & 0 \\ 0 & T_{22} & 0 \\ 0 & -\tilde{Q}_{222}\tilde{Q}_{221}^{\dagger} & I_q \end{bmatrix} \tag{4.12}$$

Using (4.11) - (4.12), it is clear that

$$T_2\tilde{Q}T_1 = \begin{matrix} \overset{n-p}{\longleftrightarrow} & \overset{p-q}{\longleftrightarrow} & \overset{q}{\longleftrightarrow} \\ \left[\begin{array}{c|c|c} T_{21} & -T_{21}\tilde{Q}_{12}\tilde{Q}_{221}^{\dagger} & 0 \\ \hline 0 & T_{22} & 0 \\ 0 & -\tilde{Q}_{222}\tilde{Q}_{221}^{\dagger} & I_q \end{array}\right] \end{matrix} \begin{bmatrix} \tilde{Q}_{11} & \tilde{Q}_{12} \\ \hline 0 & \tilde{Q}_{221} \\ 0 & \tilde{Q}_{222} \end{bmatrix} = \begin{bmatrix} 0 & 0 \\ \bar{Q}_1 & 0 \\ \hline 0 & 0 \\ 0 & \bar{Q}_2 \\ 0 & 0 \end{bmatrix} \begin{matrix} \updownarrow n-p-h+k \\ \updownarrow h-k \\ \updownarrow p-q-k \\ \updownarrow k \\ \updownarrow q \end{matrix} \tag{4.13}$$

$$\tilde{C}T_2^{-1} = \begin{bmatrix} 0 & TY_1^{-1} \end{bmatrix}, \quad Y_1 = \begin{bmatrix} T_{22} & 0 \\ -\tilde{Q}_{222}\tilde{Q}_{221}^{\dagger} & I_q \end{bmatrix}$$

The transformation T_2 does not alter $\tilde{M}$. Equating $C_2 = TY_1^{-1}$ completes the proof. ■

4.2.1 A Sliding Mode Observer for Fault Reconstruction

The sliding mode observer to be used for the system (4.1) - (4.2) for the purpose of fault reconstruction in this chapter will be of the same design methodology as the one described in Section 3.2.2.

Basically, the state observer for the system (4.1) - (4.2) is identical to the one used in (3.7) - (3.8), while the structures of ν, G_n and L have been defined in (3.9) - (3.11).

However, earlier in this chapter, through Proposition 4.1 an additional coordinate transformation was introduced such that the matrix Q has the structure shown in (4.6). As a result, $C_2 = TY_1^{-1}$ as shown in the end of the proof for Proposition 4.1, as opposed to Section 3.2.1, via (3.4), which showed that $C_2 = T$.

Therefore, the matrix $C_2 = T$ used in Section 3.2.2 shall be replaced with $C_2 = TY_1^{-1}$ in order to fit into the work to be presented in this chapter. For instance, the matrix G_n in this new form is written as

$$G_n = \begin{bmatrix} -L \\ I_p \end{bmatrix} (P_o C_2)^{-1} \tag{4.14}$$

where $P_o \in \mathbb{R}^{p \times p}$ is a symmetric positive definite (s.p.d.) matrix.

As for the state estimation error signal $e = \hat{x} - x$, it will be of the form as defined in (3.14).

Proposition 3.1 could then be used to compute the matrix P such that such that $P(A - G_l C) + (A - G_l C)^T P < 0$ is satisfied. And for a large enough choice of ρ, an ideal sliding motion takes place on $\mathcal{S} = \{e : Ce = 0\}$ in finite time.

Apply a change of coordinates such that $e_L := col(e_1, e_y) = T_L e$ using equation (3.23) and assuming that a sliding motion has taken place at the sliding surface $\mathcal{S}$, then $e_y = \dot{e}_y = 0$ and therefore the state estimation error in the coordinates of (4.5) - (4.6) can be written as had been shown in (3.32) - (3.33) where ν_{eq} has been defined to be the equivalent output error injection term required to maintain the sliding motion in Edwards *et al.* [55] and can be approximated to any degree of accuracy as defined in (3.34). Since e_y is measurable, therefore ν_{eq} can be computed online. Kindly see Edwards *et al.* [55] for full details.

To reconstruct the fault, define a fault reconstruction signal to be (3.36) where the matrix W was defined in (3.35). As a result, the fault reconstruction error can be computed as

$$e_f = -W A_3 e_1 + W Q_2 \xi \tag{4.15}$$

It is desired that $e_f = 0 \ \ (\hat{f} = f)$ and recalling from (3.37) that

$$\dot{e}_1 = (A_1 + LA_3)e_1 - (Q_1 + LQ_2)\xi \tag{4.16}$$

it is clear that ξ is an excitation signal of e_f and that the design freedom in the problem is represented by L_o and W_1. The objective is to decouple e_f from ξ by choice of L_o and W_1.

The following theorem states the main result of this chapter:

Theorem 4.1 *Suppose assumption B1 and (4.4) hold. Then the fault reconstruction error e_f will be decoupled from the disturbance ξ (and DDFR is achieved) by an appropriate choice of L_o and W_1 if the following conditions are satisfied*

C1. $rank(CM) = rank(M)$

C2. $rank\left(C \begin{bmatrix} M & Q \end{bmatrix}\right) = rank(CM) + rank(CQ)$

C3. $rank \begin{bmatrix} CAQ & CQ & CM \\ CQ & 0 & 0 \end{bmatrix} = rank(Q) + rank(M) + rank(CQ)$

C4. $\left(A, \begin{bmatrix} M & Q \end{bmatrix}, C\right)$ *is minimum phase.* □

Note that C1 - C4 are easily testable conditions in terms of the original system matrices. The following section provides a constructive proof of Theorem 4.1.

4.3 Disturbance Decoupled Fault Reconstruction

If conditions C1 - C2 are satisfied, then the coordinate transformation in Proposition 4.1 can be achieved, and assume that the structure in (4.5) - (4.6) have been obtained.

In order to make the e_f completely decoupled from ξ, a necessary condition is

$$WQ_2 = 0 \tag{4.17}$$

since WQ_2 is the direct feedthrough component in system (4.16) and (4.15). Partition Q_2 from (4.6) such that

$$Q_2 = \left[\begin{array}{cc} 0 & 0 \\ 0 & \bar{Q}_2 \\ \hline 0 & 0 \end{array}\right] = \left[\begin{array}{c} Q_{21} \\ Q_{22} \end{array}\right] \begin{array}{l} \updownarrow p-q \\ \updownarrow q \end{array} \tag{4.18}$$

and therefore $WQ_2 = W_1Q_{21}$. Thus the necessary and sufficient condition to ensure (4.17) holds is that $W_1Q_{21} = 0$.

Lemma 4.1 *A general solution for W_1 that will satisfy $W_1Q_{21} = 0$ (and hence make $WQ_2 = 0$) is given by*

$$W_1 = \left[\begin{array}{cc} W_{12} & 0 \end{array}\right] \tag{4.19}$$

where $W_{12} \in \mathbb{R}^{q\times(p-q-k)}$ is design freedom. ♯

Proof

This is straightforward; substituting (4.19) and (4.18) into WQ_2 results in (4.17) being satisfied. ■

Remark 4.1 *If C2 is not satisfied, then $rank\left(C\left[\begin{array}{cc} M & Q \end{array}\right]\right) < rank(CM) + rank(CQ)$. By definition $rank(CQ) = rank(Q_2) = k$; if C2 is not satisfied, then from the structure of M_2 in (4.6) and Q_2 in (4.18), it is clear that $rank(Q_{21}) < k$. Expanding (4.17) using (3.36) gives $WQ_2 = W_1Q_{21} + M_o^{-1}Q_{22}$. In order to satisfy (4.17), the following must be satisfied*

$$W_1Q_{21} = -M_o^{-1}Q_{22} \tag{4.20}$$

From matrix theory, to satisfy (4.20) by choice of W_1 requires

$$rank(Q_{21}) = rank\left[\begin{array}{c} Q_{21} \\ Q_{22} \end{array}\right] = rank(Q_2) \tag{4.21}$$

If C2 is not satisfied, then $rank(Q_{21}) < k$ and (4.21) is not satisfied. Therefore, C2 is a necessary condition in order for (4.17) to be satisfied.

Lemma 4.1 shows that C2 is a sufficient condition for (4.17) to be satisfied as it enables the coordinate transformation in Proposition 4.1 to be attained. Therefore, C2 is a necessary and sufficient condition in order for (4.17) to be satisfied. ♯

Partition A_1, A_3, L_o from (4.5) as

$$A_1 = \begin{bmatrix} A_{11} & A_{12} \\ A_{13} & A_{14} \end{bmatrix} \begin{matrix} \updownarrow n-p-h+k \\ \updownarrow h-k \end{matrix}, \quad A_3 = \overset{n-p-h+k}{\longleftrightarrow} \begin{bmatrix} A_{31} & A_{32} \\ A_{33} & A_{34} \\ A_{35} & A_{36} \end{bmatrix} \begin{matrix} \updownarrow p-k-q \\ \updownarrow k \\ \updownarrow q \end{matrix} \tag{4.22}$$

$$L_o = \overset{p-k-q}{\longleftrightarrow} \overset{k}{\longleftrightarrow} \begin{bmatrix} L_{11} & L_{12} \\ L_{21} & L_{22} \end{bmatrix} \tag{4.23}$$

From (4.15), define $\hat{C} := WA_3 = \begin{bmatrix} \hat{C}_1 & \hat{C}_2 \end{bmatrix}$. From (4.19) and (4.22) - (4.23), it can be expanded to be

$$\hat{C} = \begin{bmatrix} -W_{12}A_{31} - M_o^{-1}A_{35} & -W_{12}A_{32} - M_o^{-1}A_{36} \end{bmatrix} \tag{4.24}$$

Let $\hat{A} := A_1 + LA_3$ and $\hat{B} := Q_1 + LQ_2$, then both $\hat{A}$ and $\hat{B}$ when expressed using (4.22) - (4.23) will respectively produce

$$\hat{A} := \begin{bmatrix} \hat{A}_1 & \hat{A}_2 \\ \hat{A}_3 & \hat{A}_4 \end{bmatrix} = \begin{bmatrix} A_{11} + L_{11}A_{31} + L_{12}A_{33} & A_{12} + L_{11}A_{32} + L_{12}A_{34} \\ A_{13} + L_{21}A_{31} + L_{22}A_{33} & A_{14} + L_{21}A_{32} + L_{22}A_{34} \end{bmatrix} \tag{4.25}$$

$$\hat{B} := \begin{bmatrix} 0 & \hat{B}_2 \\ \hat{B}_3 & \hat{B}_4 \end{bmatrix} = \begin{bmatrix} 0 & L_{12}\bar{Q}_2 \\ \bar{Q}_1 & L_{22}\bar{Q}_2 \end{bmatrix} \tag{4.26}$$

Partition

$$e_1 = \begin{bmatrix} e_{11} \\ e_{12} \end{bmatrix} \begin{matrix} \updownarrow n-p-h+k \\ \updownarrow h-k \end{matrix}, \quad \xi = \begin{bmatrix} \xi_1 \\ \xi_2 \end{bmatrix} \begin{matrix} \updownarrow h-k \\ \updownarrow k \end{matrix} \tag{4.27}$$

Therefore, from the solution of W_1 in (4.19), the system (4.15) and (4.16) form the following state space system

$$\dot{e}_1 = \hat{A}e_1 + \hat{B}\xi \ , \qquad e_f = \hat{C}e_1 \tag{4.28}$$

It can be observed from (4.25) - (4.27) that e_{12} will always be affected by ξ_1 because $\bar{Q}_1$ is square and invertible. However, e_{11} can be decoupled from ξ by setting $L_{12} = 0$ and $\hat{A}_2 = 0$. In order for e_f not to be influenced by e_{12} (and subsequently ξ), it is necessary to make $\hat{C}_2 = 0$. Since $L_{12} = 0$, then $\hat{A}_2$ and $\hat{C}_2$ can be made zero if A_{32} has full column rank.

From (4.24), it can be shown that

$$\hat{C}_2 = 0 \Rightarrow -W_{12}A_{32} - M_o^{-1}A_{36} = 0 \tag{4.29}$$

A general solution for W_{12} that satisfies (4.29) is

$$W_{12} = -M_o^{-1}A_{36}A_{32}^{\dagger} + W_{121}(I - A_{32}A_{32}^{\dagger}) \tag{4.30}$$

where $W_{121} \in \mathbb{R}^{q\times(h-k)}$ is design freedom and $A_{32}^{\dagger} \in \mathbb{R}^{(h-k)\times(p-k-q)}$ is such that $A_{32}^{\dagger}A_{32} = I_{h-k}$. Note that $A_{32}^{\dagger}$ exists because A_{32} is full column rank.

Lemma 4.2 *The matrix A_{32} is full column rank $(h-k)$ if and only if*

$$rank \begin{bmatrix} CAQ & CQ & CM \\ CQ & 0 & 0 \end{bmatrix} = rank(Q) + rank(M) + rank(CQ) \tag{4.31}$$

♯

Proof

From the partitions in (4.5) - (4.6) and (4.22) - (4.23), it can be shown that

$$CAQ = C_2 \left[\begin{array}{c|c} A_{32} & * \\ A_{34} & * \\ A_{36} & * \end{array}\right] \left[\begin{array}{c|c} \bar{Q}_1 & 0 \\ \hline 0 & \bar{Q}_2 \end{array}\right] \tag{4.32}$$

Using the partitions of M and Q from (4.5) - (4.6), it can be shown that

$$\begin{bmatrix} CAQ & CQ & CM \\ CQ & 0 & 0 \end{bmatrix} = C_2 \left[\begin{array}{c|cccc} A_{32} & * & 0 & 0 & 0 \\ A_{34} & * & 0 & \bar{Q}_2 & 0 \\ A_{36} & * & 0 & 0 & M_o \\ \hline 0 & 0 & 0 & 0 & 0 \\ 0 & \bar{Q}_2 & 0 & 0 & 0 \\ 0 & 0 & 0 & 0 & 0 \end{array}\right] \left[\begin{array}{c|c} \bar{Q}_1 & 0 \\ \hline 0 & I_{h+k+q} \end{array}\right] \tag{4.33}$$

where (*) are matrices that play no role in the subsequent analysis.

Since $C_2, M_o, \bar{Q}_1$ and $\bar{Q}_2$ are square and invertible, it results in

$$\begin{aligned} \begin{bmatrix} CAQ & CQ & CM \\ CQ & 0 & 0 \end{bmatrix} &= rank(A_{32}) + rank(M_o) + 2rank(\bar{Q}_2) \\ &= rank(A_{32}) + rank(M) + 2rank(CQ) \end{aligned} \tag{4.34}$$

Then combining (4.34) with (4.31) results in

$$rank(A_{32}) = rank(Q) - rank(CQ) \tag{4.35}$$

It is obvious that $rank(Q) - rank(CQ) = h - k$, and the proof is complete. ■

Substituting $L_{12} = 0$ into (4.25) yields $\hat{A}_2 = A_{12} + L_{11}A_{32}$ and choosing

$$L_{11} = -A_{12}A_{32}^{\dagger} + L_{111}(I - A_{32}A_{32}^{\dagger}) \tag{4.36}$$

where L_{111} is design freedom, makes $\hat{A}_2 = 0$.

From (4.25), in order for $\hat{A}$ to be stable, $\hat{A}_1$ and $\hat{A}_4$ must be stable. Based on L_{11} in (4.36), $\hat{A}_1$ from (4.25) becomes

$$\hat{A}_1 = A_{11} - A_{12}A_{32}^{\dagger}A_{31} + L_{111}(I - A_{32}A_{32}^{\dagger})A_{31} \tag{4.37}$$

So for $\hat{A}_1$ to be stable, $\left(A_{11} - A_{12}A_{32}^{\dagger}A_{31}, (I - A_{32}A_{32}^{\dagger})A_{31}\right)$ must be detectable.

Likewise $\hat{A}_4$ can be written as

$$\hat{A}_4 \;=\; A_{14} + L_{21}A_{32} + L_{22}A_{34} \;=\; A_{14} + \begin{bmatrix} L_{21} & L_{22} \end{bmatrix} \begin{bmatrix} A_{32} \\ A_{34} \end{bmatrix} \tag{4.38}$$

which implies that $\left(A_{14}, \begin{bmatrix} A_{32} \\ A_{34} \end{bmatrix}\right)$ has to be detectable for $\hat{A}_4$ to be stable.

However, since A_{32} is full column rank, then $\left(A_{14}, \begin{bmatrix} A_{32} \\ A_{34} \end{bmatrix}\right)$ is *observable*.

Proposition 4.2 *The pair* $\left(A_{11} - A_{12}A_{32}^{\dagger}A_{31}, (I - A_{32}A_{32}^{\dagger})A_{31}\right)$ *is detectable if* $\left(A, \begin{bmatrix} M & Q \end{bmatrix}, C\right)$ *is minimum phase.*

Proof

The Rosenbrock system matrix [157] associated with the triple $\left(A, \begin{bmatrix} M & Q \end{bmatrix}, C\right)$ in (4.1) - (4.2) is given by

$$E_{a,1}(s) = \begin{bmatrix} sI - A & M & Q \\ C & 0 & 0 \end{bmatrix}$$

The invariant zeros of the system are the values of s that cause its Rosenbrock matrix to lose normal rank. From (4.5) - (4.6) and (4.22) - (4.23), it can be shown that $E_{a,1}(s)$ can be expanded to be

$$E_{a,1}(s) = \begin{bmatrix} sI - A_{11} & -A_{12} & * & 0 & 0 & 0 \\ -A_{13} & sI - A_{14} & * & 0 & \bar{Q}_1 & 0 \\ -A_{31} & -A_{32} & * & 0 & 0 & 0 \\ -A_{33} & -A_{34} & * & 0 & 0 & \bar{Q}_2 \\ -A_{35} & -A_{36} & * & M_o & 0 & 0 \\ 0 & 0 & C_2 & 0 & 0 & 0 \end{bmatrix} \tag{4.39}$$

where (*) are matrices which do not play any role in the subsequent analysis.

Since $C_2, M_o, \bar{Q}_1$ and $\bar{Q}_2$ are full rank, then $E_{1,a}(s)$ loses rank if and only if $E_{a,2}(s)$ loses rank, where

$$E_{a,2}(s) := \begin{bmatrix} sI - A_{11} & -A_{12} \\ -A_{31} & -A_{32} \end{bmatrix} \tag{4.40}$$

Hence, the values of s that make $E_{a,2}(s)$ lose rank are the invariant zeros of the quadruple $(A_{11}, A_{12}, A_{31}, A_{32})$.

Since A_{32} has full column rank, then A_{32} can be decomposed to become

$$A_{32} = X \begin{bmatrix} 0 \\ A_{322} \end{bmatrix} \tag{4.41}$$

where $A_{322} \in \mathbb{R}^{k \times k}$ is full rank and X is orthogonal.

Then partition generally

$$A_{31} = X \begin{bmatrix} A_{311} \\ A_{312} \end{bmatrix} \begin{matrix} \updownarrow p-q-2k \\ \updownarrow k \end{matrix} \tag{4.42}$$

where A_{311} and A_{312} have no specific structure.

Pre-multiply $E_{a,2}(s)$ with an invertible matrix T_z where

$$T_z = \begin{bmatrix} I & -A_{12}A_{32}^{\dagger} \\ 0 & I \end{bmatrix}$$

results in

$$E_{a,3}(s) := T_z E_{a,2}(s) = \begin{bmatrix} sI - (A_{11} - A_{12}A_{32}^{\dagger}A_{31}) & 0 \\ -A_{31} & -A_{32} \end{bmatrix} \tag{4.43}$$

Substitute from (4.41) and (4.42) into (4.43) results in

$$E_{a,3}(s) = \left[\begin{array}{c|c} I & 0 \\ \hline 0 & X \end{array}\right] \left[\begin{array}{cc} sI - (A_{11} - A_{12}A_{32}^{\dagger}A_{31}) & 0 \\ \hline -A_{311} & 0 \\ -A_{312} & -A_{322} \end{array}\right] \tag{4.44}$$

and hence the invariant zeros of $\left(A, \left[\begin{array}{cc} M & Q \end{array}\right], C\right)$ are the unobservable modes of $(A_{11} - A_{12}A_{32}^{\dagger}A_{31}, A_{311})$.

An appropriate choice of $A_{32}^{\dagger}$ is

$$A_{32}^{\dagger} = \left[\begin{array}{cc} 0 & A_{322}^{-1} \end{array}\right] X^T \tag{4.45}$$

Hence it can be shown that

$$(I - A_{32}A_{32}^{\dagger})A_{31} = X \left[\begin{array}{c} A_{311} \\ 0 \end{array}\right] \tag{4.46}$$

Following that, using the Popov-Hautus-Rosenbrock (PHR) rank test by Rosenbrock [157], the unobservable modes of $(A_{11} - A_{12}A_{32}^{\dagger}A_{31}, (I - A_{32}A_{32}^{\dagger})A_{31})$ are given by the values of s that make the following matrix pencil loses rank

$$E_{b,1}(s) = \left[\begin{array}{c|c} I & 0 \\ \hline 0 & X \end{array}\right] \left[\begin{array}{c} sI - (A_{11} - A_{12}A_{32}^{\dagger}A_{31}) \\ \hline -A_{311} \\ 0 \end{array}\right] \tag{4.47}$$

and it can be shown that the unobservable modes of $(A_{11} - A_{12}A_{32}^{\dagger}A_{31}, (I - A_{32}A_{32}^{\dagger})A_{31})$ are the invariant zeros of $(A, \left[\begin{array}{cc} M & Q \end{array}\right], C)$ and the proof is complete. ■

Proposition 4.2 corresponds to condition C4 guaranteeing a stable sliding motion and Theorem 1 is proven. □

Remark 4.2 *Condition C1 ensures that the observer is able to reconstruct the fault. Subject to the satisfaction of C1, conditions C2 - C3 ensure that the fault reconstruction is totally decoupled from the disturbances. Finally, subject to C1 - C3 being satisfied, condition C4 ensures the existence of a stable sliding motion.* ♯

Remark 4.3 *In Remark 3.6 from [56], Edwards & Tan provided an example where (4.3) is not satisfied but it is still possible to achieve DDFR. In their example, the following system matrices were obtained after the coordinate transformation in Proposition 4.1*

$$A = \begin{bmatrix} -1 & 1 & 0 \\ 1 & 2 & 1 \\ 0 & 1 & 1 \end{bmatrix}, \; Q = \begin{bmatrix} 1 \\ 0 \\ 0 \end{bmatrix}, \; C = \begin{bmatrix} 0 & 1 & 0 \\ 0 & 0 & 1 \end{bmatrix}, \; M = \begin{bmatrix} 0 \\ 0 \\ 1 \end{bmatrix}$$

It can be verified that C1 - C4 are satisfied for the example. ♯

Remark 4.4 *Note that C1 - C3 are less conservative than (4.3), and hence the construction proposed in this chapter can be applied to a wider class of systems. Equation (4.3) requires that $Q_a = \emptyset$ (empty matrix), whereas from the results in this chapter, conditions C1 - C4 do not require $Q_a = \emptyset$.* ♯

Remark 4.5 *There have been efforts to generate disturbance decoupled fault detection residuals using linear observers, for example Patton & Chen [150] as well as Xiong & Saif [206] which utilise eigenstructure assignment and the 'special coordinate basis'. However, from detailed examination of the methods by Patton & Chen [150] and Xiong & Saif [206] (as has been done by Tan* et al. *[181] and equation (13) of the work in Xiong & Saif [206]), it can be seen that certain elements of the matrix A are required to be zero. From the analysis in this chapter, no such condition is required; the only requirement on the matrix A is that A_{32} has full column rank. Hence, this chapter has also shown how the conditions for DDFR using sliding mode observers are less stringent than methods involving linear observers.* ♯

4.4 An Example

The results in this chapter will now be demonstrated using an 8th order aircraft system taken from Heck *et al.* [85]. In the notation of (4.1) - (4.2), the system matrix is

$$A = \begin{bmatrix} 0 & 0 & 1.0000 & 0 & 0 & 0 & 0 & 0 \\ 0 & -0.1540 & -0.0042 & 1.5400 & 0 & -0.7440 & -0.0320 & 0 \\ 0 & 0.2490 & -1.0000 & -5.2000 & 0 & 0.3370 & -1.1200 & 0 \\ 0.0386 & -0.9960 & -0.0003 & -2.1170 & 0 & 0.0200 & 0 & 0 \\ 0 & 0.5000 & 0 & 0 & -4.0000 & 0 & 0 & 0 \\ 0 & 0 & 0 & 0 & 0 & -20.0000 & 0 & 0 \\ 0 & 0 & 0 & 0 & 0 & 0 & -25.0000 & 0 \\ 0 & 1.0000 & 0 & 0 & 0 & 0 & 0 & 0 \end{bmatrix}$$

where the states, control inputs and outputs are

$$x = \begin{bmatrix} \text{bank angle} \\ \text{yaw rate} \\ \text{roll rate} \\ \text{sideslip angle} \\ \text{washed-out filter state} \\ \text{rudder deflection} \\ \text{aileron deflection} \\ \text{yaw angle} \end{bmatrix}, \quad u = \begin{bmatrix} \text{rudder command} \\ \text{aileron command} \end{bmatrix}$$

$$y = \begin{bmatrix} \text{bank angle} \\ \text{sideslip angle} \\ \text{rudder deflection} \\ \text{aileron deflection} \\ \text{yaw angle} \end{bmatrix}$$

Assume that both inputs are potentially faulty. Thus, the matrices B, M and C are

$$B = M = \begin{bmatrix} 0 & 0 \\ 0 & 0 \\ 0 & 0 \\ 0 & 0 \\ 0 & 0 \\ 20 & 0 \\ 0 & 25 \\ 0 & 0 \end{bmatrix}, \quad C = \begin{bmatrix} 1 & 0 & 0 & 0 & 0 & 0 & 0 & 0 \\ 0 & 0 & 0 & 1 & 0 & 0 & 0 & 0 \\ 0 & 0 & 0 & 0 & 0 & 1 & 0 & 0 \\ 0 & 0 & 0 & 0 & 0 & 0 & 1 & 0 \\ 0 & 0 & 0 & 0 & 0 & 0 & 0 & 1 \end{bmatrix}$$

Suppose that matrix A is imprecisely known and that there exists parametric uncertainty. The state equation becomes

$$\dot{x} = (A + \Delta A)x + Bu + Mf \tag{4.48}$$

where ΔA is the discrepancy between the known matrix A and its actual value. Suppose the actual value of the system matrix is given by

$$A + \Delta A = \begin{bmatrix} 0 & 0 & 1.0000 & 0 & 0 & 0 & 0 & 0 \\ 0 & -0.1600 & -0.0042 & 1.6600 & 0 & -0.7440 & -0.0500 & 0 \\ 0 & 0.2490 & -1.0000 & -5.1600 & 0 & 0.4000 & -1.2400 & 0 \\ 0.0386 & -0.9960 & -0.0003 & -2.2300 & 0 & 0.0230 & 0 & 0 \\ 0 & 0.5000 & 0 & 0 & -4.0000 & 0 & 0 & 0 \\ 0 & 0 & 0 & 0 & 0 & -20.0000 & 0 & 0 \\ 0 & 0 & 0 & 0 & 0 & 0 & -25.0000 & 0 \\ 0 & 1.0000 & 0 & 0 & 0 & 0 & 0 & 0 \end{bmatrix}$$

By inspection, only rows 2 to 4 in matrix A have uncertainties, and the other rows are certain due to the nature of the state equations. Writing (4.48) in the framework of (4.1) -

(4.2) yields

$$\Delta Ax = Q\xi = \underbrace{\begin{bmatrix} 0 & 0 & 0 \\ 1 & 0 & 0 \\ 0 & 1 & 0 \\ 0 & 0 & 1 \\ 0 & 0 & 0 \\ 0 & 0 & 0 \\ 0 & 0 & 0 \\ 0 & 0 & 0 \end{bmatrix}}_{Q} \underbrace{\begin{bmatrix} 0 & -0.0060 & 0 & 0.1200 & 0 & 0 & -0.0180 & 0 \\ 0 & 0 & 0 & 0.0400 & 0 & 0.0630 & -0.1200 & 0 \\ 0 & 0 & 0 & -0.1130 & 0 & 0.0030 & 0 & 0 \end{bmatrix}}_{\xi} x$$

Performing the coordinate transformation in Proposition 4.1 yields the following matrices

$$T_1 = \begin{bmatrix} 0 & 1 & 0 \\ 1 & 0 & 0 \\ 0 & 0 & 1 \end{bmatrix}, T_2 = \begin{bmatrix} 0 & 0 & 1 & 0 & 0 & 0 & 0 & 0 \\ 0 & 1 & 0 & 0 & 0 & 0 & 0 & 0 \\ 1 & 0 & 0 & 0 & 0 & 0 & 0 & 0 \\ 0 & 0 & 0 & 0 & 0 & 1 & 0 & 0 \\ 0 & 0 & 0 & 1 & 0 & 0 & 0 & 0 \\ 0 & 0 & 0 & 0 & 1 & 0 & 0 & 0 \\ 0 & 0 & 0 & 0 & 0 & 0 & 1 & 0 \\ 0 & 0 & 0 & 0 & 0 & 0 & 0 & 1 \end{bmatrix}, C_2 = \begin{bmatrix} 1 & 0 & 0 & 0 & 0 \\ 0 & 0 & 1 & 0 & 0 \\ 0 & 0 & 0 & 0 & 1 \\ 0 & 0 & 0 & 1 & 0 \\ 0 & 1 & 0 & 0 & 0 \end{bmatrix}$$

which gives

$$M_o = \begin{bmatrix} 0 & 25 \\ 20 & 0 \end{bmatrix}, \bar{Q}_1 = \begin{bmatrix} 0 & 1 \\ 1 & 0 \end{bmatrix}, \bar{Q}_2 = 1$$

with

$$A = \begin{bmatrix} -4.0000 & 0.5000 & 0 & 0 & 0 & 0 & 0 & 0 \\ 0 & -0.1540 & -0.0042 & 0 & 0 & 1.5400 & -0.0320 & -0.7440 \\ 0 & 0.2490 & -1.0000 & 0 & 0 & -5.2000 & -1.1200 & 0.3370 \\ 0 & 0 & 1.0000 & 0 & 0 & 0 & 0 & 0 \\ 0 & 1.0000 & 0 & 0 & 0 & 0 & 0 & 0 \\ 0 & -0.9960 & -0.0003 & 0.0386 & 0 & -2.1170 & 0 & 0.0200 \\ 0 & 0 & 0 & 0 & 0 & 0 & -25.0000 & 0 \\ 0 & 0 & 0 & 0 & 0 & 0 & 0 & -20.0000 \end{bmatrix}$$

It can be shown that conditions C1 - C4 are satisfied, hence it is possible to obtain DDFR. Since $rank(Q) = 3$, $rank(M) = 2$ and $rank(CQ) < rank(Q)$, equation (4.3) is not satisfied and it is not possible to reconstruct ξ.

4.4.1 Observer Design

After attaining the structure in (4.5), it can be shown that $A_{36} = 0$ and $I - A_{32}A_{32}^{\dagger} = 0$, which from (4.30) leads to $W_{12} = 0$. Substituting $W_{12} = 0$ into (4.19), yields $W_1 = 0$.

Since $I - A_{32}A_{32}^{\dagger} = 0$, from (4.37), $\hat{A}_1$ is independent of L and as a result, it can easily be shown that $\lambda(A_{11} - A_{12}A_{32}^{\dagger}A_{31}) = -4$.

Choosing $L_{21} = \begin{bmatrix} -1 & -1 \\ -1 & -1 \end{bmatrix}$ means $\lambda(A_{14} + L_{21}A_{32} + L_{22}A_{34}) = \{-2.5430 \quad -0.6110\}$.

Once L has been obtained, a suitable choice for G_l (in the original system coordinates of

(4.1) - (4.2)) and a P_o that satisfies Proposition 3.1 are

$$G_l = \begin{bmatrix} 0 & 0 & -19.0000 & 0 & 0 \\ -6.5090 & -17.5402 & -0.7440 & -0.0320 & 15.8779 \\ 9.3639 & 0.1599 & 0 & 0 & -0.9352 \\ -0.8084 & -2.4510 & 0 & 0 & 2.0454 \\ 14.1435 & -4.1329 & 0.3370 & -1.1200 & -2.8309 \\ -1.2330 & -3.3490 & 0 & 0 & 8.8624 \\ 0 & 0 & 0 & -23.0000 & 0 \\ 0.9517 & 7.5027 & 0.0200 & 0 & -2.7869 \end{bmatrix}$$

$$P_o = I_5$$

The gain associated with the nonlinear injection G_n in the original system coordinates of (4.1) - (4.2) can be easily computed as

$$G_n = \begin{bmatrix} 0 & 1.0000 & 0 & 0 & 0 \\ 1.0000 & 0 & 0 & 0 & 1.0000 \\ 0 & 0 & 0 & 0 & 0.5000 \\ 0 & 0 & 0 & 0 & 1.0000 \\ 1.0000 & 0 & 0 & 0 & 1.0000 \\ 0 & 0 & 1.0000 & 0 & 0 \\ 0 & 0 & 0 & 1.0000 & 0 \\ 1.0000 & 0 & 0 & 0 & 0 \end{bmatrix}$$

4.4.2 Simulation Results

In the following simulation, the upper bound of the magnitude of the fault and the disturbance associated with the nonlinear discontinuous term ν in (3.34) is set to $\rho = 80$ while the positive scalar $\delta = 0.001$. Faults have been induced in both the actuators, hence $x \neq 0 \Rightarrow \Delta A x \equiv Q\xi \neq 0 \Rightarrow \xi \neq 0$, as shown in Figure 4.1. Figure 4.2 shows the faults

and their reconstructions. It can be seen that the reconstruction signal $\hat{f}$ provides accurate estimates of f that are independent of ξ without attempting to reconstruct ξ.

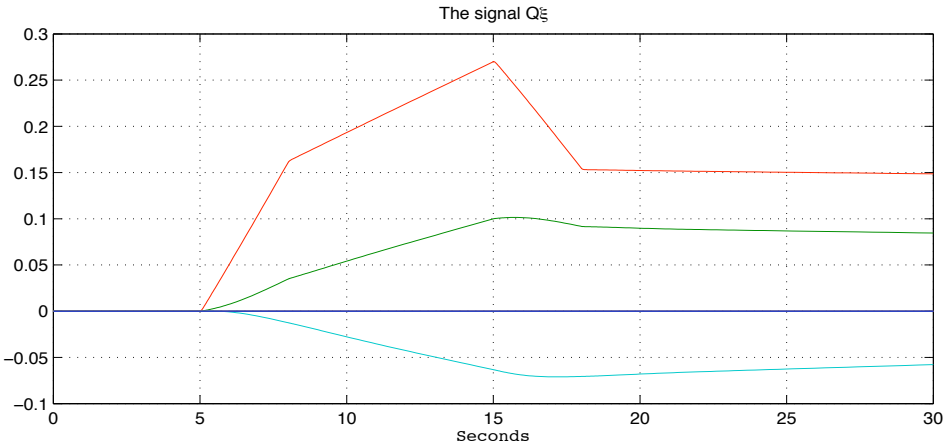

Figure 4.1: The figure shows the discrepancy/disturbance $\Delta Ax \neq 0$ acting onto the system.

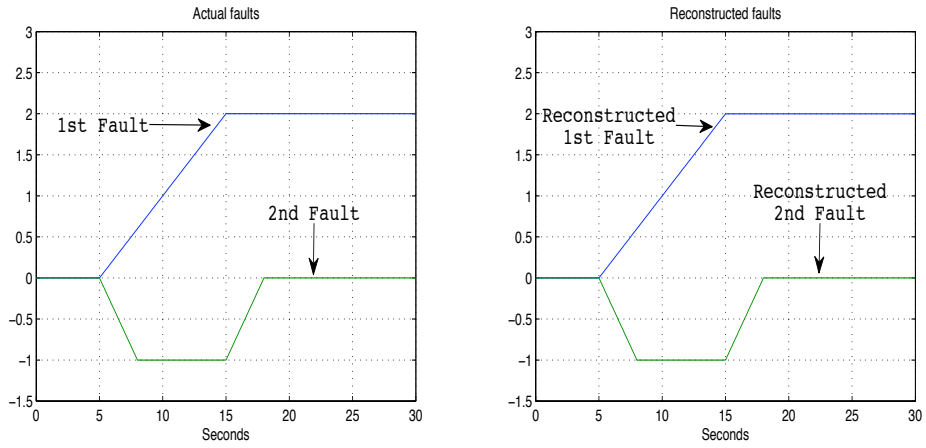

Figure 4.2: The left subfigure shows the faults, the right subfigure shows the reconstruction of the faults.

4.5 Conclusion

This chapter has investigated and presented conditions that guarantee DDFR using sliding mode observers [52], and it was found that these conditions are easily testable in terms of the original system matrices. The effects of the disturbances on the fault reconstruction were only minimised in previous work done by Tan & Edwards [177], and the conditions that guarantee disturbance decoupling were not known. Other work has achieved DDFR by reconstructing the disturbances and faults, as shown by Saif & Guan [158], but this

method requires more stringent conditions to be fulfilled. The conditions investigated in this chapter are weaker and proved that disturbance reconstruction is *not required* for robust fault reconstruction. An aircraft model has been used to validate the results.

Chapter 5

Disturbance Decoupled Sensor Fault Reconstruction

5.1 Introduction

Chapter 4 has presented the conditions that guarantee DDFR where the sliding mode observer was designed such that the fault reconstruction is robust towards the disturbances. This result was built on the work done by Tan & Edwards [177] where the effects of the disturbances on the fault reconstruction were only minimised, not fully decoupled or rejected.

Later, the work on actuator fault reconstruction has been extended to be used for sensor fault reconstruction as done in Section 5 of Tan & Edwards [177]. In general, sensor faults do not affect the process of the system directly. However, given a closed loop system where the sensors are used for feedback, the presence of sensor faults will affect the performance of the system as shown in the figure below

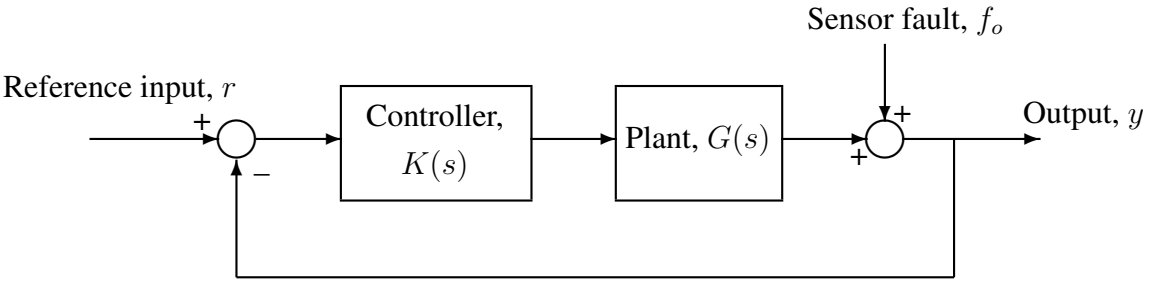

Figure 5.1: Schematic showing the presence of sensor fault in a closed-loop system

There have been some work done on sensor fault reconstruction, particularly by Chen & Speyer [21], Sreedhar *et al.* [168] and also Tan *et al.* [175, 181, 182, 183, 180]. However, their work could only reduce the effects of the disturbances on the fault reconstruction, which shared similar concept with the method shown by Tan & Edwards [177].

Tan *et al.* [57, 179, 184] have shown that a good sensor fault reconstruction scheme can be used to perform fault tolerant control. Therefore, it can be seen that should the sensor fault reconstruction scheme be completely robust towards the disturbances, a fault tolerant control scheme could then be designed such that the effects of the disturbances on the fault reconstruction are no longer minimised, but are entirely rejected and decoupled. As a result, the system is able to continue operating as efficiently as it being in a fault-free scenario.

As for the work to be presented in this chapter, it seeks to extend the results in Chapter 4 such that the conditions that guarantee DDFR for sensor faults are investigated. Generally, the work of Tan & Edwards [177] will be used to convert the sensor fault problem into an actuator fault problem, and then the work in Chapter 4 will be applied to investigate the conditions that guarantee DDFR for sensor faults.

5.2 Preliminaries and Problem Statement

Consider the following system

$$\dot{x}_s = A_s x_s + Q_s \xi_s \tag{5.1}$$

$$y_s = C_s x_s + N_s f_s \tag{5.2}$$

where $x_s \in \mathbb{R}^n, y_s \in \mathbb{R}^p, f_s \in \mathbb{R}^q, \xi_s \in \mathbb{R}^h$ are the states, outputs, unknown faults and unknown disturbances respectively. Assume without loss of generality that $rank(N_s) = q, rank(Q_s) = h$ and $rank(C_s) = p$. Futher assume that $p > q$, which implies that some sensors are not faulty. The main objective is to reconstruct the fault f_s while rejecting the effects of the disturbances ξ_s.

Let there exist an orthogonal matrix T_r such that

$$T_r C_s = \begin{bmatrix} C_{s,1} \\ C_{s,2} \end{bmatrix}, \quad T_r N = \begin{bmatrix} N_{s,o} \\ 0 \\ \underset{q}{\longleftrightarrow} \end{bmatrix} \begin{matrix} \updownarrow q \\ \updownarrow p-q \end{matrix} \tag{5.3}$$

where $N_{s,o}$ is square and invertible. The partitions of $C_{s,1}$ and $C_{s,2}$ have no particular structure.

Define

$$k_s = rank(C_{s,2}Q_s) \tag{5.4}$$

where $k_s \leq h$ and $\tilde{y}_s := T_r y_s$.

Therefore, the output of the system after being scaled by T_r can be written as

$$\tilde{y}_s = \begin{bmatrix} C_{s,1} \\ C_{s,2} \end{bmatrix} x_s + \begin{bmatrix} N_{s,o} \\ 0 \end{bmatrix} f_s \tag{5.5}$$

and as a result, it can be partitioned into faulty output and fault-free output where

$$\tilde{y}_{s,1} = C_{s,1}x_s + N_{s,o}f_s \tag{5.6}$$

$$\tilde{y}_{s,2} = C_{s,2}x_s \tag{5.7}$$

where $\tilde{y}_{s,1}$ represents the faulty output and $\tilde{y}_{s,2}$ represents the fault-free output.

Consider a new state $z_s \in \mathbb{R}^q$ that is a filtered version of $\tilde{y}_{s,1}$ satisfying

$$\dot{z}_s = -A_{s,f}z_s + A_{s,f}\tilde{y}_{s,1} \tag{5.8}$$

and substituting from (5.6) into (5.8) yields

$$\dot{z}_s = -A_{s,f}z_s + A_{s,f}C_{s,1}x_s + A_{s,f}N_{s,o}f_s \tag{5.9}$$

where $-A_{s,f} \in \mathbb{R}^{q\times q}$ is a stable filter matrix.

Equations (5.1) and (5.9) can then be combined to form an augmented state-space system of

order $n+q$

$$\underbrace{\begin{bmatrix}\dot{x}\\ \dot{z}\end{bmatrix}}_{\dot{\tilde{x}}} = \underbrace{\begin{bmatrix}A_s & 0\\ A_{s,f}C_{s,1} & -A_{s,f}\end{bmatrix}}_{\tilde{A}}\underbrace{\begin{bmatrix}x_s\\ z_s\end{bmatrix}}_{\tilde{x}} + \underbrace{\begin{bmatrix}0\\ A_{s,f}N_{s,o}\end{bmatrix}}_{\tilde{M}} f_s + \underbrace{\begin{bmatrix}Q_s\\ 0\end{bmatrix}}_{\tilde{Q}}\xi_s \tag{5.10}$$

$$\underbrace{\begin{bmatrix}\tilde{y}_{s,2}\\ z_s\end{bmatrix}}_{\tilde{y}} = \underbrace{\begin{bmatrix}C_{s,2} & 0\\ 0 & I_q\end{bmatrix}}_{\tilde{C}}\begin{bmatrix}x_s\\ z_s\end{bmatrix} \tag{5.11}$$

The equations (5.10) - (5.11) are now in the form of (4.1) - (4.2) which represents a system with the actuator fault f_s and therefore a sliding mode observer can be designed using the method discussed in Section 4 to reconstruct f_s while rejecting the effect of ξ_s.

As in Tan & Edwards [177], the sensor fault has been transformed to be an 'actuator' fault. The figure below shows the schematic to obtain the signal $\tilde{y}$.

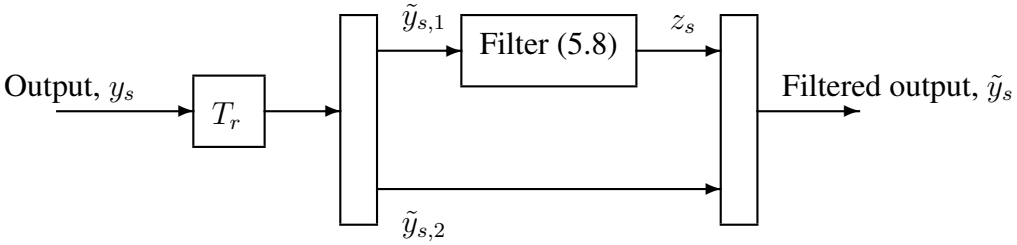

Figure 5.2: The schematic to obtain $\tilde{y}$

5.3 Disturbance Decoupled Sensor Fault Reconstruction

Proposition 5.1 *Let there exists a change of coordinates where the states x and disturbances ξ_s are transformed such that A_s, Q_s and $C_{s,2}$ can be transformed to have the following structure*

$$A_s = \left[\begin{array}{cc|c} A_{s,11} & A_{s,12} & * \\ A_{s,21} & A_{s,22} & * \\ \hline A_{s,31} & A_{s,32} & * \\ A_{s,41} & A_{s,42} & * \end{array}\right], \quad Q_s = \begin{array}{c} \left[\begin{array}{cc} 0 & 0 \\ \bar{Q}_{s,1} & 0 \\ \hline 0 & 0 \\ 0 & \bar{Q}_{s,2} \end{array}\right] \\ \overbrace{\qquad}^{h-k_s} \quad \overbrace{\qquad}^{k_s} \end{array} \begin{array}{l} \updownarrow n-p-h+k_s+q \\ \updownarrow h-k_s \\ \updownarrow p-q-k_s \\ \updownarrow k_s \end{array} \tag{5.12}$$

$$C_{s,2} = \begin{array}{c} \left[\begin{array}{ccc|c} 0 & 0 & & T \end{array}\right] \\ \underbrace{\qquad}_{n-p-h+k_s+q} \quad \underbrace{\qquad}_{h-k_s} \quad \underbrace{\qquad}_{p-q} \end{array} \updownarrow p-q \tag{5.13}$$

where $T, \bar{Q}_{s,1}$ and $\bar{Q}_{s,2}$ are square and invertible and (*) are matrices that do not play any role in the subsequent analysis while $C_{s,1}$ (partitioned conformably with $C_{s,2}$ in (5.13)) has a general structure of

$$C_{s,1} = \left[\begin{array}{ccc} C_{s,11} & C_{s,12} & C_{s,13} \end{array}\right] \tag{5.14}$$

Proof

The ideas used in this proof were taken from Tan *et al.* [180]. Without loss of generality, the states can be re-ordered such that the matrices $Q_s, C_{s,2}$ can be re-written as

$$Q_s = \left[\begin{array}{c} Q_{s,1} \\ Q_{s,2} \end{array}\right] \begin{array}{l} \updownarrow n-p+q \\ \updownarrow p-q \end{array}, \quad C_{s,2} = \left[\begin{array}{ccc} 0 & 0 & I_{p-q} \end{array}\right] \tag{5.15}$$

From (5.15) it is clear that $C_{s,2}Q_s = Q_{s,2}$ and from (5.4) it follows that $rank(Q_{s,2}) = k_s$ and there exists orthogonal matrices $T, R_{1,s}$ such that

$$T^T Q_{s,2} R_{1,s}^T = \left[\begin{array}{cc} 0 & 0 \\ 0 & \bar{Q}_{s,2} \end{array}\right]$$

where $\bar{Q}_{s,2} \in \mathbb{R}^{k \times k}$ is invertible. Then, partition $Q_{s,1}R_{1,s}^T = \left[\begin{array}{cc} Q_{s,11} & Q_{s,12} \end{array}\right]$ where $Q_{s,12}$

has k_s columns. Then, let $R_{2,s}$ be an orthogonal matrix such that $R_{2,s}Q_{s,11} = \begin{bmatrix} 0 \\ \bar{Q}_{s,1} \end{bmatrix}$ where $\bar{Q}_{s,1} \in \mathbb{R}^{(h-k_s)\times(h-k_s)}$ is invertible and define $R_{3,s} = \begin{bmatrix} 0 & -R_{2,s}Q_{s,12}\bar{Q}_{s,2}^{-1} \end{bmatrix} T^T$. Then, apply the change of coordinates $x_s \mapsto T_s x_s,\ \ \xi_s \mapsto R_{1,s}^{-1}\xi_s$ where

$$T_s = \begin{bmatrix} R_{2,s} & R_{3,s} \\ 0 & T^T \end{bmatrix}$$

The disturbance and output matrices are transformed to be

$$Q_s \mapsto T_s Q_s R_{1,s} = \begin{bmatrix} 0 & 0 \\ \bar{Q}_{s,1} & 0 \\ 0 & 0 \\ 0 & \bar{Q}_{s,2} \end{bmatrix},\ \ C_{s,2} \mapsto C_{s,2}T_s^{-1} = \begin{bmatrix} 0 & T \end{bmatrix}$$

As for the matrix A_s, it has no particular structure as shown in (5.12). ■

By substituting (5.12) - (5.13) into (5.10) - (5.11), it can be seen now that the system $(\tilde{A}, \tilde{M}, \tilde{Q}, \tilde{C})$ has the same form as the system shown in Proposition 4.1 via (4.5) - (4.6), in particular the matrices $\tilde{M}, \tilde{Q}$ and $\tilde{C}$ as shown below

$$\tilde{A} = \begin{bmatrix} A_{s,11} & A_{s,12} & * & 0 \\ A_{s,21} & A_{s,22} & * & 0 \\ A_{s,31} & A_{s,32} & * & 0 \\ A_{s,41} & A_{s,42} & * & 0 \\ A_{s,f}C_{s,11} & A_{s,f}C_{s,12} & A_{s,f}C_{s,13} & -A_{s,f} \end{bmatrix},\ \ \tilde{M} = \begin{bmatrix} 0 \\ 0 \\ 0 \\ 0 \\ A_{s,f}N_{s,o} \end{bmatrix} \tag{5.16}$$

$$\tilde{Q} = \begin{bmatrix} 0 & 0 \\ \bar{Q}_{s,1} & 0 \\ 0 & 0 \\ 0 & \bar{Q}_{s,2} \\ 0 & 0 \end{bmatrix}, \quad \tilde{C} = \begin{bmatrix} 0 & 0 & T & 0 \\ 0 & 0 & 0 & I_q \end{bmatrix} \tag{5.17}$$

Notice that by construction, conditions C1 - C2 when applied to the matrices in (5.16) - (5.17) will always be satisfied. It can be seen from Theorem 4.1 which has presented that in order for the fault reconstruction error $e_{s,f}$ to be decoupled from the disturbance ξ_s (DDFR is achieved), condition C3 has to be satisfied. By comparing (5.16) - (5.17) with (4.5) - (4.6), it is clear that $A_{s,32}$ in (5.16) - (5.17) is equivalent to A_{32} in (4.22). And this will lead to Lemma 4.2 which proved that the matrix $A_{s,32}$ has to be full rank in order for condition C3 to be true. Therefore, in the structure of the matrices in (5.16) - (5.17), the fault reconstruction error $e_{s,f}$ will be decoupled from the disturbance ξ (and DDFR is achieved) by an appropriate choice of $L_{s,o}$ and $W_{s,1}$ if the following conditions are satisfied

D1. $rank \begin{bmatrix} \tilde{C}\tilde{A}\tilde{Q} & \tilde{C}\tilde{Q} & \tilde{C}\tilde{M} \\ \tilde{C}\tilde{Q} & 0 & 0 \end{bmatrix} = rank(\tilde{Q}) + rank(\tilde{M}) + rank(\tilde{C}\tilde{Q})$

D2. $\left(\tilde{A}, \begin{bmatrix} \tilde{M} & \tilde{Q} \end{bmatrix}, \tilde{C}\right)$ is minimum phase. □

As a result, if $A_{s,32}$ is full rank, then DDFR can be achieved.

Lemma 5.1 *The matrix $A_{s,32}$ is full column rank $(h - k_s)$ if and only if*

$$rank \begin{bmatrix} C_s A_s Q_s & C_s Q_s & N_s & 0 \\ C_s Q_s & 0 & 0 & N_s \end{bmatrix} = rank(Q_s) + rank(N_s) + rank\left(\begin{bmatrix} C_s Q_s & N_s \end{bmatrix}\right) \tag{5.18}$$

♯

Proof

From the partitions in (5.12) - (5.13), it can be shown that

$$T_r C_s A_s Q_s = \begin{bmatrix} I_q & 0 \\ 0 & T \end{bmatrix} \left[\begin{array}{c|c} * & * \\ \hline A_{s,32} & * \\ A_{s,42} & * \end{array}\right] \begin{bmatrix} \bar{Q}_{s,1} & 0 \\ 0 & I_{k_s} \end{bmatrix} \tag{5.19}$$

It can then be shown that

$$\begin{bmatrix} T_r & 0 \\ 0 & T_r \end{bmatrix} \begin{bmatrix} C_s A_s Q_s & C_s Q_s & N_s & 0 \\ C_s Q_s & 0 & 0 & N_s \end{bmatrix} = \begin{bmatrix} I_q & 0 & 0 & 0 \\ 0 & T & 0 & 0 \\ 0 & 0 & I_q & 0 \\ 0 & 0 & 0 & T \end{bmatrix} \left[\begin{array}{c|cccc|c} * & * & * & * & N_{s,o} & 0 \\ \hline A_{s,32} & * & 0 & 0 & 0 & 0 \\ A_{s,42} & * & 0 & \bar{Q}_{s,2} & 0 & 0 \\ \hline * & * & 0 & 0 & 0 & N_{s,o} \\ \hline 0 & 0 & 0 & 0 & 0 & 0 \\ 0 & \bar{Q}_{s,2} & 0 & 0 & 0 & 0 \end{array}\right] \begin{bmatrix} \bar{Q}_{s,1} & 0 \\ 0 & I_{h+k_s+2q} \end{bmatrix} \tag{5.20}$$

where (*) are matrices that play no role in the subsequent analysis.

Since $T, N_{s,o}, \bar{Q}_{s,1}$ and $\bar{Q}_{s,2}$ are square and invertible and it can be seen that $rank(\bar{Q}_{s,2}) + rank(N_{s,o}) = rank\left(\begin{bmatrix} C_s Q_s & N_s \end{bmatrix}\right)$, it results in

$$\begin{aligned} rank\left(\begin{bmatrix} C_s A_s Q_s & C_s Q_s & N_s & 0 \\ C_s Q_s & 0 & 0 & N_s \end{bmatrix}\right) &= rank(A_{s,32}) + 2rank(\bar{Q}_{s,2}) + 2rank(N_{s,o}) \\ &= rank(A_{s,32}) + 2rank\left(\begin{bmatrix} C_s Q_s & N_s \end{bmatrix}\right) \end{aligned} \tag{5.21}$$

and therefore

$$rank(A_{s,32}) = rank\left(\begin{bmatrix} C_s A_s Q_s & C_s Q_s & N_s & 0 \\ C_s Q_s & 0 & 0 & N_s \end{bmatrix}\right) - 2rank\left(\begin{bmatrix} C_s Q_s & N_s \end{bmatrix}\right) \tag{5.22}$$

It is obvious that

$$rank(Q_s) - rank\left(\begin{bmatrix} C_sQ_s & N_s \end{bmatrix}\right) + rank(N_s) = h - k_s \tag{5.23}$$

It is clear that $rank(A_{s,32}) = h - k_s$ is satisfied if and only if (5.22) and (5.23) are equivalent to (5.18), and the proof is complete. ■

Lemma 5.2 *The invariant zeros of* $\left(\tilde{A}, \begin{bmatrix} \tilde{M} & \tilde{Q} \end{bmatrix}, \tilde{C}\right)$ *are identical to the invariant zeros of* $\left(A_s, \begin{bmatrix} Q_s & 0 \end{bmatrix}, C_s, \begin{bmatrix} 0 & N_s \end{bmatrix}\right)$. ♯

Proof

The Rosenbrock system matrix of $\left(\tilde{A}, \begin{bmatrix} \tilde{M} & \tilde{Q} \end{bmatrix}, \tilde{C}\right)$ is given by

$$E_{a,1}(s) := \begin{bmatrix} sI - \tilde{A} & \tilde{M} & \tilde{Q} \\ \tilde{C} & 0 & 0 \end{bmatrix}$$

and the invariant zeros of a system are the values of s that cause its Rosenbrock matrix to lose normal rank. From (5.10) - (5.11), $E_{a,1}(s)$ can be expanded to be

$$E_{a,1}(s) = \begin{bmatrix} sI - A_s & 0 & 0 & Q_s \\ -A_{s,f}C_{s,1} & sI + A_{s,f} & A_{s,f}N_{s,o} & 0 \\ C_{s,2} & 0 & 0 & 0 \\ 0 & I_q & 0 & 0 \end{bmatrix}$$

Since $A_{s,f}$ and $N_{s,o}$ are full rank, it is clear that $E_{a,1}(s)$ loses rank if and only if the following matrix loses rank

$$E_{a,2}(s) := \begin{bmatrix} sI - A_s & Q_s \\ C_{s,2} & 0 \end{bmatrix}$$

Hence, the values of s that make $E_{a,2}(s)$ loses rank are the invariant zeros of $(A_s, Q_s, C_{s,2})$. The invariant zeros of $\left(A_s, \begin{bmatrix} Q_s & 0 \end{bmatrix}, C_s, \begin{bmatrix} 0 & N_s \end{bmatrix}\right)$ are given by the values of s that

cause the following matrix to lose rank

$$E_{b,1}(s) := \begin{bmatrix} sI - A_s & Q_s & 0 \\ C_s & 0 & N_s \end{bmatrix}$$

Expanding C_s and N_s according to the structure obtained in (5.3), $E_{b,1}(s)$ can be written as

$$E_{b,1}(s) = \begin{bmatrix} sI - A_s & Q_s & 0 \\ C_{s,1} & 0 & N_{s,o} \\ C_{s,2} & 0 & 0 \end{bmatrix}$$

Since $N_{s,o}$ is square and invertible, then it can be seen that $E_{b,1}(s)$ loses rank if and only if $E_{b,2}(s)$ loses rank where

$$E_{b,2}(s) := \begin{bmatrix} sI - A_s & Q_s \\ C_{s,2} & 0 \end{bmatrix}$$

which loses rank if and only if s is an unobservable mode of $(A_s, Q_s, C_{s,2})$.

Hence, this has proven that the invariant zeros of $\left(\tilde{A}, \begin{bmatrix} \tilde{M} & \tilde{Q} \end{bmatrix}, \tilde{C}\right)$ are the invariant zeros of (A_s, Q_s, C_s, N_s). ■

5.4 An Example

The results proposed in this chapter will now be demonstrated using a double inverted pendulum system where its nonlinear equations can be expressed as

$$\ddot{x}_c = \frac{F + 0.1436\left(\dot{\theta}_1^2 \sin\theta_1 - \ddot{\theta}_1 \cos\theta_1\right) + 0.0136\left((\dot{\theta}_1+\dot{\theta}_2)^2 \sin(\theta_1+\theta_2) - (\ddot{\theta}_1+\ddot{\theta}_2)\cos(\theta_1+\theta_2)\right)}{1.051}$$

$$\ddot{\theta}_1 = \frac{0.0057\left((\dot{\theta}_1 + \dot{\theta}_2)^2 \sin\theta_2 - \ddot{\theta}_2 \cos\theta_2\right) + 1.4086\ \sin\theta_1 - 0.1436\ \ddot{x}_c \cos\theta_1}{0.0867 + 0.0057\ \cos\theta_2}$$

$$\ddot{\theta}_2 = \frac{0.1339\ \sin(\theta_1 + \theta_2) - 0.0136\ \ddot{x}_c \cos(\theta_1 + \theta_2) - 0.0057\ \dot{\theta}_1^2 \sin\theta_2 - 0.0063\ \ddot{\theta}_1}{0.0063 + 0.0057\ \cos\theta_2}$$

where x_c, θ_1 and θ_2 represent the position of the mechanical cart on the rail, the angular displacement of the first rod and the angular displacement of the second rod respectively. The parameter F would be the force applied to the mechanical cart.

In order to design a state-feedback controller using the state space approach to stabilise the pendulum with both rods at the vertical position and then ultimately to design a DDFR scheme for the system, the nonlinear equations of $\ddot{x}_c, \ddot{\theta}_1$ and $\ddot{\theta}_2$ are linearised using the small angle approximations whereby

$$\cos\theta \approx 1, \quad \sin\theta \approx \theta, \quad \dot{\theta}^2 \approx 0$$

As a result, the nonlinear equations above, separated by their linear and nonlinear parameters can be written as

$$\begin{aligned}
\ddot{x}_c &= 1.234F - 2.916\theta_1 - 0.116\theta_2 + \xi_{x_c} \\
\ddot{\theta}_1 &= -1.987F + 20.484\theta_1 - 1.299\theta_2 + \xi_{\theta_1} \\
\ddot{\theta}_2 &= 1.121F - 11.416\theta_1 + 23.973\theta_2 + \xi_{\theta_2}
\end{aligned}$$

where $\xi_{x_c}, \xi_{\theta_1}$ and ξ_{θ_2} encapsulate the nonlinearities in the equations above.

In reality, the force F supplied to move the cart originated from a DC motor where the input parameter to this motor is voltage. Therefore, by constructing a motor-force model,

$$F = V_a \frac{K_m}{rR} - \frac{K_m^2 \dot{x}_c}{r^2 R}$$

where V_a, K_m, r and R are the input voltage, motor torque constant, radius of output gear and armature resistance respectively, the state space matrices of the system with voltage as the input can be expressed as

In the notation of (5.1) - (5.2), the system matrix is

$$A_s = \begin{bmatrix} 0 & 1.0000 & 0 & 0 & 0 & 0 \\ 0 & -2.2043 & -2.9150 & 0 & -0.1160 & 0 \\ 0 & 0 & 0 & 1.0000 & 0 & 0 \\ 0 & 3.5494 & 20.4820 & 0 & -1.2990 & 0 \\ 0 & 0 & 0 & 0 & 0 & 1.0000 \\ 0 & -2.0024 & -11.4680 & 0 & 23.9770 & 0 \end{bmatrix}$$

where the states, control inputs and outputs of the system are

$$x_s = \begin{bmatrix} \text{position of cart} \\ \text{velocity of cart} \\ \text{angular displacement of first rod} \\ \text{angular velocity of first rod} \\ \text{angular displacement of second rod} \\ \text{angular velocity of second rod} \end{bmatrix}$$

$$u_s = \begin{bmatrix} \text{voltage to move cart along the rail} \end{bmatrix}$$

$$y_s = \begin{bmatrix} \text{position of cart} \\ \text{velocity of cart} \\ \text{angular displacement of first rod} \\ \text{angular displacement of second rod} \end{bmatrix}$$

Assume also that the second output (velocity of the cart) is potentially faulty. Thus, the

matrices B_s, N_s and C_s are

$$B_s = \begin{bmatrix} 0 \\ 1.3939 \\ 0 \\ -2.2445 \\ 0 \\ 1.2662 \end{bmatrix}, N_s = \begin{bmatrix} 0 \\ 1 \\ 0 \\ 0 \end{bmatrix}, C_s = \begin{bmatrix} 1 & 0 & 0 & 0 & 0 & 0 \\ 0 & 1 & 0 & 0 & 0 & 0 \\ 0 & 0 & 1 & 0 & 0 & 0 \\ 0 & 0 & 0 & 0 & 1 & 0 \end{bmatrix}$$

Suppose that matrix A_s is imprecisely known and that there exist parametric uncertainties, as shown earlier are encapsulated within the parameters $\xi_{x_c}, \xi_{\theta_1}$ and ξ_{θ_2}. The state equation becomes

$$\dot{x}_s = (A_s + \Delta A_s)x_s + B_s u_s \tag{5.24}$$

where ΔA_s is the discrepancy between the known matrix A_s and its actual value. By inspection, only the second, fourth and sixth states contain nonlinearities components as shown in matrix A_s while the other rows are certain due to the nature of the state equations. Writing (5.24) in the framework of (5.1) - (5.2) produces

$$Q_s = \begin{bmatrix} 0 & 0 & 0 \\ 1 & 0 & 0 \\ 0 & 0 & 0 \\ 0 & 1 & 0 \\ 0 & 0 & 0 \\ 0 & 0 & 1 \end{bmatrix}$$

As a result, it can be seen that the condition in (5.18) is satisfied and thus, DDFR can be achieved.

Performing the linear transformation described in Section 5.2 yields the following matrices

$$T_r = \begin{bmatrix} 0 & 1 & 0 & 0 \\ 1 & 0 & 0 & 0 \\ 0 & 0 & 1 & 0 \\ 0 & 0 & 0 & 1 \end{bmatrix}, \quad C_s = \begin{bmatrix} 0 & 1 & 0 & 0 & 0 & 0 \\ 1 & 0 & 0 & 0 & 0 & 0 \\ 0 & 0 & 1 & 0 & 0 & 0 \\ 0 & 0 & 0 & 0 & 1 & 0 \end{bmatrix}, \quad N_s = \begin{bmatrix} 1 \\ 0 \\ 0 \\ 0 \end{bmatrix}$$

Setting the filter matrix $A_{s,f} = 1$, the following matrices in the framework of (5.10) - (5.11) can be obtained as follows

$$\tilde{A} = \begin{bmatrix} 0 & 0 & 2.0024 & -23.9770 & 11.4680 & 0 & 0 \\ 0 & 0 & -3.5494 & 1.2990 & -20.4820 & 0 & 0 \\ 0 & 0 & -2.2043 & -0.1160 & -2.9150 & 0 & 0 \\ -1.0000 & 0 & 0 & 0 & 0 & 0 & 0 \\ 0 & -1.0000 & 0 & 0 & 0 & 0 & 0 \\ 0 & 0 & 1.0000 & 0 & 0 & 0 & 0 \\ 0 & 0 & 1.0000 & 0 & 0 & 0 & -1.0000 \end{bmatrix}$$

$$\tilde{M} = \begin{bmatrix} 0 \\ 0 \\ 0 \\ 0 \\ 0 \\ 0 \\ 1 \end{bmatrix}, \quad \tilde{Q} = \begin{bmatrix} -1 & 0 & 0 \\ 0 & -1 & 0 \\ 0 & 0 & 1 \\ 0 & 0 & 0 \\ 0 & 0 & 0 \\ 0 & 0 & 0 \\ 0 & 0 & 0 \end{bmatrix}, \quad \tilde{C} = \begin{bmatrix} 0 & 0 & 0 & 0 & 0 & 1 & 0 \\ 0 & 0 & 0 & 0 & 1 & 0 & 0 \\ 0 & 0 & 0 & 1 & 0 & 0 & 0 \\ 0 & 0 & 0 & 0 & 0 & 0 & 1 \end{bmatrix}$$

It was found that

$$A_{s,32} = \begin{bmatrix} -1 & 0 & 0 \\ 0 & -1 & 0 \\ 0 & 0 & 1 \end{bmatrix}$$

and that it has a full rank of 3. As result, the conditions D1 and D2 are satisfied.

Once the matrices are in the form of (4.5), it can be shown that $A_{s,36} = \begin{bmatrix} 0 & 0 & 1 \end{bmatrix}$ and $I - A_{s,32}A_{s,32}^{\dagger} = 0$, which from (4.30) leads to $W_{s,12} = \begin{bmatrix} 0 & 0 & -1 \end{bmatrix}$ and substituting this value into (4.19) yields $W_{s,1} = \begin{bmatrix} 0 & 0 & -1 \end{bmatrix}$.

The matrix $\hat{A}_1$ in (4.25) does not exist since the dimension $n-p-h+k_s+q = 0$. Choosing $L_{s,21} = I_3$ means $\lambda(A_{s,14} + L_{s,21}A_{s,32} + L_{s,22}A_{s,34}) = \{-1 \quad -1 \quad -1.2043\}$. Once L_s has been obtained, a suitable choice for $G_{s,l}$ (in the original coordinates of (4.1) - (4.2)) and a $P_{s,o}$ that satisfies Proposition 3.1 can be computed.

$$G_{s,l} = \begin{bmatrix} -1.4472 & 10.7984 & -41.3641 & -1.4472 \\ -15.1945 & -41.0844 & -6.0561 & -15.1945 \\ 1.7398 & -2.3137 & 1.8565 & 1.7398 \\ 0.6387 & 0.1922 & 9.2431 & 0.6387 \\ 2.6814 & 9.0578 & 0.8467 & 2.6814 \\ 3.7474 & 0.3966 & 0.7512 & 2.7474 \\ 2.7474 & 0.3966 & 0.7512 & 2.7474 \end{bmatrix}$$

$$P_{s,o} = I_4$$

The gain associated with the nonlinear injection $G_{s,n}$ in the original system coordinates of (4.1) - (4.2)) was computed to be

$$G_{s,n} = \begin{bmatrix} 0 & 0 & -1 & 0 \\ 0 & -1 & 0 & 0 \\ -1 & 0 & 0 & 0 \\ 0 & 0 & 1 & 0 \\ 0 & 1 & 0 & 0 \\ 1 & 0 & 0 & 0 \\ 0 & 0 & 0 & 1 \end{bmatrix}$$

5.4.1 Simulation Results

A linear observer-controller was used to stabilise the pendulum. Setting the system controller-observer parameters as

$$K = \begin{bmatrix} 15.9294 & 17.7436 & 115.685951.2155 & 423.2446 & 88.2368 \end{bmatrix}$$

for the controller and

$$L = \begin{bmatrix} 23.9193 & 1.0000 & 0 & 0 \\ 0 & 24.9701 & -2.9150 & -0.1160 \\ 0 & 0 & 46.7866 & 0 \\ 0 & 3.5494 & 765.9009 & -1.2990 \\ 0 & 0 & 0 & 46.7866 \\ 0 & -2.0024 & -11.4680 & 768.9359 \end{bmatrix}$$

for the observer, a simulation is carried out whereby the upper bound of the magnitude of the fault and the disturbance associated with the nonlinear discontinuous term ν in (3.34) is set to $\rho = 50$ while the positive scalar $\delta = 0.001$.

In order to stabilise the system with both rods of the pendulum being kept in the upright position, a state feedback controller was designed. The controller was also designed in such a way that it will lead the cart to move to a reference position (a tracking system). It can be seen that the cart failed to follow the position of its reference signal, as shown in Figure 5.3 due to a ramp fault being induced in the second sensor from 0s to 20s. Figure 5.5 shows the fault and its reconstruction and it can be seen that the fault could be reconstructed while being independent of the disturbance of ξ_s, which is non-zero where $Q_s\xi_s \neq 0 \Rightarrow \xi_s \neq 0$, as shown in Figure 5.4.

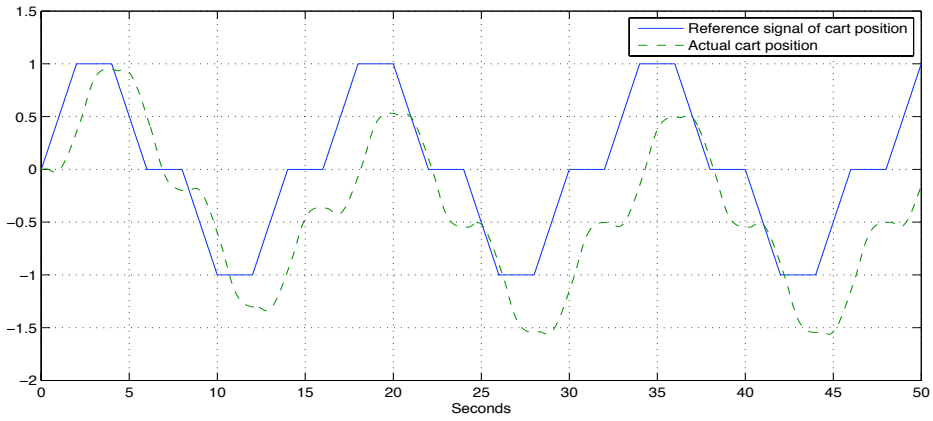

Figure 5.3: The reference signal for the cart position and its actual position.

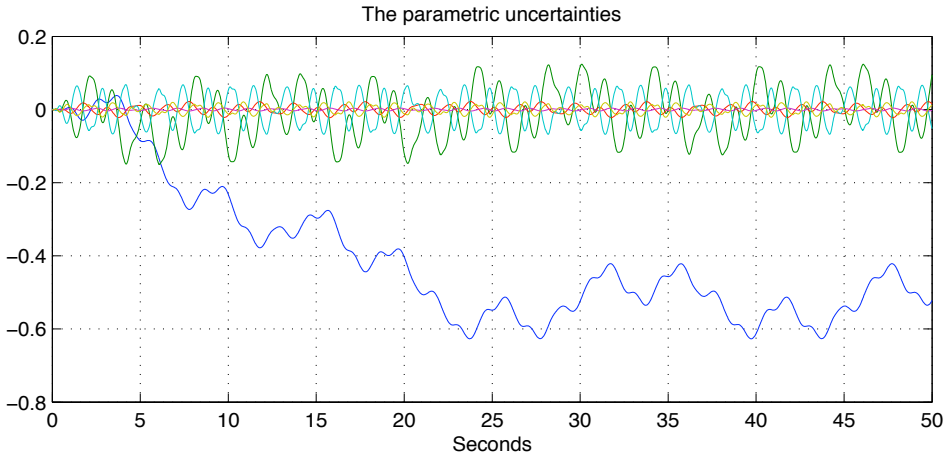

Figure 5.4: The uncertainties arise in the modelling of the system due to the nonlinearities encapsulated in ξ_{π_c},ξ_{θ_1} and ξ_{θ_2}.

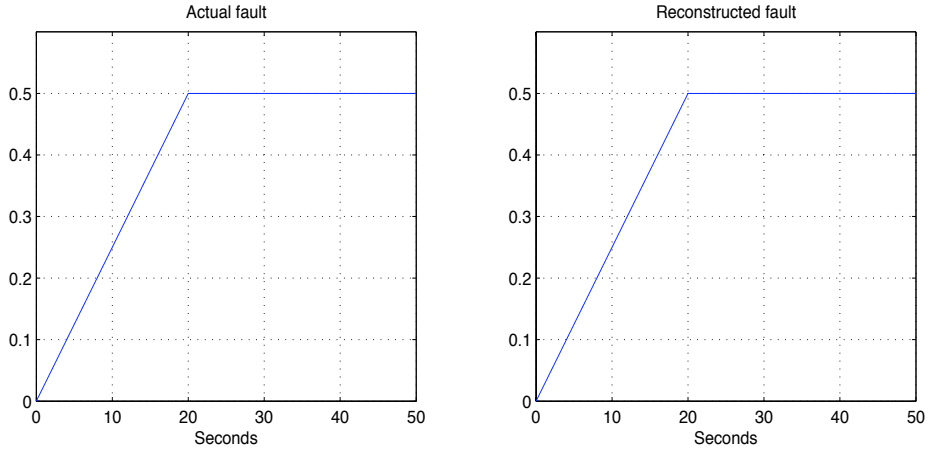

Figure 5.5: The left subfigure shows the fault, the right subfigure shows its reconstruction.

5.5 Conclusion

This chapter has successfully presented on how the work introduced in Chapter 4 could provide the platform and be extended to achieve robust sensor fault reconstruction, when it is combined with the method shown in Tan & Edwards [177] and investigated the conditions (in terms of the original system matrices) that guarantee DDFR for sensor fault.

The results discussed in this chapter was demonstrated with a double inverted pendulum model. The results had shown that the sensor fault reconstruction was completely decoupled from the disturbances, and this can be further extended to be used for the purpose of fault tolerant control. For example, in the simulation shown in this chapter, a fault tolerant control scheme can be used such that the cart will track the position of its reference signal without being affected by the fault.

Chapter 6

DDFR Using Multiple Sliding Mode Observers in Cascade

6.1 Introduction

It was found in Chapter 4 that the sliding mode observer can achieve DDFR with less stringent conditions compared with the linear observer.

This chapter addresses the case when DDFR cannot be guaranteed and presents a scheme that can achieve DDFR even though Condition C3 in Chapter 4 is not satisfied by using *cascaded observers*. It will be shown that the signals from an observer are found to be the output of a 'fictitious' system that is driven by the faults and disturbances. These signals are then fed into the subsequent observer which will be arranged in cascade form with the previous observer. This process is repeated until a fictitious system can successfully achieve DDFR. It is found that the scheme proposed in this chapter is applicable to a wider class of systems compared to the case if only one observer was used, as in Chapter 4. In addition, this chapter also presents a systematic method for the designer to check if DDFR is achievable for a system in terms of the original system matrices, together with the precise number of observers needed such that DDFR can be guaranteed. A rotational system will be used to validate the findings in this chapter.

For the notations used throughout this chapter, as an arbitrary number of observers is used in cascade, X^i indicates that the parameter X is analysed and evaluated for the i-th observer. Should the parameter X be raised to a certain power i, it shall be denoted by $(X)^i$.

The preliminary ideas of the work in this chapter has been submitted as a journal paper [142] and has been accepted as a conference paper [137].

6.2 Problem Statement and Design Algorithm

Consider the following system

$$\dot{x}^1 = A^1x^1 + M^1f + Q^1\xi^1 \tag{6.1}$$

$$y^1 = C^1x^1 \tag{6.2}$$

where $x^1 \in \mathbb{R}^{n^1}$ are the states, $y^1 \in \mathbb{R}^{p^1}$ are the outputs and $f \in \mathbb{R}^q$ are unknown faults with $n^1 \geq p^1$. The signals $\xi^1 \in \mathbb{R}^h$ are uncertainties or dynamics that represent the mismatch between the linear model (6.1) - (6.2) and the real plant. Without loss of generality assume that $rank(M^1) = q, rank(C^1) = p^1$ and $rank(C^1Q^1) = \bar{k}^1 < h$. The objective is to reconstruct the fault f whilst rejecting the effects of ξ on the fault reconstruction.

Assume also the following

E1. $rank(C^1M^1) = rank(M^1)$

E2. $rank\left(C^1\begin{bmatrix} M^1 & Q^1 \end{bmatrix}\right) = rank(C^1M^1) + rank(C^1Q^1)$

If Conditions E1 - E2 hold, then Proposition 4.1 can be used to transform the system (A^1, M^1, C^1, Q^1) such that it has the specific structures shown in (4.5) - (4.6),

$$A^1 = \begin{bmatrix} A_1^1 & A_2^1 \\ A_3^1 & A_4^1 \end{bmatrix}, M^1 = \begin{bmatrix} 0 \\ M_2^1 \end{bmatrix}, Q^1 = \begin{bmatrix} Q_1^1 \\ Q_2^1 \end{bmatrix} \begin{matrix} \updownarrow n^1 - p^1 \\ \updownarrow p^1 \end{matrix}, C^1 = \begin{bmatrix} 0 & C_2^1 \end{bmatrix} \updownarrow p^1 \tag{6.3}$$

where Q_1^1, Q_2^1 and M_2^1 can be further partitioned to be

$$Q_1^1 = \begin{bmatrix} 0 & 0 \\ \bar{Q}_1^1 & 0 \end{bmatrix} \begin{matrix} \updownarrow n^1 - p^1 - h + \bar{k}^1 \\ \updownarrow h - \bar{k}^1 \end{matrix}, Q_2^1 = \begin{bmatrix} 0 & 0 \\ 0 & \bar{Q}_2^1 \\ 0 & 0 \end{bmatrix}, M_2^1 = \begin{bmatrix} 0 \\ 0 \\ M_o \end{bmatrix} \begin{matrix} \updownarrow p - q - \bar{k}^1 \\ \updownarrow \bar{k}^1 \\ \updownarrow q \end{matrix} \tag{6.4}$$

where $C_2^1, \bar{Q}_1^1, \bar{Q}_2^1$ and M_o are square and invertible.

6.2.1 Design Algorithm

Set the index variable $i = 1$. Define

$$\bar{k}^i := \bar{k}^{i-1} + k^i \tag{6.5}$$

and enter the following iterative design procedure.

1. **Check for algorithm termination**

   The system associated with the i^{th} observer be defined as

$$\dot{x}^i = A^i x^i + Q^i \xi^i + M^i f^i \tag{6.6}$$

$$y^i = C^i x^i \tag{6.7}$$

   For the case when $i = 1$, define $Q_2^0 = \emptyset$ (empty matrix), $p^0 = 0$ and $\bar{k}^0 = 0$ (hence the definition of $\bar{k}^i$ from (6.5) results in $\bar{k}^1 = k^1$).

   The matrices Q^i, C^i and M^i have the following structure

$$Q^i = \begin{bmatrix} Q_1^i \\ Q_2^i \end{bmatrix} = \left[\begin{array}{cc} 0 & 0 \\ \bar{Q}_1^i & 0 \\ \hline 0 & 0 \\ 0 & \bar{Q}_2^i \\ 0 & 0 \end{array}\right] \begin{array}{l} \updownarrow n^i - p^i - h + \bar{k}^i \\ \updownarrow h - \bar{k}^i \\ \updownarrow p^i - q - \bar{k}^i \\ \updownarrow \bar{k}^i \\ \updownarrow q \end{array} \quad , \bar{Q}_2^i = \begin{bmatrix} Q_2^i & 0 \\ 0 & \bar{Q}_2^{i-1} \end{bmatrix} \begin{array}{l} \updownarrow k^i \\ \updownarrow \bar{k}^{i-1} \end{array} \tag{6.8}$$

   and

$$C^i = \begin{bmatrix} 0 & C_2^i \end{bmatrix}, \quad M^i = \begin{bmatrix} 0 \\ M_o \end{bmatrix} \tag{6.9}$$

   where C_2^i and M_o are square and invertible. Then let A^i be partitioned generally as

$$A^i = \left[\begin{array}{cc|c} \breve{A}^i_{11} & \breve{A}^i_{12} & * \\ \breve{A}^i_{13} & \breve{A}^i_{14} & * \\ \hline \breve{A}^i_{31} & \breve{A}^i_{32} & * \\ \breve{A}^i_{33} & \breve{A}^i_{34} & * \\ \breve{A}^i_{35} & \breve{A}^i_{36} & * \end{array}\right] \begin{array}{l} \updownarrow n^i - p^i - h + \bar{k}^i \\ \updownarrow h - \bar{k}^i \\ \updownarrow p^i - q - \bar{k}^i \\ \updownarrow \bar{k}^i \\ \updownarrow q \end{array} \tag{6.10}$$

where $\breve{A}^i_{11}, \breve{A}^i_{14}$ are square matrices, and (*) are matrices of p^i columns and do not play any role in the subsequent analysis.

a) If $\breve{A}^i_{32}$ has full column rank of $h - \bar{k}^i$, then from the results in Chapter 4 it is possible to implement a sliding mode observer and reconstruct the fault while being robust to the disturbances and the algorithm can be terminated. Let $m = i$, where m denotes the number of observers needed for robust fault reconstruction. Return to Section 4.3 of Chapter 4 to design the observer for DDFR.

b) If $\breve{A}^i_{32}$ does not have full column rank and $i = n^1 - p^1$, then DDFR cannot be guaranteed[1] and the algorithm is terminated.

If neither conditions (a) nor (b) are satisfied, proceed with the algorithm.

2. **Transform system to obtain special structure in system matrix**

Define

$$k^{i+1} := rank(\breve{A}^i_{32}) \,, \quad p^{i+1} := rank \left[\begin{array}{cc} \breve{A}^i_{31} & \breve{A}^i_{32} \end{array}\right] + q + \bar{k}^i \tag{6.11}$$

Since from (6.10), $\left[\begin{array}{cc} \breve{A}^i_{31} & \breve{A}^i_{32} \end{array}\right]$ has $p^i - q - \bar{k}^i$ rows, then it is obvious from the definition of p^{i+1} in (6.11) that $p^{i+1} \leq p^i$.

Let $R^i_1 \in \mathbb{R}^{(p^i - q - \bar{k}^i) \times (p^i - q - \bar{k}^i)}$ be an orthogonal matrix such that

$$R^i_1 \left[\begin{array}{cc} \breve{A}^i_{31} & \breve{A}^i_{32} \end{array}\right] = \underset{\substack{\longleftrightarrow \\ n^i - p^i - h + \bar{k}^i}}{\left[\begin{array}{c} 0 \\ A^{i\,o}_{31} \end{array}\right.} \quad \underset{\substack{\longleftrightarrow \\ h - \bar{k}^i}}{\left.\begin{array}{c} 0 \\ A^{i\,o}_{32} \end{array}\right]} \begin{array}{l} \updownarrow p^i - p^{i+1} \\ \updownarrow p^{i+1} - q - \bar{k}^i \end{array} \tag{6.12}$$

[1]The reason for this is given in Proposition 6.1.

From the definition of k^{i+1} in (6.11) and (6.12), it is obvious that $rank(A_{32}^{i\ o}) = k^{i+1}$. Hence, there exist orthogonal matrices $R_2^i \in \mathbb{R}^{(p^{i+1}-q-\bar{k}^i)\times(p^{i+1}-q-\bar{k}^i)}$ and $R_3^i \in \mathbb{R}^{(h-\bar{k}^i)\times(h-\bar{k}^i)}$ such that

$$R_2^i A_{32}^{i\ o} R_3^i = \underbrace{\begin{bmatrix} 0 & 0 \\ 0 & A_{322}^{i\ o} \end{bmatrix}}_{h-\bar{k}^{i+1}\quad k^{i+1}} \begin{matrix} \updownarrow p^{i+1}-q-\bar{k}^{i+1} \\ \updownarrow k^{i+1} \end{matrix} \tag{6.13}$$

where $A_{322}^{i\ o}$ has full rank, and partition generally (and partition conformably with (6.13)) the following

$$\begin{aligned} \breve{A}_{12}^i R_3^i &= \begin{bmatrix} A_{121}^i & A_{122}^i \\ A_{123}^i & A_{124}^i \end{bmatrix} \begin{matrix} \updownarrow n^i-p^i-h+\bar{k}^i-p^{i+1}+q+\bar{k}^{i+1} \\ \updownarrow p^{i+1}-q-\bar{k}^{i+1} \end{matrix} \\ \breve{A}_{36}^i R_3^i &= \underbrace{\begin{bmatrix} A_{361}^i & A_{362}^i \end{bmatrix}}_{\qquad\quad k^{i+1}} \updownarrow q \end{aligned} \tag{6.14}$$

Using (6.11) - (6.13), there exists an orthogonal matrix $R_4^i \in \mathbb{R}^{(n^i-p^i-h+\bar{k}^i)\times(n^i-p^i-h+\bar{k}^i)}$ such that

$$R_2^i A_{31}^{i\ o} R_4^i = \underbrace{\begin{bmatrix} 0 & A_{3112}^{i\ o} \\ A_{3121}^{i\ o} & A_{3122}^{i\ o} \end{bmatrix}}_{n^i-p^i-h+\bar{k}^i-p^{i+1}+q+\bar{k}^{i+1}\quad p^{i+1}-q-\bar{k}^{i+1}} \begin{matrix} \updownarrow p^{i+1}-q-\bar{k}^{i+1} \\ \updownarrow k^{i+1} \end{matrix} \tag{6.15}$$

where $A_{3112}^{i\ o}$ is full rank. Using (6.12), (6.13) and (6.15), it is straightforward to show that

$$\begin{bmatrix} I_{p^i-p^{i+1}} & 0 \\ 0 & R_2^i \end{bmatrix} R_1^i \begin{bmatrix} \breve{A}_{31}^i & \breve{A}_{32}^i \end{bmatrix} \begin{bmatrix} R_4^i & 0 \\ 0 & R_3^i \end{bmatrix} = \underbrace{\begin{bmatrix} 0 & 0 & 0 & 0 \\ 0 & A_{3112}^{i\ o} & 0 & 0 \\ A_{3121}^{i\ o} & A_{3122}^{i\ o} & 0 & A_{322}^{i\ o} \end{bmatrix}}_{p^{i+1}-q-\bar{k}^{i+1}\quad h-\bar{k}^{i+1}\quad k^{i+1}} \begin{matrix} \updownarrow p^i-p^{i+1} \\ \updownarrow p^{i+1}-q-\bar{k}^{i+1} \\ \updownarrow k^{i+1} \end{matrix}$$

Define a coordinate transformation $T_2^i := T_{23}^i T_{22}^i T_{21}^i$ where

$$T_{21}^i := \left[\begin{array}{cc|cc} (R_4^i)^{-1} & 0 & 0 & 0 \\ 0 & (R_3^i)^{-1} & 0 & 0 \\ \hline 0 & 0 & R_5^i & 0 \\ 0 & 0 & 0 & I \end{array}\right] \begin{array}{l} \updownarrow n^i - p^i - h + \bar{k}^i \\ \updownarrow h - \bar{k}^i \\ \updownarrow p^i - q - \bar{k}^i \\ \updownarrow q + \bar{k}^i \end{array} \tag{6.16}$$

$$T_{22}^i := \left[\begin{array}{ccccc|c} & I & & 0 & 0 & 0 & 0 \\ & 0 & & I & 0 & 0 & 0 \\ & 0 & & 0 & I & 0 & 0 \\ (A_{322}^{i\ o})^{-1} A_{3121}^{i\ o} & & & 0 & 0 & I & 0 \\ \hline & 0 & & 0 & 0 & 0 & I \end{array}\right] \begin{array}{l} \updownarrow n^i - p^i - h + \bar{k}^i - p^{i+1} + q + \bar{k}^{i+1} \\ \updownarrow p^{i+1} - q - \bar{k}^{i+1} \\ \updownarrow h - \bar{k}^{i+1} \\ \updownarrow k^{i+1} \\ \updownarrow p^i \end{array} \tag{6.17}$$

$$T_{23}^i = \left[\begin{array}{cccc|c} I & 0 & 0 & 0 & 0 \\ 0 & 0 & I & 0 & 0 \\ 0 & I & 0 & 0 & 0 \\ 0 & 0 & 0 & I & 0 \\ \hline 0 & 0 & 0 & 0 & I \end{array}\right] \begin{array}{l} \updownarrow n^i - p^i - h + \bar{k}^i - p^{i+1} + q + \bar{k}^{i+1} \\ \updownarrow h - \bar{k}^{i+1} \\ \updownarrow p^{i+1} - q - \bar{k}^{i+1} \\ \updownarrow k^{i+1} \\ \updownarrow p^i \end{array} \tag{6.18}$$

where $R_5^i = \begin{bmatrix} I_{p^i - p^{i+1}} & 0 \\ 0 & R_2^i \end{bmatrix} R_1^i$ in order to obtain

$$\begin{aligned} T_2^i A^i (T_2^i)^{-1} &= \left[\begin{array}{c|c} A_1^i & A_2^i \\ \hline A_3^i & A_4^i \end{array}\right] \begin{array}{l} \updownarrow n^i - p^i \\ \updownarrow p^i \end{array} \\ &= \left[\begin{array}{c|c} A_1^i & * \\ \hline A_{31}^i & * \\ A_{32}^i & * \end{array}\right] \begin{array}{l} \updownarrow n^i - p^i \\ \updownarrow p^i - q - \bar{k}^i \\ \updownarrow q + \bar{k}^i \end{array} \end{aligned} \tag{6.19}$$

and it can be further expanded to be

$$T_2^i A^i (T_2^i)^{-1} = \left[\begin{array}{cc|c} A_{11}^i & A_{12}^i & * \\ A_{13}^i & A_{14}^i & * \\ \hline 0 & A_{312}^i & * \\ A_{321}^i & A_{322}^i & * \end{array}\right] \begin{array}{l} \updownarrow\, n^i - p^i + \bar{k}^i - p^{i+1} + q \\ \updownarrow\, p^{i+1} - q - \bar{k}^i \\ \updownarrow\, p^i - q - \bar{k}^i \\ \updownarrow\, q + \bar{k}^i \end{array} \tag{6.20}$$

and subsequently

$$T_2^i A^i (T_2^i)^{-1} = \left[\begin{array}{cccc|c} A_{111}^i & A_{121}^i & A_{112}^i & A_{122}^i & * \\ A_{131}^i & A_{141}^i & A_{132}^i & A_{142}^i & * \\ A_{113}^i & A_{123}^i & A_{114}^i & A_{124}^i & * \\ A_{133}^i & A_{143}^i & A_{134}^i & A_{144}^i & * \\ \hline 0 & 0 & 0 & 0 & * \\ 0 & 0 & A_{3112}^{i\ o} & 0 & * \\ 0 & 0 & A_{3122}^{i\ o} & A_{322}^{i\ o} & * \\ A_{331}^i & A_{341}^i & A_{332}^i & A_{342}^i & * \\ A_{351}^i & A_{361}^i & A_{352}^i & A_{362}^i & * \end{array}\right] \begin{array}{l} \updownarrow\, n^i - p^i - h + \bar{k}^i - p^{i+1} + q + \bar{k}^{i+1} \\ \updownarrow\, h - \bar{k}^{i+1} \\ \updownarrow\, p^{i+1} - q - \bar{k}^{i+1} \\ \updownarrow\, k^{i+1} \\ \updownarrow\, p^i - p^{i+1} \\ \updownarrow\, p^{i+1} - q - \bar{k}^{i+1} \\ \updownarrow\, k^{i+1} \\ \updownarrow\, \bar{k}^i \\ \updownarrow\, q \end{array} \tag{6.21}$$

where (*) are matrices with p^i columns and play no role in the following analysis. Comparing (6.20) with (6.21), it is obvious that A_{312}^i has full column rank. Let there be an invertible matrix $T_\xi^i \in \mathbb{R}^{(h-\bar{k}^i)\times(h-\bar{k}^i)}$ such that

$$(R_3^i)^{-1} \bar{Q}_1^i (T_\xi^i)^{-1} = \begin{bmatrix} \bar{Q}_1^{i+1} & 0 \\ 0 & Q_2^{i+1} \end{bmatrix}$$

where $Q_2^{i+1} \in \mathbb{R}^{k^{i+1}\times k^{i+1}}$ is invertible. Therefore, it follows that

$$T_2^i Q^i (T_\xi^i)^{-1} = \begin{bmatrix} Q_1^i \\ Q_2^i \end{bmatrix} = \left[\begin{array}{ccc} 0 & 0 & 0 \\ \bar{Q}_1^{i+1} & 0 & 0 \\ 0 & 0 & 0 \\ 0 & Q_2^{i+1} & 0 \\ \hline 0 & 0 & 0 \\ 0 & 0 & 0 \\ 0 & 0 & 0 \\ 0 & 0 & \bar{Q}_2^i \\ 0 & 0 & 0 \end{array}\right], \quad T_2^i M^i = \begin{bmatrix} 0 \\ M_2^i \end{bmatrix} = \left[\begin{array}{c} 0 \\ 0 \\ 0 \\ 0 \\ \hline 0 \\ 0 \\ 0 \\ 0 \\ M_o \end{array}\right] \tag{6.22}$$

$$C^i (T_2^i)^{-1} = \begin{bmatrix} 0 & \bar{C}_2^i \end{bmatrix} \tag{6.23}$$

where

$$\bar{C}_2^i = C_2^i \begin{bmatrix} (R_5^i)^{-1} & 0 \\ 0 & I_{q+k^i} \end{bmatrix}$$

Note that the row dimensions of the matrices in (6.22) are conformable to those in (6.21).

3. **Implement sliding mode observer**

The sliding mode observer for the system (6.6) - (6.7) will be designed based on the method that has been discussed in Section 4.2.1 where $C_2 = T$ used in Section 3.2.2 shall be replaced with $\bar{C}_2^i$ in order to fit into the framework that is to be presented in this chapter. For example, the matrix G_n^i in this new form is written as

$$G_n^i = \begin{bmatrix} -L^i \\ I_{p^i} \end{bmatrix} (\bar{P}_o^i \bar{C}_2^i)^{-1}, \quad L^i = \underset{\substack{\longleftarrow \\ p^i - q - \bar{k}^i}}{\begin{bmatrix} L_o^i & 0 \end{bmatrix}} \updownarrow n^i - p^i \quad \underset{q + \bar{k}^i}{\longleftrightarrow} \tag{6.24}$$

where $\bar{P}_o^i$ is a symmetric positive definite (s.p.d.) matrix.

Then assume a sliding motion has taken place at $\mathcal{S}^i(e_y^i = \dot{e}_y^i = 0)$. From the structure of L^i in (6.24) and M_2^i and Q_2^i in (6.22), it is clear that $L^i M_2^i = 0, L^i Q_2^i = 0$ and therefore the error system (3.14) in the new coordinates of (6.21) - (6.23) can be partitioned to be (see Section 4.2.1)

$$\begin{aligned} \dot{e}_1^i &= (A_1^i + L^i A_3^i)e_1^i - Q_1^i \xi^{i+1} && (6.25) \\ 0 &= \bar{C}_2^i A_3^i e_1^i + (\bar{P}_o^i)^{-1}\nu_{eq}^i - \bar{C}_2^i M_2^i f - \bar{C}_2^i Q_2^i \xi^{i+1} && (6.26) \end{aligned}$$

Define $w^i := (\bar{P}_o^i \bar{C}_2^i)^{-1}\nu_{eq}^i$ and $v^i := -e_1^i$. Pre-multiplying (6.26) with $(\bar{C}_2^i)^{-1}$ and re-arrange (6.25) - (6.26) to obtain

$$\begin{aligned} \dot{v}^i &= (A_1^i + L^i A_3^i)v^i + Q_1^i \xi^{i+1} && (6.27) \\ w^i &= A_3^i v^i + Q_2^i \xi^{i+1} + M_2^i f && (6.28) \end{aligned}$$

4. **Obtain system for next observer**

Partition (6.28) using (6.19) and (6.22) to get

$$\begin{aligned} w_1^i &= A_{31}^i v^i && (6.29) \\ w_2^i &= A_{32}^i v^i + Q_{22}^i \xi^{i+1} + M_{22}^i f && (6.30) \end{aligned}$$

where Q_{22}^i and M_{22}^i are the bottom of $q + \bar{k}^i$ rows of Q_2^i and M_2^i respectively.

Then define z^i to be a filtered version of w_2^i representing

$$\begin{aligned} \dot{z}^i &= -\alpha^i z^i + \alpha^i w_2^i, \quad \alpha^i \in \mathbb{R}_+ && (6.31) \\ &= -\alpha^i z^i + \alpha^i A_{32}^i v^i + \alpha^i Q_{22}^i \xi^{i+1} + \alpha^i M_{22}^i f && (6.32) \end{aligned}$$

Combine (6.27), (6.29) and (6.32) to obtain the system for the $(i+1)^{th}$ observer of

order $n^{i+1} := n^i - p^i + q + \bar{k}^i$

$$\dot{x}^{i+1} = A^{i+1}x^{i+1} + Q^{i+1}\xi^{i+1} + M^{i+1}f \tag{6.33}$$

$$y^{i+1} = C^{i+1}x^{i+1} \tag{6.34}$$

where $x^{i+1} := \begin{bmatrix} v^i \\ z^i \end{bmatrix}, y^{i+1} := \begin{bmatrix} w_1^i \\ z^i \end{bmatrix}$ and

$$A^{i+1} = \begin{bmatrix} A_1^i + L^i A_3^i & 0 \\ \alpha^i A_{32}^i & -\alpha^i I \end{bmatrix}, Q^{i+1} = \begin{bmatrix} Q_1^i \\ \alpha^i Q_{22}^i \end{bmatrix}, M^{i+1} = \begin{bmatrix} 0 \\ M_{22}^i \end{bmatrix} \begin{matrix} \updownarrow n^i - p^i \\ \updownarrow q + \bar{k}^i \end{matrix} \tag{6.35}$$

$$C^{i+1} = \begin{bmatrix} A_{31}^i & 0 \\ 0 & I \end{bmatrix} \begin{matrix} \updownarrow p^{i+1} - q - \bar{k}^i \\ \updownarrow q + \bar{k}^i \end{matrix} \tag{6.36}$$

Further expanding $A^{i+1}, M^{i+1}, C^{i+1}, Q^{i+1}$ in (6.35) - (6.36) using (6.21) - (6.23) to get

$$A^{i+1} = \left[\begin{array}{cc|c} A_{111}^i & A_{121}^i & * \\ A_{131}^i & A_{141}^i & * \\ \hline A_{113}^i & A_{123}^i & * \\ A_{133}^i & A_{143}^i & * \\ A_{331}^i & A_{341}^i & * \\ A_{351}^i & A_{361}^i & * \end{array}\right], Q^{i+1} = \left[\begin{array}{ccc} 0 & 0 & 0 \\ \bar{Q}_1^{i+1} & 0 & 0 \\ \hline 0 & 0 & 0 \\ 0 & Q_2^{i+1} & 0 \\ 0 & 0 & \bar{Q}_2^i \\ 0 & 0 & 0 \end{array}\right], M^{i+1} = \left[\begin{array}{c} 0 \\ 0 \\ \hline 0 \\ 0 \\ 0 \\ M_o \end{array}\right] \begin{matrix} \updownarrow n^i - p^i - h + \bar{k}^i - p^{i+1} + q + \bar{k}^{i+1} \\ \updownarrow h - \bar{k}^{i+1} \\ \updownarrow p^{i+1} - q - \bar{k}^{i+1} \\ \updownarrow k^{i+1} \\ \updownarrow \bar{k}^i \\ \updownarrow q \end{matrix} \tag{6.37}$$

$$C^{i+1} = \left[\begin{array}{cc|cccc} 0 & 0 & A_{3112}^{i\,o} & 0 & 0 & 0 \\ 0 & 0 & A_{3122}^{i\,o} & A_{322}^{i\,o} & 0 & 0 \\ 0 & 0 & 0 & 0 & I & 0 \\ 0 & 0 & 0 & 0 & 0 & I \end{array}\right] \begin{matrix} \updownarrow p^{i+1} - q - \bar{k}^{i+1} \\ \updownarrow k^{i+1} \\ \updownarrow \bar{k}^i \\ \updownarrow q \end{matrix} \tag{6.38}$$

From the definition of $\bar{Q}_2^i$ in (6.8), it is obvious that $\bar{Q}_2^{i+1} := diag\{Q_2^{i+1}, \bar{Q}_2^i\}$.

Notice that Q^{i+1}, M^{i+1} and C^{i+1} from (6.37) - (6.38) are in exactly the same structure as Q^i, M^i and C^i in (6.8) - (6.9), where

- the bottom q rows of M^j form a square and invertible matrix, whilst the remaining rows are zero.
- the last p^j columns of C^j form a square and invertible matrix, whilst the remaining columns are zero.
- the bottom q rows of Q^j are zero, the next $\bar{k}^j$ rows are full row rank (where the last $\bar{k}^j$ columns form an invertible matrix, the remaining columns are zero), the next $p^j - q - \bar{k}^j$ rows are zero, the next $h - \bar{k}^j$ rows are full row rank (the first $h - \bar{k}^j$ columns form an invertible matrix, the remaining columns are zero) and the remaining rows are zero.

Increment i by 1 and repeat the algorithm.

Remark 6.1 *From (6.25) - (6.26), it is clear that the output estimation error e_y^i vanishes when sliding motion occurs in observer i, which also causes the last p^i columns of A^i to vanish from the analysis in (6.25) - (6.26). This is due to the structure of C^i from (6.23) which causes the 'output' states to be the last p^i states. Since C^{i+1} has the same structure as C^i, therefore the last p^{i+1} columns of A^{i+1} will also vanish during the sliding motion of observer $i+1$. By expanding $A_1^i + L^i A_3^i$ from (6.25) using (6.21), and comparing with A^{i+1} in (6.37), it can be seen that the elements of L^i appear only in the last p^{i+1} columns of A^{i+1} and therefore L^i plays no role in the sliding motion of observer $(i+1)$, and does not affect the quality of the fault reconstruction. It is obvious that the observer gain G_l^i also vanishes during sliding motion as it is multiplied with e_y^i. Hence, it can be concluded that the design of an observer, the matrices (G_l^i, L^i) does not affect the sliding motion of subsequent observers (and the quality of fault reconstruction), and more importantly does not affect the ability of the subsequent observers (and the overall cascade scheme) to achieve DDFR.* ♯

Remark 6.2 *The design of P^i and G_l^i that satisfy Proposition 3.1 can be performed systematically as in Edwards & Spurgeon [52] where system (3.14) is transformed using T_L^i in (3.23) and the design of P^i and G_l^i can be performed in the new coordinates. An alternative design method can be found in Tan & Edwards [172] where L_o^i, G_l^i and $\bar{P}_o^i$ are deigned simultaneously using Linear Matrix Inequalities as shown by Boyd* et al. *[13].* ♯

6.3 Existence Conditions

From the algorithm, comparing $(A^{i+1}, M^{i+1}, Q^{i+1}, C^{i+1})$ in equations (6.37) - (6.38) with (A^i, M^i, Q^i, C^i) in (6.8) - (6.10) shows that $A_{123}^i = \breve{A}_{32}^{i+1}$. Therefore, comparing with Conditions C3 and C4 in Chapter 4, it is possible to generate a reconstruction of the fault that is decoupled from the disturbances using m observers if the following conditions are satisfied

F1. A_{123}^{m-1} has full rank.

F2. All observers have a stable sliding motion.

It is of interest to find existence conditions for the method proposed in this chapter in terms of the original matrices (A^1, M^1, C^1, Q^1), so that it can be easily ascertained from the beginning whether the method proposed in this chapter is applicable or not. To conveniently analyze the existence conditions, (A^1, M^1, C^1, Q^1) will be transformed into a special structure.

6.3.1 Overall Coordinate Transformation

To achieve a convenient representation of (A^1, M^1, C^1, Q^1), parts of the transformations T_2^i and T_ξ^i in the algorithm will be used. However, some modifications need to be made to those transformation matrices as the structure that will be aimed for will be of different order from the original system.

It can be seen that before the algorithm is entered, the system firstly undergoes the transformations shown introduced in Proposition 4.1. Then, the algorithm is repeated $m-1$ times

and terminated at step 1 of the m-th time the algorithm is entered. In each iteration of the algorithm, the states and disturbances undergo (respectively) the transformations T_2^i and T_ξ^i. Then, the bottom p^i states are removed due to sliding motion, followed by the augmentation of $q + \bar{k}^i$ states at the bottom of the state vector.

In order to obtain the transformation matrices for the original system (A^i, M^i, Q^i, C^i), the process of state removal and augmentation need to be reversed $m - 1$ times. The reversal of changes can be summarised to: remove the last $\bar{k}^i + q$ rows and columns, and augment with I_{p^i}. From (6.11), it is clear that $p^i > \bar{k}^i + q$; hence the reversal for each step simply involves only augmenting with $I_{p^i - \bar{k}^i - q}$. Hence, to make T_2^i compatible with the original system, each of them need to be augmented with $I_{\Sigma_{j=1}^i p^j - \bar{k}^j - jq}$.

Define the following transformation matrices $T_2 \in \mathbb{R}^{n^1 \times n^1}, T_\xi \in \mathbb{R}^{h \times h}$

$$T_2 := \bar{T}_2^{m-1} \bar{T}_2^{m-2} \dots \bar{T}_2^2 \bar{T}_2^1 \,, \quad T_\xi := \bar{T}_\xi^{m-1} \bar{T}_\xi^{m-2} \dots \bar{T}_\xi^2 \bar{T}_\xi^1 \tag{6.39}$$

where

$$\bar{T}_2^i = \begin{bmatrix} T_2^i & 0 \\ 0 & I_{\sum_{j=0}^{i-1}(p^j - \bar{k}^j - jq)} \end{bmatrix}, \quad \bar{T}_\xi^i = \begin{bmatrix} T_\xi^i & 0 \\ 0 & I_{\bar{k}^i} \end{bmatrix} \tag{6.40}$$

Assume that (A^1, M^1, C^1, Q^1) are already in the form in Proposition 4.1. Then by using the results in Step 2 of the algorithm, performing the transformation $x^1 \mapsto T_2 x^1, \xi^1 \mapsto T_\xi \xi^1$ results in (6.41) - (6.43) as shown on the next few pages.

Remark 6.3 *From step 2 in the algorithm, it can be seen that the coordinate transformation T_2^i, T_ξ^i (and hence $\bar{T}_2^i, \bar{T}_\xi^i$) depend only on $\breve{A}_{31}^i, \breve{A}_{32}^i$ and $\bar{Q}_1^i$. Then it can be seen that $A_{111}^i, A_{121}^i, A_{131}^i, A_{141}^i, A_{113}^i, A_{123}^i$ and $\bar{Q}_1^{i+1}$ are obtained from transformations and partitions of $\breve{A}_{11}^i, \breve{A}_{12}^i, \breve{A}_{13}^i, \breve{A}_{14}^i$ and $\bar{Q}_1^i$. By comparing (A^i, M^i, Q^i, C^i) in (6.8) - (6.10) with $(A^{i+1}, M^{i+1}, Q^{i+1}, C^{i+1})$ in (6.37) - (6.38), it can be seen that $\breve{A}_{31}^{i+1} = A_{113}^i$, $\breve{A}_{32}^{i+1} = A_{123}^i$, $\breve{A}_{11}^{i+1} = A_{111}^i$, $\breve{A}_{12}^{i+1} = A_{121}^i$, $\breve{A}_{13}^{i+1} = A_{131}^i$, $\breve{A}_{14}^{i+1} = A_{141}^i$ and the coordinate transform for the next observer T_2^{i+1}, T_ξ^{i+1} (and also $\bar{T}_2^{i+1}, \bar{T}_\xi^{i+1}$) depend on A_{113}^i, A_{123}^i and $\bar{Q}_1^{i+1}$.*

Therefore, after the system is in the form of Proposition 4.1, the coordinate transformations

depend only on the partitions of A^1 and Q^1. Hence, the transformations $\bar{T}_2^i$ and $\bar{T}_\xi^i$ can be systematically computed using an automated algorithm based on the transformed and partitioned parts of A^1 and Q^1 until a value of m is obtained (and the structures in (6.41) - (6.43) are achieved) such that A_{123}^{m-1} is full column rank (and m is the sufficient number of observers to guarantee DDFR for the system).

If $A_{123}^{n^1-p^1-1}$ is not full column rank, then DDFR cannot be guaranteed as proven in the following proposition. ♯

$$A^1 = \left[\begin{array}{cc|c|c|c|c|c|l}
* & A_{121}^{m-1} & * & * & \dots & * & * & * \\
* & * & * & * & \dots & * & * & * \\
* & A_{123}^{m-1} & * & * & \dots & * & * & * \\
* & * & * & * & \dots & * & * & * \\
\hline
0 & 0 & 0 & * & \dots & * & * & * \\
0 & 0 & Y^{m-1} & * & \dots & * & * & * \\
* & * & * & * & \dots & * & * & * \\
\hline
0 & 0 & 0 & 0 & \dots & * & * & * \\
0 & 0 & 0 & Y^{m-2} & \dots & * & * & * \\
* & * & * & * & \dots & * & * & * \\
\hline
\vdots & \vdots & \vdots & \vdots & \ddots & \vdots & \vdots & \vdots \\
\hline
0 & 0 & 0 & 0 & \dots & 0 & * & * \\
0 & 0 & 0 & 0 & \dots & Y^2 & * & * \\
* & * & * & * & \dots & * & * & * \\
\hline
0 & 0 & 0 & 0 & \dots & 0 & 0 & * \\
0 & 0 & 0 & 0 & \dots & 0 & Y^1 & * \\
* & * & * & * & \dots & * & * & * \\
* & A_{361}^{m-1} & * & * & \dots & * & * & *
\end{array}\right]
\begin{array}{l}
\updownarrow n^{m-1}-p^{m-1}-p^m-h+k^m+q+2\bar{k}^{m-1} \\
\updownarrow h-\bar{k}^{m-1}-k^m \\
\updownarrow p^m-q-\bar{k}^{m-1}-k^m \\
\updownarrow k^m \\
\updownarrow p^{m-1}-p^m \\
\updownarrow p^m-q-\bar{k}^{m-1} \\
\updownarrow k^{m-1} \\
\updownarrow p^{m-2}-p^{m-1} \\
\updownarrow p^{m-1}-q-\bar{k}^{m-2} \\
\updownarrow k^{m-2} \\
\\
\updownarrow p^2-p^3 \\
\updownarrow p^3-q-\bar{k}^2 \\
\updownarrow k^2 \\
\updownarrow p^1-p^2 \\
\updownarrow p^2-q-\bar{k}^1 \\
\updownarrow \bar{k}^1 \\
\updownarrow q
\end{array} \tag{6.41}$$

$$
Q^1 = \left[\begin{array}{ccccc|cc|l}
0 & 0 & 0 & 0 & \dots & 0 & 0 & \updownarrow n^{m-1} - p^{m-1} - p^m - h + k^m + q + 2\bar{k}^{m-1} \\
\bar{Q}_1^m & 0 & 0 & 0 & \dots & 0 & 0 & \updownarrow h - \bar{k}^{m-1} - k^m \\
0 & 0 & 0 & 0 & \dots & 0 & 0 & \updownarrow p^m - q - \bar{k}^{m-1} - k^m \\
0 & Q_2^m & 0 & 0 & \dots & 0 & 0 & \updownarrow k^m \\
\hline
0 & 0 & 0 & 0 & \dots & 0 & 0 & \updownarrow p^{m-1} - p^m \\
0 & 0 & 0 & 0 & \dots & 0 & 0 & \updownarrow p^m - q - \bar{k}^{m-1} \\
0 & 0 & Q_2^{m-1} & 0 & \dots & 0 & 0 & \updownarrow k^{m-1} \\
\hline
0 & 0 & 0 & 0 & \dots & 0 & 0 & \updownarrow p^{m-2} - p^{m-1} \\
0 & 0 & 0 & 0 & \dots & 0 & 0 & \updownarrow p^{m-1} - q - \bar{k}^{m-2} \\
0 & 0 & 0 & Q_2^{m-2} & \dots & 0 & 0 & \updownarrow k^{m-2} \\
\hline
\vdots & \vdots & \vdots & \vdots & \ddots & \vdots & \vdots & \\
\hline
0 & 0 & 0 & 0 & \dots & 0 & 0 & \updownarrow p^2 - p^3 \\
0 & 0 & 0 & 0 & \dots & 0 & 0 & \updownarrow p^3 - q - \bar{k}^2 \\
0 & 0 & 0 & 0 & \dots & Q_2^2 & 0 & \updownarrow k^2 \\
\hline
0 & 0 & 0 & 0 & \dots & 0 & 0 & \updownarrow p^1 - p^2 \\
0 & 0 & 0 & 0 & \dots & 0 & 0 & \updownarrow p^2 - q - \bar{k}^1 \\
0 & 0 & 0 & 0 & \dots & 0 & Q_2^1 & \updownarrow \bar{k}^1 \\
0 & 0 & 0 & 0 & \dots & 0 & 0 & \updownarrow q
\end{array}\right] \tag{6.42}
$$

$$
M^1 = \left[\begin{array}{c} 0 \\ M_o \end{array}\right] \begin{array}{l} \updownarrow n^1 - q \\ \updownarrow q \end{array}, \qquad C^1 = \left[\begin{array}{cc} 0 & \bar{C}_2^1 \end{array}\right] \tag{6.43}
$$

where $Y^{m-1} = \left[\begin{array}{cc} A_{3112}^{m-1\ o} & 0 \\ A_{3122}^{m-1\ o} & A_{322}^{m-1\ o} \end{array}\right]$ is square and invertible.

Proposition 6.1 *The maximum number of observers for any particular system is* $m \leq n^1 - p^1$*, where* m *denotes the observers count.*

Proof

Denote $\mathcal{J}(X)$ and $\mathcal{K}(X)$ to respectively represent the number of rows and columns of the matrix X. From (6.11), it has been established that $p^{i+1} \leq p^i$; this results in

$$\mathcal{K}(Y^{i+1}) \leq \mathcal{K}(Y^i) \tag{6.44}$$

Denote A_r to be the elements to the right of Y^1 in (6.41), hence $\mathcal{K}(A_r) = p^1$ which results in

$$\mathcal{K}(A_{123}^{m-1}) + \sum_{j=1}^{m-1} \mathcal{K}(Y^j) \leq n^1 - p^1 \tag{6.45}$$

To guarantee DDFR, it requires $rank(A_{123}^{m-1}) \geq 1$ and subsequently from (6.45)

$$\sum_{j=1}^{m-1} \mathcal{K}(Y^j) \leq n^1 - p^1 - 1 \tag{6.46}$$

It can be seen that $\mathcal{J}(Y^{m-1}) = \mathcal{K}(A_{123}^{m-1})$ which results in $\mathcal{J}(Y^{m-1}) = \mathcal{K}(Y^{m-1}) \geq 1$ and therefore from (6.44) yields

$$\mathcal{K}(Y^{m-1}), \mathcal{K}(Y^{m-2}), \ldots, \mathcal{K}(Y^1) \geq 1 \tag{6.47}$$

Combining (6.46) and (6.47), it is straightforward to show that

$$m - 1 \leq n^1 - p^1 - 1 \Rightarrow m \leq n^1 - p^1$$

Hence the proof is complete. ■

Theorem 6.1 *All m observers will have a stable sliding motion if $\left(A^1, \begin{bmatrix} M^1 & Q^1 \end{bmatrix}, C^1\right)$ is minimum phase.*

The remainder of this section will provide a constructive proof of Theorem 6.1.

From (6.27), the reduced order sliding motion for each observer is governed by $A_1^i + L_o^i A_{31}^i$. Hence the pair (A_1^i, A_{31}^i) from (6.19) must be detectable. ♯

Proposition 6.2 *Partition Q^i from (6.22) as $Q^i = \begin{bmatrix} Q_a^i & Q_b^i \end{bmatrix}$ where Q_a^i has $h-\bar{k}^i$ columns and Q_b^i has $\bar{k}^i$ columns and the unobservable modes of (A_1^i, A_{31}^i) are given by the invariant zeros of $\left(A^i, \begin{bmatrix} Q_b^i & M^i \end{bmatrix}, C^i\right)$.*

Proof

The Rosenbrock system matrix [157] of the triple $\left(A^i, \begin{bmatrix} Q_b^i & M^i \end{bmatrix}, C^i\right)$ is given by

$$\mathcal{P}_1(s) := \begin{bmatrix} sI - A^i & Q_b^i & M^i \\ C^i & 0 & 0 \end{bmatrix} \tag{6.48}$$

According to Rosenbrock [157], the invariant zeros of the system are the values of s that cause its Rosenbrock matrix to lose normal rank.

Substituting for A^i, Q_b^i, M^i, C^i from (6.19), (6.22) and (6.23) into $\mathcal{P}_1(s)$ yields

$$\mathcal{P}_1(s) = \begin{bmatrix} sI - A_1^i & * & 0 & 0 \\ -A_{31}^i & * & 0 & 0 \\ -A_{32a}^i & * & \bar{Q}_2^i & 0 \\ -A_{32b}^i & * & 0 & M_o \\ 0 & \bar{C}_2^i & 0 & 0 \end{bmatrix}$$

where A_{32a}^i and A_{32b}^i are the top $\bar{k}^i$ rows and bottom q rows of the matrix A_{32}^i respectively. Since $\bar{Q}_2^i, M_o$ and $\bar{C}_2^i$ are square and invertible, then $\mathcal{P}_1(s)$ loses rank if and only if $\mathcal{P}_2(s)$ loses rank where

$$\mathcal{P}_2(s) := \begin{bmatrix} sI - A_1^i \\ -A_{31}^i \end{bmatrix} \tag{6.49}$$

From the Popov-Hautus-Rosenbrock (PHR) rank test by Rosenbrock [157], it is clear that $\mathcal{P}_2(s)$ loses rank when s is an unobservable mode of (A_1^i, A_{31}^i) and hence, the proof is complete. ■

Proposition 6.3 *The unobservable modes of observer i are the unobservable modes of observer $(i+1)$.*

Proof

From Proposition 6.2, the unobservable modes of observer i are the values of s that make

$$\mathcal{P}_2(s) = \begin{bmatrix} sI - A_1^i \\ -A_{31}^i \end{bmatrix} \tag{6.50}$$

loses rank.

Substitute for A_1^i and A_{31}^i from (6.20) using PHR rank test by Rosenbrock [157],

$$\mathcal{P}_2(s) := \begin{bmatrix} sI - A_{11}^i & -A_{12}^i \\ -A_{13}^i & sI - A_{14}^i \\ 0 & -A_{312}^i \end{bmatrix}$$

and given the fact that A_{312}^i has full column rank, the unobservable modes of observer i are the unobservable modes of (A_{11}^i, A_{13}^i) and they are the values of s that make the following matrix pencil to lose rank

$$\mathcal{R}_1(s) := \begin{bmatrix} sI - A_{11}^i \\ -A_{13}^i \end{bmatrix} \tag{6.51}$$

From Proposition 6.2, the unobservable modes of observer $(i+1)$ are the invariant zeros of $\left(A^{i+1}, \begin{bmatrix} Q_b^{i+1} & M^{i+1} \end{bmatrix}, C^{i+1}\right)$. Using the definition of $\bar{Q}_2^i$ from (6.8), it is clear that

$$Q_b^{i+1} = \begin{bmatrix} 0 & 0 \\ 0 & 0 \\ Q_2^{i+1} & 0 \\ 0 & \bar{Q}_2^i \\ 0 & 0 \end{bmatrix} \begin{matrix} \\ \\ \updownarrow k^{i+1} \\ \updownarrow \bar{k}^i \\ \updownarrow q \end{matrix}$$

From (6.35) - (6.38), the Rosenbrock system matrix of $\left(A^{i+1}, \begin{bmatrix} Q_b^{i+1} & M^{i+1} \end{bmatrix}, C^{i+1}\right)$, is

given by

$$\mathcal{P}_3(s) := \left[\begin{array}{cccccc|cc|c} sI - A^i_{111} & -A^i_{121} & * & 0 & 0 & 0 & 0 & 0 \\ -A^i_{131} & sI - A^i_{141} & * & 0 & 0 & 0 & 0 & 0 \\ -A^i_{113} & -A^i_{123} & * & 0 & 0 & 0 & 0 & 0 \\ -A^i_{133} & -A^i_{143} & * & 0 & 0 & Q_2^{i+1} & 0 & 0 \\ -A^i_{331} & -A^i_{341} & * & -\alpha_1 I_{\bar{k}^i} & 0 & 0 & \bar{Q}_2^i & 0 \\ -A^i_{351} & -A^i_{361} & * & 0 & -\alpha_2 I_q & 0 & 0 & M_o \\ \hline 0 & 0 & 0 & 0 & 0 & 0 & 0 & 0 \\ 0 & 0 & Y^i & 0 & 0 & 0 & 0 & 0 \\ 0 & 0 & 0 & I_{\bar{k}^i} & 0 & 0 & 0 & 0 \\ 0 & 0 & 0 & 0 & I_q & 0 & 0 & 0 \end{array}\right] \tag{6.52}$$

Since $Q_2^{i+1}, \bar{Q}_2^i, M_o$ and Y^i are square and invertible, the matrix $\mathcal{P}_3(s)$ will lose rank if and only if the following matrix loses rank

$$\mathcal{R}_2(s) := \left[\begin{array}{cc} sI - A^i_{111} & -A^i_{121} \\ -A^i_{131} & sI - A^i_{141} \\ -A^i_{113} & -A^i_{123} \end{array}\right] \tag{6.53}$$

Therefore, the unobservable modes of observer $(i+1)$ are the values of s that make the matrix pencil $\mathcal{R}_2(s)$ to lose rank.

By expanding A^i_{11} and A^i_{13} using (6.21), it is clear that if $\mathcal{R}_1(s)$ loses rank, then $\mathcal{R}_2(s)$ loses rank too. Hence an unobservable mode of observer i will also be an unobservable mode of observer $(i+1)$. ■

Proposition 6.4 *If the system* $\left(A^1, \left[\begin{array}{cc} M^1 & Q^1 \end{array}\right], C^1\right)$ *is minimum phase, then it can also be shown that* $\left(A^m, \left[\begin{array}{cc} M^m & Q^m \end{array}\right], C^m\right)$ *is also minimum phase.*

Proof

The Rosenbrock system matrix of $\left(A^1, \begin{bmatrix} M^1 & Q^1 \end{bmatrix}, C^1\right)$ can be written as

$$\mathcal{P}_4(s) := \begin{bmatrix} sI - A^1 & Q^1 & M^1 \\ C^1 & 0 & 0 \end{bmatrix} \tag{6.54}$$

Substituting from the structures obtained in (6.41) - (6.43), $\mathcal{P}_4(s)$ can be written as

$$\left[\begin{array}{cc|ccccccc|c|cccc|cc}
sI-A_{111}^{m-1} & -A_{121}^{m-1} & * & * & \dots & * & * & * & 0 & 0 & 0 & 0 & 0 & \dots & 0 & 0 \\
-A_{131}^{m-1} & sI-A_{141}^{m-1} & * & * & \dots & * & * & * & 0 & \bar{Q}_1^m & 0 & 0 & 0 & \dots & 0 & 0 \\
-A_{113}^{m-1} & -A_{123}^{m-1} & * & * & \dots & * & * & * & 0 & 0 & 0 & 0 & 0 & \dots & 0 & 0 \\
-A_{133}^{m-1} & -A_{143}^{m-1} & * & * & \dots & * & * & * & 0 & 0 & Q_2^m & 0 & 0 & \dots & 0 & 0 \\
\hline
0 & 0 & 0 & * & \dots & * & * & * & 0 & 0 & 0 & 0 & 0 & \dots & 0 & 0 \\
0 & 0 & Y^{m-1} & * & \dots & * & * & * & 0 & 0 & 0 & 0 & 0 & \dots & 0 & 0 \\
* & * & * & * & \dots & * & * & * & 0 & 0 & 0 & Q_2^{m-1} & 0 & \dots & 0 & 0 \\
\hline
0 & 0 & 0 & 0 & \dots & * & * & * & 0 & 0 & 0 & 0 & 0 & \dots & 0 & 0 \\
0 & 0 & 0 & Y^{m-2} & \dots & * & * & * & 0 & 0 & 0 & 0 & 0 & \dots & 0 & 0 \\
* & * & * & * & \dots & * & * & * & 0 & 0 & 0 & 0 & Q_2^{m-2} & \dots & 0 & 0 \\
\hline
\vdots & \vdots & \vdots & \vdots & \ddots & \vdots & \vdots & \vdots & \vdots & \vdots & \vdots & \vdots & \vdots & \ddots & \vdots & \vdots \\
\hline
0 & 0 & 0 & 0 & \dots & 0 & * & * & 0 & 0 & 0 & 0 & 0 & \dots & 0 & 0 \\
0 & 0 & 0 & 0 & \dots & Y^2 & * & * & 0 & 0 & 0 & 0 & 0 & \dots & 0 & 0 \\
* & * & * & * & \dots & * & * & * & 0 & 0 & 0 & 0 & 0 & \dots & Q_2^2 & 0 \\
\hline
0 & 0 & 0 & 0 & \dots & 0 & 0 & * & 0 & 0 & 0 & 0 & 0 & \dots & 0 & 0 \\
0 & 0 & 0 & 0 & \dots & 0 & Y^1 & * & 0 & 0 & 0 & 0 & 0 & \dots & 0 & 0 \\
* & * & * & * & \dots & * & * & * & 0 & 0 & 0 & 0 & 0 & \dots & 0 & Q_2^1 \\
* & -A_{361}^{m-1} & * & * & \dots & * & * & * & M_o & 0 & 0 & 0 & 0 & \dots & 0 & 0 \\
\hline
0 & 0 & 0 & 0 & \dots & 0 & 0 & \bar{C}_2^1 & 0 & 0 & 0 & 0 & 0 & \dots & 0 & 0
\end{array}\right] \tag{6.55}$$

Since $M_o, \bar{C}_2^1, Q_2^m \dots Q_2^1, Y^{m-1} \dots Y^1$ and Q_{11}^m are square and invertible, the matrix $\mathcal{P}_4(s)$

loses rank if and only if the following matrix loses rank

$$\mathcal{R}_3(s) := \begin{bmatrix} sI - A_{111}^{m-1} & -A_{121}^{m-1} \\ -A_{113}^{m-1} & -A_{123}^{m-1} \end{bmatrix} \tag{6.56}$$

As for $\left(A^m, \begin{bmatrix} M^m & Q^m \end{bmatrix}, C^m\right)$, its Rosenbrock matrix $\mathcal{P}_5(s)$, expanding using (6.37) - (6.38) yields

$$\mathcal{P}_5(s) := \left[\begin{array}{cc|cccc|cccc} sI - A_{111}^{m-1} & -A_{121}^{m-1} & * & * & * & * & 0 & 0 & 0 & 0 \\ -A_{131}^{m-1} & sI - A_{141}^{m-1} & * & * & * & * & 0 & \bar{Q}_1^m & 0 & 0 \\ -A_{113}^{m-1} & -A_{123}^{m-1} & * & * & * & * & 0 & 0 & 0 & 0 \\ -A_{133}^{m-1} & -A_{143}^{m-1} & * & * & * & * & 0 & 0 & Q_2^m & 0 \\ -A_{331}^{m-1} & -A_{341}^{m-1} & * & * & * & * & 0 & 0 & 0 & \bar{Q}_2^{m-1} \\ -A_{351}^{m-1} & -A_{361}^{m-1} & * & * & * & * & M_o & 0 & 0 & 0 \\ \hline 0 & 0 & A_{3112}^{m-1\ o} & 0 & 0 & 0 & 0 & 0 & 0 & 0 \\ 0 & 0 & A_{3122}^{m-1\ o} & A_{322}^{m-1\ o} & 0 & 0 & 0 & 0 & 0 & 0 \\ 0 & 0 & 0 & 0 & I & 0 & 0 & 0 & 0 & 0 \\ 0 & 0 & 0 & 0 & 0 & I & 0 & 0 & 0 & 0 \end{array}\right] \tag{6.57}$$

Since $\bar{Q}_1^m, Q_2^m, \bar{Q}_2^{m-1}, A_{3112}^{m-1\ o}$ and $A_{322}^{m-1\ o}$ are square and invertible, therefore $\mathcal{P}_5(s)$ will lose rank if and only if $\mathcal{R}_4(s)$ loses rank where

$$\mathcal{R}_4(s) := \begin{bmatrix} sI - A_{111}^{m-1} & -A_{121}^{m-1} \\ -A_{113}^{m-1} & -A_{123}^{m-1} \end{bmatrix} = \mathcal{R}_3(s) \tag{6.58}$$

$\left(A^m, \begin{bmatrix} M^m & Q^m \end{bmatrix}, C^m\right)$ and $\left(A^1, \begin{bmatrix} M^1 & Q^1 \end{bmatrix}, C^1\right)$ have the same zeros and therefore the proposition is proven. ■

Proposition 6.5 *If* $\left(A^m, \begin{bmatrix} M^m & Q^m \end{bmatrix}, C^m\right)$ *is minimum phase, then it can also be shown that* $\left(A^m, \begin{bmatrix} M^m & Q_b^m \end{bmatrix}, C^m\right)$ *is minimum phase.*

Proof

From Proposition 6.2 and (6.53), the invariant zeros of $\left(A^m, \left[M^m \; Q_b^m\right], C^m\right)$ is given by

$$\mathcal{R}_2(s) = \begin{bmatrix} sI - A_{111}^{m-1} & -A_{121}^{m-1} \\ -A_{131}^{m-1} & sI - A_{141}^{m-1} \\ -A_{113}^{m-1} & -A_{123}^{m-1} \end{bmatrix}$$

and from Proposition 6.4 through (6.58), the invariant zeros of $\left(A^m, \left[M^m \; Q^m\right], C^m\right)$ is

$$\mathcal{R}_4(s) = \begin{bmatrix} sI - A_{111}^{m-1} & -A_{121}^{m-1} \\ -A_{113}^{m-1} & -A_{123}^{m-1} \end{bmatrix}$$

If $\mathcal{R}_2(s)$ loses rank then $\mathcal{R}_4(s)$ also loses rank, but the converse is not necessarily true.

As a result, the invariant zeros of $\left(A^m, \begin{bmatrix} M^m & Q_b^m \end{bmatrix}, C^m\right)$ will also be the invariant zeros of $\left(A^m, \begin{bmatrix} M^m & Q^m \end{bmatrix}, C^m\right)$. ■

Hence, combining Propositions 6.2 and 6.4 mean that if $\left(A^1, \begin{bmatrix} M^1 & Q^1 \end{bmatrix}, C^1\right)$ is minimum phase, then observer m will be detectable since $Q^i = \begin{bmatrix} Q_a^i & Q_b^i \end{bmatrix}$. Then, using Proposition 6.3, it further implies that all previous observers are also detectable. Therefore, if $\left(A^1, \begin{bmatrix} M^1 & Q^1 \end{bmatrix}, C^1\right)$ is minimum phase, then all observers have a stable sliding motion and Theorem 6.1 is proven.

6.4 An Example

The method described in this chapter will be demonstrated using a simulation example. Consider a 2nd order rotational system

$$\ddot{\theta} + 3\dot{\theta} + 2\theta = u \tag{6.59}$$

where θ is the position while u is the applied torque. Assume that the torque is generated by a device where

$$\dot{u} = -0.1u + 0.1u_c + \xi$$

where u_c is the torque command (measurable control input) and ξ is an unknown nonlinearity in the device generating the torque. Assume that θ and u are measurable, and that the sensor for u is faulty, which results in $u_m = u + f$ where u_m is the sensor measurement of u and f is the sensor fault. Filter the faulty measurement of u using the equation $\dot{z}_f = -z_f + u_m$. Therefore, by defining $x = \begin{bmatrix} \dot{\theta} & u & \theta & z_f \end{bmatrix}^T$ the following state-space system can be generated

$$\dot{x}^1 = A^1x^1 + B^1u_c + M^1f + Q^1\xi^1 \tag{6.60}$$

$$y^1 = C^1x^1 \tag{6.61}$$

where

$$A^1 := \left[\begin{array}{cc|cc} -3 & 1 & -2 & 0 \\ 0 & -0.1 & 0 & 0 \\ \hline 1 & 0 & 0 & 0 \\ 0 & 1 & 0 & -1 \end{array}\right], Q^1 := \left[\begin{array}{c} 0 \\ 1 \\ \hline 0 \\ 0 \end{array}\right], C^1 := \begin{bmatrix} 0 & I_2 \end{bmatrix} \tag{6.62}$$

$$M^1 := \left[\begin{array}{c} 0 \\ 0 \\ \hline 0 \\ 1 \end{array}\right], B^1 := \begin{bmatrix} 0 \\ 0.1 \\ 0 \\ 0 \end{bmatrix} \tag{6.63}$$

6.4.1 Preliminary Checks

From the parameters above, it can be seen that $n^1 = 4, p^1 = 2, q^1 = 1, h^1 = 1, C^1Q^1 = 0 \Rightarrow \bar{k}^1 = 0$. By comparing (6.62) - (6.63) with (6.8) - (6.10), note that $\breve{A}^1_{36} \neq 0$. In the scenario where $\breve{A}^1_{36} \neq 0$ and $\breve{A}^1_{32} = 0$, notice that $\hat{C}_2$ from (4.24) in Chapter 4 will be non-zero and therefore DDFR will be impossible. Hence, for the system (6.62) - (6.63), it is impossible

to achieve DDFR using only 1 observer.

It then follows that $k^2 = rank(\breve{A}^1_{32}) = 0$ and $p^2 = 2$ (refer to (6.11)). From the values of $\breve{A}^1_{31}$ and $\breve{A}^1_{32}$, it can be shown that $R^1_1 = R^1_2 = R^1_3 = R^1_4 = R^1_5$ which results in

$$T^1_2 = \bar{T}^1_2 = \begin{bmatrix} 0 & 1 & 0 & 0 \\ 1 & 0 & 0 & 0 \\ 0 & 0 & 1 & 0 \\ 0 & 0 & 0 & 1 \end{bmatrix}$$

Apply the change of coordinates $\bar{T}^1_2$ to the matrices in (6.62) - (6.63) places them in the structure of (6.21) - (6.23) where

$$A^1 = \begin{bmatrix} -0.1000 & 0 & 0 & 0 \\ 1.0000 & -3.0000 & -2.0000 & 0 \\ 0 & 1.0000 & 0 & 0 \\ 1.0000 & 0 & 0 & -1.0000 \end{bmatrix}, \quad Q^1 = \begin{bmatrix} 1 \\ 0 \\ 0 \\ 0 \end{bmatrix}$$

$A^1_{141} = -0.1, A^1_{132} = 0, A^1_{123} = 1, A^1_{114} = -3, A^1_{3112^o} = 1, A^1_{361} = 1, A^1_{352} = 0$ and the other parameters in (6.21) are empty matrices (do not exist). This satisfies condition F1 and thus confirms that DDFR is possible with 2 observers using the method proposed in this chapter. It can also be verified that $\left(A^1, \begin{bmatrix} M^1 & Q^1 \end{bmatrix}, C^1\right)$ is minimum phase.

6.4.2 Observers Design

Choosing $L^1_o = \begin{bmatrix} 0 \\ -3 \end{bmatrix}$ causes $\lambda(A^1_1 + L^1 A^1_3) = \{-6, -0.1\}$. Then the following choices of $\bar{P}^1_o, G^1_l, G^1_n$

$$\bar{P}_o^1 = I_2,\ \ G_l^1 = \begin{bmatrix} 10.7115 & 12.2511 \\ 5.0883 & 5.1838 \\ 8.5494 & 1.4967 \\ 2.2864 & 7.3506 \end{bmatrix},\ \ G_n^1 = \begin{bmatrix} 0 & 0 \\ 3 & 0 \\ 1 & 0 \\ 0 & 1 \end{bmatrix}$$

guarantee a sliding motion on the first observer.

Choosing $\alpha_1^1 = \alpha_2^1 = 1$ results in the following matrices

$$A^2 = \left[\begin{array}{c|cc} -0.1000 & 0 & 0 \\ \hline 1.0000 & -6.0000 & 0 \\ 1.0000 & 0 & -1.0000 \end{array}\right],\ \ Q^2 = \left[\begin{array}{c} 1 \\ \hline 0 \\ 0 \end{array}\right],\ \ M^2 = \left[\begin{array}{c} 0 \\ \hline 0 \\ 1 \end{array}\right],\ \ C^2 = \begin{bmatrix} 0 & I_2 \end{bmatrix}$$

To design the second observer, $L_o^2 = -3$ is chosen and therefore $\lambda(A_1^2 + L^2 A_3^2) = -3.1$, and with that the choices of $\bar{P}_o^2, G_l^2$ and G_n^2 whereby

$$\bar{P}_o^2 = I_2,\ \ G_l^2 = \begin{bmatrix} 5.8544 & 5.3534 \\ 0.0754 & 1.8857 \\ 2.0070 & 4.8246 \end{bmatrix},\ \ G_n^2 = \begin{bmatrix} 3 & 0 \\ 1 & 0 \\ 0 & 1 \end{bmatrix}$$

will guarantee a stable sliding motion for the second observer.

Then choosing $W_1^2 = 1$ to get $W^2 = \begin{bmatrix} -1 & 1 \end{bmatrix}$ and DDFR can be achieved.

6.4.3 Simulation Results

A fault is injected into the sensor of u together with the disturbance ξ. The left subfigure of Figure 6.1 shows the actual fault while the right subfigure of it shows the fault reconstruction, which is identical to the fault despite the presence of the disturbance ξ as shown in Figure 6.2, thus achieving DDFR. The simulation is then repeated with a different fault scenario where the fault signal is set to be a ramp signal. The result is shown in Figure 6.3.

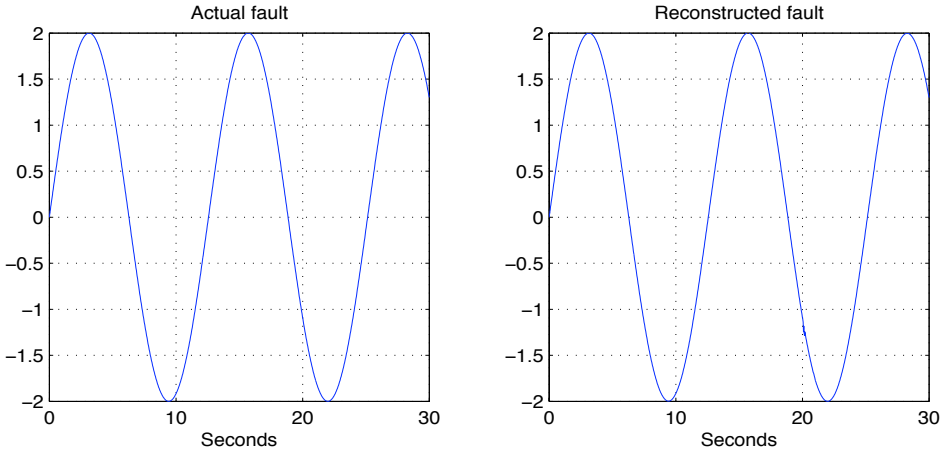

Figure 6.1: The left subfigure is f, the right subfigure is $\hat{f}$.

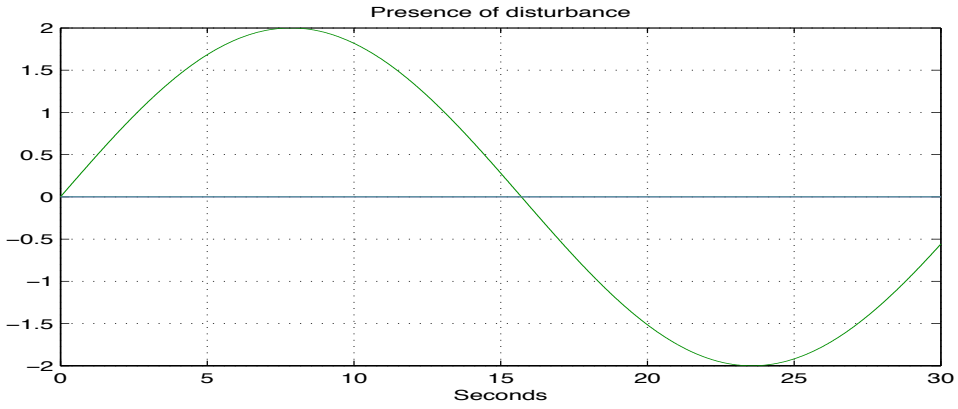

Figure 6.2: The disturbance ξ acting onto the system.

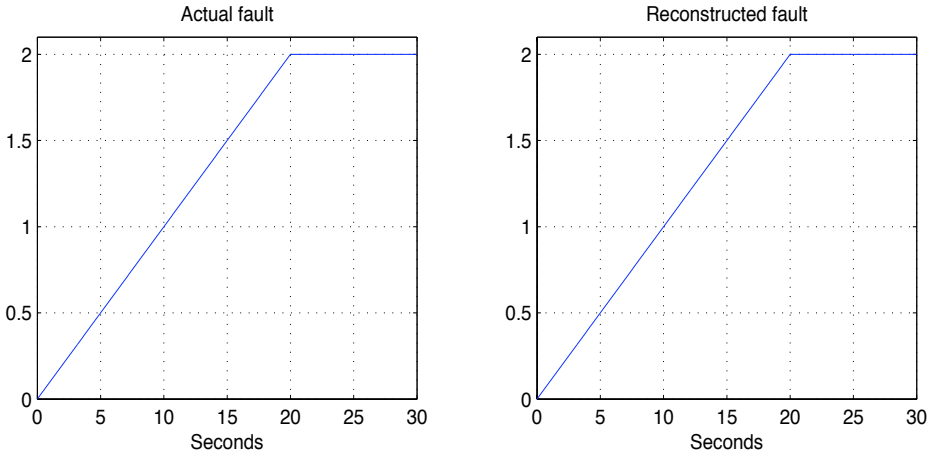

Figure 6.3: The left subfigure is f, the right subfigure is $\hat{f}$.

6.5 Conclusion

This chapter has presented new results in DDFR using multiple sliding mode observers in cascade mode. Measurable signals from a previous observer are treated as the output for the subsequent observer. The faults are then reconstructed using the final observer in the cascade arrangement. It was found that by using cascaded sliding mode observers, DDFR could then be applicable to a wider class of systems, compared to situations if only one observer is being used. The chapter has presented a systematic way to check if DDFR is achievable from the original system matrices, thus making it easier for the designer to know if DDFR is feasible. And if the method is applicable, the sufficient number of observers needed could be known as well. It is also possible to know if DDFR is not guaranteed for the system under observation. A rotational system model was used to demonstrate the claims made in this chapter and for the example, it was found that a single observer is not able to reconstruct the faults. However, by using 2 observers in cascade, the faults were successfully reconstructed despite the presence of disturbances.

Chapter 7

Robust Fault Reconstruction for Systems with Deficient First Markov Matrices

7.1 Introduction

The previous few chapters of this thesis have discussed the concept of DDFR on actuator and sensor faults (Chapters 4 and 5 respectively) as well as the use of multiple sliding mode observers for DDFR (Chapter 6) when Condition C3 in Chapter 4 is not satisfied. However, the work in those previous chapters assumed that the first Markov parameter (the product of output and fault matrices) is full rank. If this condition is not fulfilled, then DDFR is not feasible. In addition, this is one of the necessary conditions that some of the existing work in the literature, most notably by Edwards *et al.* [55, 54, 177] and Saif & Guan [158], need to meet in order to achieve fault reconstruction. As a result, this limits the class of systems where the schemes by Edwards *et al.* [55, 54, 177] and Saif & Guan [158] are applicable.

Recently, there have been developments in the area of fault reconstruction for systems where the first Markov parameter is not full rank. Floquet & Barbot [62] transformed the system into an 'output information' form such that existing sliding mode observer techniques could be implemented to perfectly estimate the states in finite time and reconstruct faults. However, their algorithm does not consider disturbances, unless the unknown inputs (faults) vectors are augmented with the disturbances vector, as done by Saif & Guan [158]. In addition to that, the class of systems for which the transformation is feasible is not known, and therefore it is not easy for the designer to immediately recognise whether the algorithm is suitable for the system under consideration. Davila *et al.* [36] developed a 2nd order sliding

mode observer for nonlinear mechanical systems, i.e. 2nd order differential equations, arising from Newton's laws where only position (and not velocity) is measured. The work by Davila *et al.* [36] could be easily extended to the case of robust fault reconstruction for actuator faults occurring in the acceleration equation. However, it is applicable only to a limited class of systems as it requires that *all* position signals of the system to be measurable.

This chapter presents a robust fault reconstruction method for a class of systems of which the first Markov parameter is not full rank, relaxing the condition required by the previous work by Edwards *et al.* [55, 54, 177]. The method to be discussed in this chapter essentially uses two sliding mode observers in cascade, which are designed based on the method shown in Edwards & Spurgeon [52]. Suitable processing of the equivalent output error injection in the first observer yields the measurable output of a 'fictitious' system where the first Markov parameter is full rank. This signifies that the robust fault reconstruction method by Tan & Edwards [177] is applicable to the fictitious system and a second observer is implemented on the fictitious system to generate a reconstruction of the fault that is robust to the disturbances. This approach is applicable to a wider class of systems for which the methods by Edwards *et al.* [54, 55, 177] are not applicable. Furthermore, this chapter considers robustness against disturbances, as opposed to the work by Floquet & Barbot [62], and the scheme may be feasible for systems for which the method by Davila *et al.* [36] is not applicable. An aircraft system model taken from the FDI literature will be used to demonstrate the method proposed in this chapter.

The work described in this chapter has been published as a journal paper [140] as well as a conference paper [141].

7.2 Preliminaries and Statement of Main Result

Consider a system

$$\dot{\tilde{x}} = \tilde{A}\tilde{x} + \tilde{B}u + \tilde{M}f + \tilde{Q}\tilde{\xi} \tag{7.1}$$

$$y = \tilde{C}\tilde{x} \tag{7.2}$$

where $\tilde{x} \in \mathbb{R}^{\tilde{n}}$, $y \in \mathbb{R}^p, u \in \mathbb{R}^m$ are the states, outputs and inputs respectively with $\tilde{n} \geq p$. The vector $f \in \mathbb{R}^q$ is an unknown fault and $\tilde{\xi} \in \mathbb{R}^h$ is an unknown disturbance, which encapsulates all nonlinearities and unknowns in the system as shown in Chen & Patton [16]. Assume without loss of generality that $rank(\tilde{M}) = q, rank(\tilde{Q}) = h, rank(\tilde{C}) = p$ and suppose that $rank(\tilde{C}\tilde{M}) = r < q < p$. In previous chapters, it was assumed that $rank(\tilde{C}\tilde{M}) = q$. Also assume that $(\tilde{A}, \tilde{C})$ is observable.

The objective is to reconstruct the fault f whilst being robust to $\tilde{\xi}$. Edwards *et al.* [55, 54] have reconstructed the fault f for the case when $\tilde{\xi} = 0$. Tan & Edwards [177] built on this early work and presented a method that minimises the $\mathcal{L}_2$ gain from $\tilde{\xi}$ to the fault reconstruction. In the work by Edwards *et al.* [55, 54, 177], the fault reconstruction scheme is feasible if and only if the following conditions are satisfied

G1. $rank(\tilde{C}\tilde{M}) = rank(\tilde{M}) = q$

G2. The invariant zeros of $(\tilde{A}, \tilde{M}, \tilde{C})$ (if any) are stable

Condition G1 implies that the first Markov parameter of the system is full rank, and condition G2 implies that the system is minimum phase. These conditions are also often assumed if Unknown Input Observers (UIOs) are employed for fault reconstruction, as shown by Saif & Guan [158] and Edwards & Tan [56]. This chaper proposes a method to robustly reconstruct the fault when condition G1 is not satisfied.

With reference to Saif & Guan [158], assume that the disturbance $\tilde{\xi}$ is piecewise continuous such that

$$\dot{\tilde{\xi}} = A_\Omega \tilde{\xi} + B_\Omega \xi \tag{7.3}$$

where $\xi \in \mathbb{R}^h$ and $A_\Omega \in \mathbb{R}^{h \times h}$ is stable and $B_\Omega \in \mathbb{R}^{h \times h}$. This is not an unreasonable assumption provided the frequency content of $\tilde{\xi}$ is known. If $\tilde{\xi}$ is known to be a signal in the frequency region $\omega_1 < \omega < \omega_2$, then the system (7.3) can be taken to be first order filters with cut-off frequency ω_2.

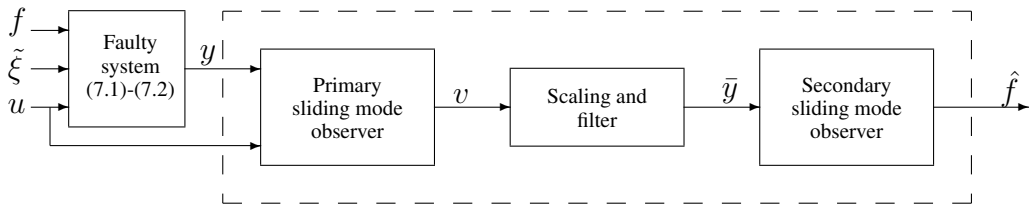

Figure 7.1: Schematic diagram of the scheme proposed in this chaper

Theorem 7.1 *For the case when G1 is not satisfied, i.e.* $r = rank(\tilde{C}\tilde{M}) < rank(\tilde{M}) = q$*, then the fault* f *can be reconstructed by the scheme given in Figure 7.1 such that the* $\mathcal{L}_2$ *gain from* ξ *to the fault reconstruction will be bounded if and only if*

H1. $rank \begin{bmatrix} \tilde{C}\tilde{A}\tilde{M} & \tilde{C}\tilde{M} \\ \tilde{C}\tilde{M} & 0 \end{bmatrix} = rank(\tilde{C}\tilde{M}) + rank(\tilde{M})$

H2. The invariant zeros of $(\tilde{A}, \tilde{M}, \tilde{C})$ (if any) must be stable □

In the scheme in Figure 7.1 $\hat{f}$ is the reconstruction of the fault f, whilst v and $\bar{y}$ are intermediate signals that will be defined later.

Comparing Conditions H1 and G1, it is clear that H1 is less restrictive than G1, i.e. if G1 is satisfied then H1 will also be satisfied, but the converse is not necessarily true. In the case when G1 is satisfied, the method proposed in this chaper is also applicable since $\hat{f}$ can be calculated directly from the output of the primary observer in Figure 7.1. In practice however, the simpler scheme shown by Tan & Edwards [177] would be used in preference.

The next section will provide a constructive proof for Theorem 7.1.

7.3 Robust Fault Reconstruction

Firstly, four lemmas will be introduced to provide a canonical form which underpins the scheme that will be developed. The first is concerned with the system in (7.1) - (7.2) and imposes specific structures on the output and fault distribution matrices.

Lemma 7.1 *There exist appropriately dimensioned nonsingular linear transformations of* $\tilde{x} \mapsto T_1\tilde{x}, f \mapsto T_2 f$ *such that the triple* $\tilde{A}, \tilde{M}, \tilde{C}$ *from (7.1) - (7.2) in the new coordinates are given by*

$$\tilde{A} = \begin{bmatrix} \tilde{A}_1 & \tilde{A}_2 \\ \tilde{A}_3 & \tilde{A}_4 \end{bmatrix}, \tilde{C} = \begin{bmatrix} 0 & \tilde{T} \end{bmatrix}, \tilde{M} = \begin{bmatrix} \tilde{M}_1 \\ \tilde{M}_2 \end{bmatrix} \tag{7.4}$$

where $\tilde{A}_1 \in \mathbb{R}^{(\tilde{n}-p)\times(\tilde{n}-p)}, \tilde{M}_2 \in \mathbb{R}^{p\times q}$ *and* $\tilde{T} \in \mathbb{R}^{p\times p}$ *is orthogonal.*

Furthermore, the matrices $\tilde{M}_1, \tilde{M}_2$ *can be partitioned to have the form*

$$\tilde{M}_1 = \begin{bmatrix} \overset{q-r}{\longleftrightarrow} & \overset{r}{\longleftrightarrow} & \\ 0 & 0 & \updownarrow_{\tilde{n}-p-q+r} \\ M_{11} & 0 & \updownarrow_{q-r} \end{bmatrix} \quad \tilde{M}_2 = \begin{bmatrix} \overset{q-r}{\longleftrightarrow} & \overset{r}{\longleftrightarrow} & \\ 0 & 0 & \updownarrow_{p-r} \\ 0 & M_{22} & \updownarrow_{r} \end{bmatrix} \tag{7.5}$$

where M_{11}, M_{22} *are invertible. In this coordinate system,* $f \mapsto T_2 f = col(f_1, f_2)$ *where* $f_2 \in \mathbb{R}^r$. ♯

Proof

Since $\tilde{C}$ has full row rank, there exists an invertible change of coordinates $T_a = \begin{bmatrix} N_c \\ \tilde{C} \end{bmatrix}$ where N_c spans the null space of $\tilde{C}$, such that

$$M_a := T_a\tilde{M} = \begin{bmatrix} M_{a,1} \\ M_{a,2} \end{bmatrix}, \; C_a := \tilde{C}T_a^{-1} = \begin{bmatrix} 0 & I_p \end{bmatrix}$$

where $M_{a,2} \in \mathbb{R}^{p\times q}$. Since $rank(\tilde{C}\tilde{M}) = r$, then $rank(M_{a,2}) = r$. Hence, there exist orthogonal matrices $\tilde{T} \in \mathbb{R}^{p\times p}, T_2 \in \mathbb{R}^{q\times q}$ such that

$$\tilde{T}^T M_{a,2} T_2^T = \begin{bmatrix} 0 & 0 \\ 0 & M_{22} \end{bmatrix}$$

where $M_{22} \in \mathbb{R}^{r\times r}$ is invertible. Partition $M_{a,1}T_2^T = \begin{bmatrix} M_{a,11} & M_{a,12} \end{bmatrix}$ where $M_{a,12}$ has r columns. Then, let X_1 be an orthogonal matrix such that

$$X_1 M_{a,11} = \begin{bmatrix} 0 \\ M_{11} \end{bmatrix}$$

where $M_{11} \in \mathbb{R}^{(q-r)\times(q-r)}$ is invertible. Define $X_2 = \begin{bmatrix} 0 & -X_1 M_{a,12} M_{22}^{-1} \end{bmatrix} \tilde{T}^T$. Then apply the change of coordinates T_1 to M_a and C_a where

$$T_1 = \begin{bmatrix} X_1 & X_2 \\ 0 & \tilde{T}^T \end{bmatrix}$$

and post-multiply M_a by T_2^T to get

$$M = T_1 M_a T_2^T = \begin{bmatrix} 0 & 0 \\ M_{11} & 0 \\ 0 & 0 \\ 0 & M_{22} \end{bmatrix}, C = C_a T_1^{-1} = \begin{bmatrix} 0 & \tilde{T} \end{bmatrix}$$

and the coordinate transformation is complete.

Note that if $rank(\tilde{C}\tilde{M}) = q$, then M_{11} will not exist. ■

In the coordinate system of (7.4) - (7.5), further partition $\tilde{A}$ and $\tilde{Q}$ (generally) as

$$\tilde{A} = \begin{bmatrix} \tilde{A}_1 & \tilde{A}_2 \\ \tilde{A}_3 & \tilde{A}_4 \end{bmatrix} = \left[\begin{array}{cc|cc} \tilde{A}_{11} & \tilde{A}_{12} & \tilde{A}_{13} & \tilde{A}_{14} \\ \tilde{A}_{21} & \tilde{A}_{22} & \tilde{A}_{23} & \tilde{A}_{24} \\ \hline \tilde{A}_{31} & \tilde{A}_{32} & \tilde{A}_{33} & \tilde{A}_{34} \\ \tilde{A}_{41} & \tilde{A}_{42} & \tilde{A}_{43} & \tilde{A}_{44} \end{array}\right], \tilde{Q} = \begin{bmatrix} \tilde{Q}_1 \\ \tilde{Q}_2 \end{bmatrix} = \left[\begin{array}{c} \tilde{Q}_{11} \\ \tilde{Q}_{12} \\ \hline \tilde{Q}_{21} \\ \tilde{Q}_{22} \end{array}\right] \begin{array}{l} \updownarrow \tilde{n}-p-q+r \\ \updownarrow q-r \\ \updownarrow p-r \\ \updownarrow r \end{array} \tag{7.6}$$

Now the system equations (7.1) - (7.2) and the uncertainty/disturbance model from (7.3) will be augmented to form the system which will be studied in the remainder of the chaper.

Combine (7.1) - (7.2) and (7.3) to obtain the following augmented system of order $n := \tilde{n}+h$

$$\underbrace{\begin{bmatrix} \dot{\tilde{\xi}} \\ \dot{\tilde{x}} \end{bmatrix}}_{\dot{x}} = \underbrace{\begin{bmatrix} A_\Omega & 0 \\ \tilde{Q} & \tilde{A} \end{bmatrix}}_{A} \underbrace{\begin{bmatrix} \tilde{\xi} \\ \tilde{x} \end{bmatrix}}_{x} + \underbrace{\begin{bmatrix} 0 \\ \tilde{B} \end{bmatrix}}_{B} u + \underbrace{\begin{bmatrix} 0 \\ \tilde{M} \end{bmatrix}}_{M} f + \underbrace{\begin{bmatrix} B_\Omega \\ 0 \end{bmatrix}}_{Q} \xi \tag{7.7}$$

$$y = \underbrace{\begin{bmatrix} 0 & \tilde{C} \end{bmatrix}}_{C} \underbrace{\begin{bmatrix} \tilde{\xi} \\ \tilde{x} \end{bmatrix}}_{x} \tag{7.8}$$

Now expand the matrices in (7.7) - (7.8) as in (7.4) - (7.5) to obtain

$$A = \left[\begin{array}{ccc|cc} A_\Omega & 0 & 0 & 0 & 0 \\ \tilde{Q}_{11} & \tilde{A}_{11} & \tilde{A}_{12} & \tilde{A}_{13} & \tilde{A}_{14} \\ \tilde{Q}_{12} & \tilde{A}_{21} & \tilde{A}_{22} & \tilde{A}_{23} & \tilde{A}_{24} \\ \hline \tilde{Q}_{21} & \tilde{A}_{31} & \tilde{A}_{32} & \tilde{A}_{33} & \tilde{A}_{34} \\ \tilde{Q}_{22} & \tilde{A}_{41} & \tilde{A}_{42} & \tilde{A}_{43} & \tilde{A}_{44} \end{array}\right] \begin{array}{l} \updownarrow_h \\ \updownarrow_{n-p-q+r-h} \\ \updownarrow_{q-r} \\ \updownarrow_{p-r} \\ \updownarrow_r \end{array} \tag{7.9}$$

$$M = \left[\begin{array}{cc} 0 & 0 \\ 0 & 0 \\ M_{11} & 0 \\ \hline 0 & 0 \\ 0 & M_{22} \end{array}\right], Q = \left[\begin{array}{c} B_\Omega \\ 0 \\ 0 \\ \hline 0 \\ 0 \end{array}\right], C = \begin{bmatrix} 0 & \tilde{T} \end{bmatrix} \tag{7.10}$$

Lemma 7.2 *The augmented pair (A, C) from (7.7) - (7.8) is detectable.* ♯

Proof

Let the matrices (A, C) be in the partitions of (7.9) - (7.10). By performing the Popov-Hautus-Rosenbrock (PHR) rank test [157] on the pair (A, C),

$$J_{a,1}(s) := \begin{bmatrix} sI - A \\ C \end{bmatrix}$$

and expanding $J_{a,1}(s)$ according to the coordinates in (7.9) - (7.10) produces

$$J_{a,1}(s) = \begin{bmatrix} sI - A_\Omega & 0 & 0 \\ -\tilde{Q}_1 & sI - \tilde{A}_1 & -\tilde{A}_2 \\ -\tilde{Q}_2 & -\tilde{A}_3 & sI - \tilde{A}_4 \\ 0 & 0 & \tilde{T} \end{bmatrix}$$

Since $\tilde{T}$ is square and invertible, therefore the matrix $J_{a,1}(s)$ will lose rank if and only if the following matrix loses rank

$$J_{a,2}(s) := \begin{bmatrix} sI - A_\Omega & 0 \\ -\tilde{Q}_1 & sI - \tilde{A}_1 \\ -\tilde{Q}_2 & -\tilde{A}_3 \end{bmatrix}$$

where it is obvious to see that $(\tilde{A}_\Omega, \tilde{Q}, \tilde{A}_1, \tilde{A}_3)$ are the unobservable modes of the pair (A, C). As for the Popov-Hautus-Rosenbrock (PHR) rank test [157] on $(\tilde{A}, \tilde{C})$, it is given by

$$J_{b,1}(s) := \begin{bmatrix} sI - \tilde{A} \\ \tilde{C} \end{bmatrix}$$

where it can be further partitioned according to (7.4) and (7.6) to be

$$J_{b,1}(s) = \begin{bmatrix} sI - \tilde{A}_1 & -\tilde{A}_2 \\ -\tilde{A}_3 & sI - \tilde{A}_4 \\ 0 & \tilde{T} \end{bmatrix}$$

Since $\tilde{T}$ is full rank, therefore $J_{b,1}(s)$ loses rank if and only if $J_{b,2}(s)$ loses rank where

$$J_{b,2}(s) := \begin{bmatrix} sI - \tilde{A}_1 \\ -\tilde{A}_3 \end{bmatrix}$$

As a result, it can be seen that the unobservable modes of $(\tilde{A}, \tilde{C})$ are given by $(\tilde{A}_1, \tilde{A}_3)$. Using the fact that $(\tilde{A}, \tilde{C})$ is observable if and only if $rank \begin{bmatrix} sI - \tilde{A}_1 \\ -\tilde{A}_3 \end{bmatrix} = \tilde{n} - p$ for all $s \in \mathbb{C}$, it is clear that the unobservable modes of (A, C) are given by $\lambda(A_\Omega)$. By assumption A_Ω is a stable matrix and therefore, (A, C) is detectable. ■

Lemma 7.3 *Condition H1 from the statement of Theorem 7.1 is satisfied if and only if $\tilde{A}_{32}$ from (7.6) has full column rank $q - r$.* ♯

Proof

Define

$$H := \begin{bmatrix} \tilde{C}\tilde{A}\tilde{M} & \tilde{C}\tilde{M} \\ \tilde{C}\tilde{M} & 0 \end{bmatrix} \tag{7.11}$$

Therefore from (7.4) - (7.5),

$$\begin{aligned} H &= \begin{bmatrix} \tilde{T} & 0 \\ 0 & \tilde{T} \end{bmatrix} \begin{bmatrix} \tilde{A}_3\tilde{M}_1 + \tilde{A}_4\tilde{M}_2 & \tilde{M}_2 \\ \tilde{M}_2 & 0 \end{bmatrix} \\ &= \begin{bmatrix} \tilde{T} & 0 \\ 0 & \tilde{T} \end{bmatrix} \left[\begin{array}{cc|cc} \tilde{A}_{32}M_{11} & \tilde{A}_{34}M_{22} & 0 & 0 \\ \tilde{A}_{42}M_{11} & \tilde{A}_{44}M_{22} & 0 & M_{22} \\ \hline 0 & 0 & 0 & 0 \\ 0 & M_{22} & 0 & 0 \end{array}\right] \end{aligned}$$

It is clear that $rank(H) = rank(M_{22}) + rank(M_{22}) + rank(\tilde{A}_{32}M_{11})$. Then it follows that $rank(H) = r + r + rank(\tilde{A}_{32}) = rank(\tilde{C}\tilde{M}) + r + rank(\tilde{A}_{32})$ since M_{11}, M_{22} are square and invertible. It is then straightforward to see that as $rank(\tilde{M}) = q$, Condition H1 holds if and only if $rank(\tilde{A}_{32}) = q - r$. ■

Define $\bar{p} := rank \begin{bmatrix} \tilde{Q}_{21} & \tilde{A}_{31} & \tilde{A}_{32} \end{bmatrix} + r$. It follows that $\bar{p} - r \leq min\{p - r, n - p\}$ and therefore $\bar{p} \leq p$. Since condition H1 implies that $\tilde{A}_{32}$ has full column rank, then $\bar{p} - r \geq q - r$ which implies that $\bar{p} \geq q$.

Lemma 7.4 *There exists a nonsingular linear change of coordinates such that* $x \to T_5 x$ *and the matrices* A, M, Q, C *from (7.9) - (7.10) when partitioned have the structure*

$$A = \begin{bmatrix} A_1 & A_2 \\ A_3 & A_4 \end{bmatrix} = \left[\begin{array}{ccc|cc} A_{11} & A_{12} & A_{13} & A_{14} & A_{15} \\ A_{21} & A_{22} & A_{23} & A_{24} & A_{25} \\ A_{31} & A_{32} & A_{33} & A_{34} & A_{35} \\ \hline 0 & A_{42} & A_{43} & A_{44} & A_{45} \\ A_{51} & A_{52} & A_{53} & A_{54} & A_{55} \end{array}\right] \begin{array}{l} \updownarrow n-\bar{p}+r-p \\ \updownarrow \bar{p}-q \\ \updownarrow q-r \\ \updownarrow p-r \\ \updownarrow r \end{array} \tag{7.12}$$

$$M = \begin{bmatrix} M_1 \\ M_2 \end{bmatrix} = \left[\begin{array}{cc} 0 & 0 \\ 0 & 0 \\ M_{11} & 0 \\ \hline 0 & 0 \\ 0 & M_{22} \end{array}\right], \; Q = \begin{bmatrix} Q_1 \\ 0 \end{bmatrix} = \left[\begin{array}{c} Q_{11} \\ Q_{12} \\ Q_{13} \\ \hline 0 \\ 0 \end{array}\right], \; C = \begin{bmatrix} 0 & T \end{bmatrix} \tag{7.13}$$

where $\begin{bmatrix} A_{42} & A_{43} \end{bmatrix} \in \mathbb{R}^{(p-r)\times(\bar{p}-r)}$ *which can be further partitioned to have the form*

$$\begin{array}{c} \overset{\bar{p}-q}{\longleftrightarrow} \quad \overset{q-r}{\longleftrightarrow} \\ \begin{bmatrix} A_{42} & A_{43} \end{bmatrix} \end{array} = \begin{array}{c} \overset{\bar{p}-q}{\longleftrightarrow} \quad \overset{q-r}{\longleftrightarrow} \\ \begin{bmatrix} 0 & 0 \\ A^o_{42} & A^o_{43} \end{bmatrix} \end{array} \begin{array}{l} \updownarrow p-\bar{p} \\ \updownarrow \bar{p}-r \end{array} \tag{7.14}$$

where $\begin{bmatrix} A^o_{42} & A^o_{43} \end{bmatrix}$ *is square and invertible and* $rank(\tilde{A}_{32}) = rank(A^o_{43})$. *The matrix* $T \in \mathbb{R}^{p\times p}$ *is orthogonal.* ♯

Proof

In the coordinates of (7.9) - (7.10), define

$$R_1 = \begin{bmatrix} \tilde{Q}_{21} & \tilde{A}_{31} & \tilde{A}_{32} \end{bmatrix},\ R_2 = \begin{bmatrix} 0 \\ 0 \\ M_{11} \end{bmatrix} \begin{matrix} \updownarrow h \\ \updownarrow n-h-p-q+r \\ \updownarrow q-r \end{matrix} \tag{7.15}$$

Therefore M in (7.10) is

$$\begin{bmatrix} R_2 & 0 \\ 0 & 0 \\ 0 & M_{22} \end{bmatrix} \begin{matrix} \updownarrow n-p \\ \updownarrow p-r \\ \updownarrow r \end{matrix}$$

Recall that $rank(R_1) = \bar{p}-r$ and that $\tilde{A}_{32}$ has full column rank $q-r$. Let $X_3 \in \mathbb{R}^{(n-p)\times(n-p)}$ and $X_4 \in \mathbb{R}^{(p-r)\times(p-r)}$ be orthogonal matrices such that

$$X_4 R_1 X_3^T = \left[\begin{array}{c|cc} 0 & A_{a,42} & A_{a,43} \end{array}\right] = \left[\begin{array}{c|c} 0 & 0 \\ 0 & U \end{array}\right] \tag{7.16}$$

where $U \in \mathbb{R}^{(\bar{p}-r)\times(\bar{p}-r)}$ is invertible.

Then define a nonsingular change of coordinates $T_3 \in \mathbb{R}^{n\times n}$ where

$$T_3 = \left[\begin{array}{c|cc} X_3 & 0 & 0 \\ \hline 0 & X_4 & 0 \\ 0 & 0 & I_r \end{array}\right]$$

Apply the change of coordinates T_3 to A, M, Q, C in (7.9) - (7.10) to get

$$A_a = \begin{bmatrix} A_{a,1} & A_{a,2} \\ A_{a,3} & A_{a,4} \end{bmatrix},\ M_a = \begin{bmatrix} M_{a,1} \\ M_{a,2} \end{bmatrix},\ Q_a = \begin{bmatrix} Q_{a,1} \\ 0 \end{bmatrix}, C_a = \begin{bmatrix} 0 & T_a \end{bmatrix} \tag{7.17}$$

where $A_a := T_3 A T_3^{-1},\ M_a := T_3 M,\ Q_a := T_3 Q,\ C_a := C T_3^{-1}$. Further partition

$$A_{a,1} = \begin{bmatrix} A_{a,11} & A_{a,12} & A_{a,13} \\ A_{a,21} & A_{a,22} & A_{a,23} \\ A_{a,31} & A_{a,32} & A_{a,33} \end{bmatrix} \begin{matrix} \updownarrow n-\bar{p}+r-p \\ \updownarrow \bar{p}-q \\ \updownarrow q-r \end{matrix},\ A_{a,3} = \begin{bmatrix} 0 & A_{a,42} & A_{a,43} \\ A_{a,51} & A_{a,52} & A_{a,53} \end{bmatrix} \begin{matrix} \updownarrow p-r \\ \updownarrow r \end{matrix} \tag{7.18}$$

$$Q_{a,1} = \begin{bmatrix} Q_{a,11} \\ Q_{a,12} \\ Q_{a,13} \end{bmatrix},\ M_{a,1} = \begin{bmatrix} M_{a,11} & 0 \\ M_{a,12} & 0 \\ M_{a,13} & 0 \end{bmatrix},\ M_{a,2} = \begin{bmatrix} 0 & 0 \\ 0 & M_{22} \end{bmatrix} \tag{7.19}$$

where T_a is still orthogonal.

It is straightforward to show that $R_1 R_2 = \tilde{A}_{32} M_{11}$. Since the matrix $\tilde{A}_{32}$ has full column rank $q-r$ and $det(M_{11}) \neq 0$, then $rank(R_1 R_2) = q - r$.

Clearly $R_1 R_2 = R_1 X_3^{-1} X_3 R_2$, which from (7.16) can be expanded to be

$$\underbrace{X_4^{-1} \begin{bmatrix} 0 & A_{a,42} & A_{a,43} \end{bmatrix}}_{R_1 X_3^{-1}} \underbrace{\begin{bmatrix} M_{a,11} \\ M_{a,12} \\ M_{a,13} \end{bmatrix}}_{X_3 R_2} = X_4^{-1} \begin{bmatrix} A_{a,42} & A_{a,43} \end{bmatrix} \begin{bmatrix} M_{a,12} \\ M_{a,13} \end{bmatrix} = X_4^{-1} \begin{bmatrix} 0 \\ U \end{bmatrix} \begin{bmatrix} M_{a,12} \\ M_{a,13} \end{bmatrix}$$

Since X_4 is orthogonal and $\bar{p} > q$, it follows that

$$rank(\tilde{A}_{32}) = q - r \Rightarrow rank(R_1 R_2) = q - r \Rightarrow rank \begin{bmatrix} M_{a,12} \\ M_{a,13} \end{bmatrix} = q - r$$

Define two nonsingular matrices $X_5 \in \mathbb{R}^{(q-r)\times(\bar{p}-r)}$ and $X_6 \in \mathbb{R}^{(\bar{p}-r)\times(\bar{p}-r)}$ so that

$$X_5 \begin{bmatrix} M_{a,12} \\ M_{a,13} \end{bmatrix} = I_{q-r},\ X_6 \begin{bmatrix} M_{a,12} \\ M_{a,13} \end{bmatrix} = \begin{bmatrix} 0 \\ M_{11} \end{bmatrix}$$

Then introduce the final change of coordinates

$$T_4 = \left[\begin{array}{cc|c} I_{n-\bar{p}+r-p} & -M_{a,11}X_5 & 0 \\ 0 & X_6 & 0 \\ \hline 0 & 0 & I_p \end{array}\right]$$

so that A_a, M_a, Q_a, C_a are transformed to be

$$A_b = \begin{bmatrix} A_{b,1} & A_{b,2} \\ A_{b,3} & A_{b,4} \end{bmatrix},\ M_b = \begin{bmatrix} M_{b,1} \\ M_{b,2} \end{bmatrix},\ C_b = \begin{bmatrix} 0 & T_a \end{bmatrix},\ Q_b = \begin{bmatrix} Q_{b,1} \\ 0 \end{bmatrix} \tag{7.20}$$

where

$$A_{b,3} = \begin{bmatrix} 0 & A_{b,42} & A_{b,43} \\ A_{b,51} & A_{b,52} & A_{b,53} \end{bmatrix}, M_{b,2} = \begin{bmatrix} 0 & 0 \\ 0 & M_{22} \end{bmatrix} \begin{matrix} \updownarrow p-r \\ \updownarrow r \end{matrix}, M_{b,1} = \begin{bmatrix} 0 & 0 \\ 0 & 0 \\ M_{11} & 0 \end{bmatrix} \begin{matrix} \updownarrow n-p-\bar{p}+r \\ \updownarrow \bar{p}-q \\ \updownarrow q-r \end{matrix}$$

and from (7.16)

$$\begin{bmatrix} A_{b,42} & A_{b,43} \end{bmatrix} = \begin{bmatrix} 0 \\ UX_6^{-1} \end{bmatrix} \begin{matrix} \updownarrow p-\bar{p} \\ \updownarrow \bar{p}-r \end{matrix}$$

By defining the nonsingular transformation matrix $T_5 := T_4T_3$ and partitioning

$$UX_6^{-1} = \begin{bmatrix} A_{42}^o & A_{43}^o \end{bmatrix} \tag{7.21}$$

where $A_{43}^o \in \mathbb{R}^{(\bar{p}-r)\times(q-r)}$, the matrices $A_b,\ M_b,\ Q_b,\ C_b$ and their partitions are now in the same form as the matrices A, M, Q, C in (7.12) - (7.13) in the statement of Lemma 7.4.

To prove that $rank(A_{43}^o) = rank(\tilde{A}_{32})$, define

$$X_7 = \begin{bmatrix} I_{n-\bar{p}-p+r} & -M_{a,11}X_5 \\ 0 & X_6 \end{bmatrix}$$

From the coordinate transformations T_3, T_4 and by observing the structure of A_b and M_b, it is clear from (7.16) and (7.21) that

$$X_4 R_1 X_3^{-1} X_7^{-1} = \begin{bmatrix} 0 & 0 & 0 \\ 0 & A_{42}^o & A_{43}^o \end{bmatrix}, \; X_7 X_3 R_2 = \begin{bmatrix} 0 \\ 0 \\ M_{11} \end{bmatrix} \Rightarrow X_4 R_1 R_2 = \begin{bmatrix} 0 \\ A_{43}^o M_{11} \end{bmatrix}$$

Recalling that $rank(R_1 R_2) = rank(\tilde{A}_{32}) = q - r$, and using the fact that X_4 and M_{11} are invertible, it follows that $rank(A_{43}^o) = rank(\tilde{A}_{32})$. ■

The canonical form in (7.12) - (7.13) associated with Lemma 7.4 is the basis for the proof of Theorem 7.1 which will be developed in the next section. Also partition $A_3 \in \mathbb{R}^{p \times (n-p)}$ from (7.12) as

$$A_3 = \begin{bmatrix} A_{311} \\ A_{312} \end{bmatrix} \begin{matrix} \updownarrow p-\bar{p} \\ \updownarrow \bar{p}-r \end{matrix} \Rightarrow A_{311} = \begin{bmatrix} 0 & A_{42} & A_{43} \end{bmatrix}, A_{312} = \begin{bmatrix} A_{51} & A_{52} & A_{53} \end{bmatrix} \quad (7.22)$$

Assume that the unknown signals f, ξ are norm bounded by known scalars α, β so that

$$\|f\| < \alpha, \; \|\xi\| < \beta$$

The remainder of this section develops a fault estimation scheme for f based on a pair of sliding mode observers as illustrated in Figure 7.1.

7.3.1 A Fault Reconstruction Scheme (proof of Theorem 7.1)

A sliding mode observer for the system (7.7) - (7.8) which fulfills the role of the primary observer in Figure 7.1) is designed based on the method that has been discussed in Section 3.2.2.

Once the matrix T_L in (3.23) has been obtained, the matrices in (7.12) - (7.13) are trans-

formed to be

$$T_L A T_L^{-1} = \begin{bmatrix} A_1 + LA_3 & * \\ TA_3 & * \end{bmatrix}, T_L M = \begin{bmatrix} M_1 + LM_2 \\ TM_2 \end{bmatrix}, CT_L^{-1} = \begin{bmatrix} 0 & I_p \end{bmatrix} \tag{7.23}$$

$$T_L Q = \begin{bmatrix} Q_1 \\ 0 \end{bmatrix}, T_L G_n = \begin{bmatrix} 0 \\ P_o^{-1} \end{bmatrix}, T_L x = \begin{bmatrix} x_1 \\ y \end{bmatrix} \tag{7.24}$$

where $x_1 \in \mathbb{R}^{n-p}$ are the 'non-output' states, and (*) are matrices that play no role in the analysis that follows. Partition the error system (3.14) according to (7.23) and (7.24), and let e_1 be the estimation error of x_1. According to Edwards *et al.* [52, 55, 54], assume that an ideal sliding motion has taken place on $\mathcal{S}$ so that $e_y = \dot{e}_y = 0$, then the error system (3.14) can be partitioned and re-arranged as

$$\dot{e}_1 = (A_1 + LA_3)e_1 - (M_1 + LM_2)f - Q_1\xi \tag{7.25}$$

$$T^T P_o^{-1} \nu_{eq} = -A_3 e_1 + M_2 f \tag{7.26}$$

where ν_{eq} is the equivalent output error injection required to maintain a sliding motion according to Edwards *et al.* [55, 54] and can be approximated to any degree of accuracy by replacing ν with

$$\nu = -\rho \frac{e_y}{\|e_y\| + \delta} \tag{7.27}$$

where δ is a small positive scalar. As the term e_y is a measurable signal, the signal ν_{eq} is computable online. For full details, kindly see Edwards *et al.* [55, 54].

Define v in Figure 7.1 as $v := T^T P_o^{-1} \nu_{eq}$ and partition $v = \text{col}(v_1, v_2)$ where $v_2 \in \mathbb{R}^r$. The contents of the scaling and filter block from Figure 7.1 will now be described to extract the signal $\bar{y}$ from v. Partition (7.26) conformably according to (7.22) as

$$v_1 = -A_{311} e_1 \tag{7.28}$$

$$v_2 = -A_{312} e_1 + M_{22} f_2 \tag{7.29}$$

where f_2 is a partition of f in Lemma 7.1.

Then define a matrix $Z \in \mathbb{R}^{(\bar{p}-r)\times(p-r)}$ as $Z = \begin{bmatrix} 0 & I_{\bar{p}-r} \end{bmatrix}$ and multiply (7.28) by Z to get

$$\bar{v}_1 := Zv_1 = -ZA_{311}e_1 \tag{7.30}$$

From (7.14) and the partitions of A_{311} in (7.22) it is clear that $ZA_{311} = \begin{bmatrix} 0 & A_{42}^o & A_{43}^o \end{bmatrix}$ which is full row rank of $\bar{p} - r$ as deduced from Lemma 7.4.

Now low-pass filter v_2 to produce v_f according to

$$\dot{v}_f = -A_f v_f + A_f v_2 = -A_f v_f - A_f A_{312} e_1 + A_f M_{22} f_2 \tag{7.31}$$

where $-A_f \in \mathbb{R}^{r\times r}$ is a stable design matrix, and combine (7.25), (7.31), and (7.30) to get the following system of order $\bar{n} := n - p + r$

$$\begin{bmatrix} \dot{e}_1 \\ \dot{v}_f \end{bmatrix} = \underbrace{\begin{bmatrix} A_1 + LA_3 & 0 \\ -A_f A_{312} & -A_f \end{bmatrix}}_{\mathcal{A}} \underbrace{\begin{bmatrix} e_1 \\ v_f \end{bmatrix}}_{z} + \underbrace{\begin{bmatrix} -(M_1 + LM_2) \\ \begin{bmatrix} 0 & A_f M_{22} \end{bmatrix} \end{bmatrix}}_{\mathcal{M}} f + \underbrace{\begin{bmatrix} -Q_1 \\ 0 \end{bmatrix}}_{\mathcal{Q}} \xi \tag{7.32}$$

$$\underbrace{\begin{bmatrix} \bar{v}_1 \\ v_f \end{bmatrix}}_{\bar{y}} = \underbrace{\begin{bmatrix} -ZA_{311} & 0 \\ 0 & I_r \end{bmatrix}}_{\mathcal{C}} \underbrace{\begin{bmatrix} e_1 \\ v_f \end{bmatrix}}_{z} \tag{7.33}$$

Define a nonsingular transformation matrix $\mathcal{T} \in \mathbb{R}^{\bar{n}\times\bar{n}}$ so that $\bar{x} = \mathcal{T}z$ where

$$\mathcal{T} = \begin{bmatrix} I_{\bar{n}-r} & \tilde{L}A_f^{-1} \\ 0 & I_r \end{bmatrix}$$

where $\tilde{L}$ represents the last r columns of L. Then the matrices $\mathcal{A}, \mathcal{M}, \mathcal{C}, \mathcal{Q}$ from (7.32) -

(7.33) are transformed ($\bar{A} = \mathcal{T}\mathcal{A}\mathcal{T}^{-1}, \bar{M} = \mathcal{T}\mathcal{M}, \bar{C} = \mathcal{C}\mathcal{T}^{-1}, \bar{Q} = \mathcal{T}\mathcal{Q}$) to be

$$\bar{A} = \left[\begin{array}{c|ccc} A_{11} & * & * & * \\ \hline A_{21} & * & * & * \\ A_{31} & * & * & * \\ -A_f A_{51} & * & * & * \end{array}\right] = \begin{array}{c} \overset{\bar{n}-\bar{p}}{\longleftrightarrow}\ \overset{\bar{p}}{\longleftrightarrow} \\ \left[\begin{array}{cc} \bar{A}_1 & \bar{A}_2 \\ \bar{A}_3 & \bar{A}_4 \end{array}\right] \end{array} \begin{array}{l} \updownarrow \bar{n}-\bar{p} \\ \updownarrow \bar{p} \end{array}, \ \bar{M} = \left[\begin{array}{cc} 0 & 0 \\ \hline 0 & 0 \\ -M_{11} & 0 \\ 0 & A_f M_{22} \end{array}\right] = \left[\begin{array}{c} 0 \\ \bar{M}_2 \end{array}\right] \quad (7.34)$$

$$\bar{C} = \left[\begin{array}{c|ccc} 0 & A_{42}^o & A_{43}^o & * \\ 0 & 0 & 0 & I_r \end{array}\right] = \left[\begin{array}{cc} 0 & \bar{T} \end{array}\right], \ \bar{Q} = \left[\begin{array}{c} Q_{11} \\ \hline Q_{12} \\ Q_{13} \\ 0 \end{array}\right] = \left[\begin{array}{c} \bar{Q}_1 \\ \bar{Q}_2 \end{array}\right] \quad (7.35)$$

where (*) are terms that play no role in the subsequent analysis. Clearly, the matrix $\bar{T} \in \mathbb{R}^{\bar{p}\times\bar{p}}$ is invertible since $\left[\begin{array}{cc} A_{42}^o & A_{43}^o \end{array}\right]$ is square and invertible. Define $\bar{M}_o$ to be the bottom q rows of $\bar{M}_2$, therefore $\bar{M}_o$ is square and invertible. From (7.34) - (7.35) it is easy to verify

$$\bar{C}\bar{M} = \left[\begin{array}{cc} -A_{43}^o M_{11} & * \\ 0 & A_f M_{22} \end{array}\right]$$

By construction M_{11} and M_{22} are invertible, and it can be seen that from Lemma 7.4, $rank(A_{43}^o) = rank(\tilde{A}_{32}) = q - r$, therefore $\bar{C}\bar{M}$ is full rank. It is shown in Lemma 7.2 that condition H1 implies that $rank(\tilde{A}_{32}) = q - r$, hence H1 implies that $\bar{C}\bar{M}$ is full rank.

Remark 7.1 *The purpose of the filter in (7.31) is to force the fault f_2 to appear in the dynamics of the 'state' equation (7.32) so that it is in the framework for fault reconstruction according to Tan & Edwards [177].* ♯

Remark 7.2 *The special structure of $\bar{C}$ in (7.35) (where the first $\bar{n} - \bar{p}$ columns are zero) is obtained because of the coordinate transform in Lemma 7.4.* ♯

Lemma 7.5 *The invariant zeros of* $(\bar{A}, \bar{M}, \bar{C})$ *are identical to the invariant zeros of the triple* $(\tilde{A}, \tilde{M}, \tilde{C})$ *together with the eigenvalues of* A_Ω. ♯

Proof

The Rosenbrock system matrix [157] of $(\bar{A}, \bar{M}, \bar{C})$ is given by

$$E_{a,1}(s) = \begin{bmatrix} sI - \bar{A} & \bar{M} \\ \bar{C} & 0 \end{bmatrix}$$

and the invariant zeros of a system are the values of s that cause its Rosenbrock matrix to lose normal rank. From (7.34) - (7.35), $E_{a,1}(s)$ can be expanded to be

$$E_{a,1}(s) = \begin{bmatrix} sI - \bar{A}_1 & -\bar{A}_2 & 0 \\ -\bar{A}_3 & sI - \bar{A}_4 & \bar{M}_2 \\ 0 & \bar{T} & 0 \end{bmatrix}$$

Since $\bar{T}$ has full rank, it is clear that $E_{a,1}(s)$ loses rank if and only if the following matrix loses rank

$$E_{a,2}(s) := \begin{bmatrix} sI - \bar{A}_1 & 0 \\ -\bar{A}_3 & \bar{M}_2 \end{bmatrix}$$

Substituting for $\bar{A}_1, \bar{A}_3, \bar{M}_2$ from (7.34) - (7.35), $E_{a,2}(s)$ can be expanded to be

$$E_{a,2}(s) = \left[\begin{array}{c|cc} sI - A_{11} & 0 & 0 \\ \hline -A_{21} & 0 & 0 \\ -A_{31} & -M_{11} & 0 \\ A_f A_{51} & 0 & A_f M_{22} \end{array}\right]$$

It is then obvious to see that $E_{a,2}(s)$ loses rank if and only if $E_{a,3}(s)$ loses rank where

$$E_{a,3}(s) := \begin{bmatrix} sI - A_{11} \\ -A_{21} \end{bmatrix}$$

From the rank test in [157], the values of s that make $E_{a,3}(s)$ lose rank are the unobservable modes of (A_{11}, A_{21}).

The invariant zeros of (A, M, C) are given by the values of s that cause the following matrix to lose rank

$$E_{b,1}(s) = \begin{bmatrix} sI - A & M \\ C & 0 \end{bmatrix}$$

From (7.12) - (7.13), $E_{b,1}(s)$ is

$$E_{b,1}(s) = \left[\begin{array}{cc|c} sI - A_1 & -A_2 & M_1 \\ -A_3 & sI - A_4 & M_2 \\ \hline 0 & T & 0 \end{array}\right]$$

Since T is orthogonal, then $E_{b,1}(s)$ loses rank if and only if $E_{b,2}(s)$ loses rank where

$$E_{b,2}(s) = \begin{bmatrix} sI - A_1 & M_1 \\ -A_3 & M_2 \end{bmatrix}$$

Substituting for A_1, A_3, M_1, M_2 from (7.12) - (7.13), $E_{b,2}(s)$ becomes

$$E_{b,2}(s) = \left[\begin{array}{ccc|cc} sI - A_{11} & -A_{12} & -A_{13} & 0 & 0 \\ -A_{21} & sI - A_{22} & -A_{23} & 0 & 0 \\ -A_{31} & -A_{32} & sI - A_{33} & M_{11} & 0 \\ \hline 0 & -A_{42} & -A_{43} & 0 & 0 \\ -A_{51} & -A_{52} & -A_{53} & 0 & M_{22} \end{array}\right]$$

From Lemma 7.4, $\begin{bmatrix} A_{42} & A_{43} \end{bmatrix}$ has a special structure which together with the fact that M_{11}, M_{22} are square and invertible, means $E_{b,2}(s)$ loses rank if and only if $E_{b,3}(s)$ loses rank where

$$E_{b,3}(s) = \begin{bmatrix} sI - A_{11} \\ -A_{21} \end{bmatrix}$$

which loses rank if and only if s is an unobservable mode of (A_{11}, A_{21}). This shows that $(\bar{A}, \bar{M}, \bar{C})$ and (A, M, C) have the same invariant zeros.

By using the partitions of (A, M, C) in (7.9) - (7.10), it can be easily shown the Rosenbrock matrix of (A, M, C) loses rank if and only if the following matrix $E_{c,1}(s)$ loses rank

$$E_{c,1}(s) = \begin{bmatrix} sI - A_\Omega & 0 & 0 \\ -\tilde{Q}_{11} & sI - \tilde{A}_{11} & -\tilde{A}_{12} \\ -\tilde{Q}_{21} & -\tilde{A}_{31} & -\tilde{A}_{32} \end{bmatrix}$$

It is clear that $E_{c,1}(s)$ loses rank when $s = \lambda(A_\Omega)$ or when s is an invariant zero of $(\tilde{A}_{11}, \tilde{A}_{12}, \tilde{A}_{31}, \tilde{A}_{32})$. Then, by finding the Rosenbrock matrix of $(\tilde{A}, \tilde{M}, \tilde{C})$ using the partitions in (7.4) - (7.6), it can be proven that the invariant zeros of $(\tilde{A}, \tilde{M}, \tilde{C})$ are the invariant zeros of $(\tilde{A}_{11}, \tilde{A}_{12}, \tilde{A}_{31}, \tilde{A}_{32})$.

Hence, it is proven that the invariant zeros of $(\bar{A}, \bar{M}, \bar{C})$ are the invariant zeros of $(\tilde{A}, \tilde{M}, \tilde{C})$ and $\lambda(A_\Omega)$. ■

Since from H2 it is assumed that $(\tilde{A}, \tilde{M}, \tilde{C})$ has stable invariant zeros, the system $(\bar{A}, \bar{M}, \bar{C})$ has stable invariant zeros. So by construction the system in (7.32) - (7.33) meets the Necessary and Sufficient conditions of the reconstruction method by Tan & Edwards [177], if and only if conditions H1 and H2 are satisfied.

Since the signal $\bar{y}$ defined in (7.33) is measurable, the approach from Tan & Edwards [177] will be used to design the secondary sliding mode observer from Figure 7.1 based on (7.32) - (7.33) to reconstruct the fault f whilst being robust to ξ. From (7.34) - (7.35), notice that $\bar{M}_{22}, \bar{T}$ are both invertible. Therefore, the triple $(\bar{A}, \bar{M}, \bar{C})$ is already in the coordinates where the robustness analysis in Tan & Edwards [177] is carried out, hence no further coordinate transformations are required[1].

The proposed observer for the system (7.32) - (7.33) (the secondary sliding mode observer

[1]However, there is a slight difference in that $\bar{T}$ is invertible but not necessarily orthogonal as in Tan & Edwards [177]. This is of no major consequence as will be shown in the proceeding analysis.

in Figure 7.1) in the coordinates of (7.34) - (7.35) can be written as

$$\dot{\hat{\bar{x}}} = \bar{A}\hat{\bar{x}} - \bar{G}_l\bar{e}_y + \bar{G}_n\bar{\nu} \tag{7.36}$$

$$\hat{\bar{y}} = \bar{C}\hat{\bar{x}} \tag{7.37}$$

where $\bar{e}_y := \hat{\bar{y}} - \bar{y}$ and the rest of the design process for the observer gains is similar to the method shown in Section 3.3 where the fault reconstruction signal is defined to be

$$\hat{f} = f + G(s)\xi \tag{7.38}$$

where $G(s) := \bar{W}\bar{A}_3\left(sI - (\bar{A}_1 + \bar{L}\bar{A}_3)\right)^{-1}(\bar{Q}_1 + \bar{L}\bar{Q}_2) + \bar{W}\bar{Q}_2$. ■

7.3.2 Design of Observers

This section discusses the design of the gains of the two observers from Figure 7.1. In this chaper, the observers will be designed using the Linear Matrix Inequality (LMI) Control Toolbox discussed in Gahinet *et al.* [74], which is a commonly available commercial software package.

For the design of the primary observer (3.7) - (3.8), G_l needs to be calculated such that Proposition 3.1 is satisfied so that a stable sliding motion can take place on $\mathcal{S}$. Then the matrices L and P_o can be calculated from P as defined in (3.12), and subsequently G_n can be calculated from (3.10).

Key observation: Notice that $G(s)$ in (7.38) not affected by the elements of L because $(\bar{A}_1, \bar{A}_3)$ are independent of L (see (7.34)). *This means the transfer function $G(s)$ (and hence the quality of the fault reconstruction) is unaffected by the design parameters of the primary observer (L and G_l), which therefore can be designed using any method as long as P and G_l satisfy Proposition 3.1.* Obviously G_l will not affect $G(s)$ since $G(s)$ is derived/valid based on the fact that the sliding motion has happened in observer 1 (since G_l will vanish during sliding motion of observer 1 as it is multiplied with e_y) ♯

Remark 7.3 *The observer (3.7) - (3.8) and (3.10) is slightly different to the one by Edwards* et al. *[52, 177], in that here the matrix L is unconstrained. In Edwards* et al. *[52, 177], the matrix L is forced to have a special structure. The observer in this chaper treats all the unknown signals col(ξ, f) as an 'unmatched' disturbance, because in general the distribution matrices M and Q are not matched to G_n, i.e. $rank \begin{bmatrix} G_n & M & Q \end{bmatrix} > rank(G_n)$. As L is unconstrained, the observer can be considered to be a modified Utkin observer [188] with the additional term $G_l e_y$.* ♯

The secondary observer in (7.36) - (7.37) will be designed to satisfy Proposition 3.1 and the same design process as the one shown in Section 3.2.2 will be used [177]. *The design of the secondary observer is crucial to the quality of the reconstruction.* An LMI method will be used.

Define the following symmetric decision variable

$$\bar{P}_{lmi} = \begin{bmatrix} \bar{P}_{11} & \bar{P}_{12} \\ \bar{P}_{12}^T & \bar{P}_{22} \end{bmatrix}, \; \bar{P}_{12} = \begin{bmatrix} \bar{P}_{121} & 0 \end{bmatrix}$$

where $\bar{P}_{11} \in \mathbb{R}^{(\bar{n}-\bar{p})\times(\bar{n}-\bar{p})}, \bar{P}_{22} \in \mathbb{R}^{\bar{p}\times\bar{p}}, \bar{P}_{121} \in \mathbb{R}^{(\bar{n}-\bar{p})\times(\bar{p}-q)}$. Also, define other decision variables $\bar{\gamma} \in \mathbb{R}$ and $\bar{W}_1 \in \mathbb{R}^{q\times(\bar{p}-q)}$. Notice that the structure of $\bar{P}_{12}$ causes $\bar{P}_{lmi}$ to have the same structure as $\bar{P}$ in (3.12).

The design proposed by Tan & Edwards [177] can be summarised as follows: Minimise $\bar{\gamma}$ subject to the following inequalities

$$\begin{bmatrix} \bar{P}_{11}\bar{A}_1 + \bar{A}_1^T\bar{P}_{11} + \bar{P}_{12}\bar{A}_3 + \bar{A}_3^T\bar{P}_{12}^T & * & * \\ -(\bar{P}_{11}\bar{Q}_1 + \bar{P}_{12}\bar{Q}_2)^T & -\bar{\gamma}I_h & * \\ -\bar{W}\bar{A}_3 & \bar{W}\bar{Q}_2 & -\bar{\gamma}I_q \end{bmatrix} < 0 \tag{7.39}$$

$$\begin{bmatrix} \bar{P}_{lmi}\bar{A} + \bar{A}^T\bar{P}_{lmi} - \bar{\gamma}_o\bar{C}^T(\bar{D}_d\bar{D}_d^T)^{-1}\bar{C} & * & * \\ -\bar{B}_d^T\bar{P} & -\bar{\gamma}_o I_{\bar{p}+h} & * \\ \bar{E} & \bar{H} & -\bar{\gamma}_o I_q \end{bmatrix} < 0 \qquad (7.40)$$

$$\bar{P}_{lmi} > 0 \qquad (7.41)$$

where (*) are terms that make (7.39) - (7.40) symmetric. The fixed matrices are $\bar{B}_d := \begin{bmatrix} 0 & \bar{Q} \end{bmatrix}, \bar{D}_d := \begin{bmatrix} \bar{D}_1 & 0 \end{bmatrix}$ whilst $\bar{H} = \begin{bmatrix} 0 & \bar{W}\bar{Q}_2 \end{bmatrix}$ where $\bar{D}_1 \in \mathbb{R}^{\bar{p}\times\bar{p}}$ and $\bar{\gamma}_o$ are user-specified parameters to tune the gains $\bar{G}_l, \bar{G}_n$. After the LMI solver returns the values of $\bar{W}, \bar{P}$, the gain $\bar{G}_l$ can be calculated as $\bar{G}_l = \bar{\gamma}_o^{-1}\bar{P}_{lmi}^{-1}\bar{C}^T(\bar{D}_d\bar{D}_d^T)^{-1}$ and $\bar{G}_n$ as in (3.10). This algorithm ensures inequality shown in Proposition 3.1 is satisfied and the $\mathcal{L}_2$ gain from ξ to $\hat{f}$ is bounded by $\bar{\gamma}$. Then choosing the gain from (3.9) as

$$\bar{\rho} > 2\|\bar{P}_o\bar{T}\bar{A}_3\|\bar{\mu}_1\beta/\bar{\mu}_0 + \|\bar{P}_o\bar{T}\bar{Q}_2\|\beta + \|\bar{P}_o\bar{T}\bar{M}_2\|\alpha$$

where

$$\bar{\mu}_0 = -\lambda_{max}(\bar{P}(\bar{A} - \bar{G}_l\bar{C}) + (\bar{A} - \bar{G}_l\bar{C})^T\bar{P}), \;\; \bar{\mu}_1 = \|\bar{P}\bar{Q}\|$$

ensures a sliding motion of the secondary observer on $\bar{\mathcal{S}}$. For full details, see Tan & Edwards [177]. The secondary observer now treats the fault vector f as the matched fault (in the sense that its distribution matrix is 'matched' to $\bar{G}_n$, i.e. $rank \begin{bmatrix} \bar{G}_n & \bar{M} \end{bmatrix} = rank(\bar{G}_n)$) and ξ as the unmatched disturbance.

Remark 7.4 *The matrix H in (7.11) associated with condition H1 is formed from Markov parameters and is system realization independent. (It is also a sub-block of the Hankel matrix shown in Zhou* et al. *[226]). Intuitively it is related to the system $(\tilde{A}, \tilde{M}, \tilde{C})$ having*

relative degree two for single-input-single-output systems since for example if

$$\tilde{A} = \begin{bmatrix} 0 & 1 \\ 0 & 0 \end{bmatrix}, \ \tilde{M} = \begin{bmatrix} 0 \\ 1 \end{bmatrix}, \ \tilde{C} = \begin{bmatrix} 1 & 0 \end{bmatrix}$$

(i.e. a double integrator realization) then H1 is satisfied although $\tilde{C}\tilde{M} = 0$. ♯

7.3.3 Design Algorithm Summary

The design algorithm for the method in this chaper can be summarised as follows:

1. Preliminary checks and coordinate transformations:

   (a) Check that $rank(\tilde{C}\tilde{M}) < rank(\tilde{M})$. Otherwise, stop, and the existing methods by Tan & Edwards [177] for example can be used. Then, ensure that Conditions H1 and H2 are satisfied. If not, the method in this chaper is not applicable.

   (b) From the knowledge of the frequency of $\tilde{\xi}$, select the matrices A_Ω and B_Ω.

   (c) Find the coordinate transformations T_1, T_2, following the steps shown in the proof of Lemma 7.1. Then, apply the coordinate transformation to $\tilde{A}, \tilde{M}, \tilde{C}$ and $\tilde{Q}$. The matrices $\tilde{C}$ and $\tilde{M}$ will then have the special structures shown in (7.4) and (7.5) so that the analysis of the observer in (7.25) - (7.26) and (7.28) - (7.29) is simplified without loss of generality.

   (d) Use the matrices obtained in the previous step to form the matrices A, M, Q, C of the augmented system in (7.7) and (7.8).

   (e) Find the coordinate transformation T_5, following the steps shown in the proof of Lemma 7.4. Then, apply the coordinate transformation to the matrices A, M, C and Q, which should then have the structures in (7.12) - (7.14). Obtain the partitions in Lemma 7.4 and equation (7.22). The purpose of the coordinate transformation T_5 is to give the matrix A the special structure in (7.12) and (7.14) so that the analysis of the secondary observer in (7.34) - (7.35) can be simplified without loss of generality.

2. Design observers

   (a) Design the primary observer using the method in Section 7.3.2 (although in fact any method of choice can be used). Full details of this design method are available in Tan & Edwards [172]. The design method will yield the gains G_l, G_n, L and the matrix P_o. Note that other methods can be used to design the primary observer, as long as the designed parameters satisfy Proposition 3.1.

   (b) Define a stable matrix $-A_f$ as in (7.31). Then obtain the matrices for the system in (7.32) - (7.33), in particular $\mathcal{A}, \mathcal{M}, \mathcal{Q}$ and $\mathcal{C}$.

   (c) Perform the coordinate transformation $\mathcal{T}$ on $\mathcal{A}, \mathcal{M}, \mathcal{Q}, \mathcal{C}$ to obtain $\bar{A}, \bar{M}, \bar{Q}, \bar{C}$ as in (7.34) - (7.35). The purpose of the coordinate transformation $\mathcal{T}$ is to make the system in (7.32) - (7.33) have the canonical observer structure from Tan & Edwards [177] as described in (7.34) - (7.35).

   (d) Design the secondary observer using the method in Section 3.3, in particular from (7.39) - (7.41). Full details of this design method are available in Tan & Edwards [177]. This design method will synthesise the gains $\bar{G}_l, \bar{G}_n, \bar{W}$ and also minimise the $\mathcal{L}_2$ gain from ξ to $\hat{f}$.

3. Implement the observers and generate the fault reconstruction as shown in Figure 7.1.

   (a) Implement the primary observer (3.7) - (3.8) on the original system (7.1) - (7.2). The observer will generate the signal ν as in (7.27).

   (b) Process the signal ν as in (7.30) - (7.31) to generate the output $\bar{y}$.

   (c) Implement the secondary observer (7.36) - (7.37) on the fictitious system (7.32) - (7.33), using the (measurable) signal $\bar{y}$ as the driving signal.

   (d) Generate the fault reconstruction as in (3.36) from $\bar{\nu}_{eq}$.

7.4 An Example

The method proposed in this chaper will now be demonstrated by an example, which is a 7th order model of an aircraft used in Heck *et al.* [85]. In the notation of (7.1) - (7.2), the

matrices that describe the system are as follows

$$\tilde{A} = \begin{bmatrix} 0 & 0 & 1.0000 & 0 & 0 & 0 & 0 \\ 0 & -0.1540 & -0.0042 & 1.5400 & 0 & -0.7440 & -0.0320 \\ 0 & 0.2490 & -1.0000 & -5.2000 & 0 & 0.3370 & -1.1200 \\ 0.0386 & -0.9960 & -0.0003 & -2.1170 & 0 & 0.0200 & 0 \\ 0 & 0.5000 & 0 & 0 & -4.0000 & 0 & 0 \\ 0 & 0 & 0 & 0 & 0 & -20.0000 & 0 \\ 0 & 0 & 0 & 0 & 0 & 0 & -25.0000 \end{bmatrix}$$

where the states, control inputs and outputs are

$$x = \begin{bmatrix} \text{bank angle} \\ \text{yaw rate} \\ \text{row rate} \\ \text{sideslip angle} \\ \text{washed-out filter state} \\ \text{rudder deflection} \\ \text{aileron deflection} \end{bmatrix}, \quad u = \begin{bmatrix} \text{rudder command} \\ \text{aileron command} \end{bmatrix}$$

$$y = \begin{bmatrix} \text{bank angle} \\ \text{yaw rate} \\ \text{sideslip angle} \end{bmatrix}$$

and assume that the first actuator is faulty. Therefore the matrices $\tilde{C}$ and $\tilde{M}$ are

$$\tilde{C} = \begin{bmatrix} 1 & 0 & 0 & 0 & 0 & 0 & 0 \\ 0 & 1 & 0 & 0 & 0 & 0 & 0 \\ 0 & 0 & 0 & 1 & 0 & 0 & 0 \end{bmatrix}, \tilde{M} = \begin{bmatrix} 0 \\ 0 \\ 0 \\ 0 \\ 0 \\ 20 \\ 0 \end{bmatrix}$$

Suppose that the matrix $\tilde{A}$ is imprecisely known and that there exists parametric uncertainty. Therefore the state equation of the system becomes

$$\dot{\tilde{x}} = (\tilde{A} + \triangle\tilde{A})x + \tilde{B}u + \tilde{M}f \tag{7.42}$$

where $\triangle\tilde{A}$ is the discrepancy between the known matrix $\tilde{A}$ and its actual value. For simplicity let $u \equiv 0$. Notice that the first, fifth, sixth and seventh rows of the matrix $\tilde{A}$ do not contain any uncertainty due to the nature of the state equations. Hence, any parametric uncertainty will appear in the second, third and fourth rows of $\tilde{A}$. Let the actual value of the system matrix be

$$\tilde{A}+\triangle\tilde{A} = \begin{bmatrix} 0 & 0 & 1.0000 & 0 & 0 & 0 & 0 \\ 0 & -0.1600 & -0.0042 & 1.6600 & 0 & -0.7440 & -0.0500 \\ 0 & 0.2490 & -1.0000 & -5.1600 & 0 & 0.4000 & -1.2400 \\ 0.0386 & -0.9960 & -0.0003 & -2.2300 & 0 & 0.0230 & 0 \\ 0 & 0.5000 & 0 & 0 & -4.0000 & 0 & 0 \\ 0 & 0 & 0 & 0 & 0 & -20.0000 & 0 \\ 0 & 0 & 0 & 0 & 0 & 0 & -25.0000 \end{bmatrix}$$

Equation (7.42) can be placed in the same framework as (7.1) by writing

$$\triangle\tilde{A}\tilde{x} = \tilde{Q}\tilde{\xi} = \underbrace{\begin{bmatrix} 0 & 0 & 0 \\ 1 & 0 & 0 \\ 0 & 1 & 0 \\ 0 & 0 & 1 \\ 0 & 0 & 0 \\ 0 & 0 & 0 \\ 0 & 0 & 0 \end{bmatrix}}_{\tilde{Q}} \underbrace{\begin{bmatrix} 0 & -0.0060 & 0 & 0.1200 & 0 & 0 & -0.0180 \\ 0 & 0 & 0 & 0.0400 & 0 & 0.0630 & -0.1200 \\ 0 & 0 & 0 & -0.1130 & 0 & 0.0030 & 0 \end{bmatrix} \tilde{x}}_{\tilde{\xi}}$$

The disturbance $\tilde{\xi}$ will be generated by the states $\tilde{x}$, which is in turn generated by the fault f. Assuming f is bounded, then $\tilde{x}$ and $\tilde{\xi}$ will also be bounded since $\tilde{A} + \triangle\tilde{A}$ is stable. Notice that the method by Floquet & Barbot [62] cannot be used on this system as there is no consideration of the disturbance $\tilde{\xi}$. If the signals f and $\tilde{\xi}$ are augmented to form a new 'fault' vector, as has been done by Saif & Guan [158], this would result in the new 'fault' having 4 components. The number of outputs in this system is only 3, resulting in a 'more faults than outputs' scenario, and hence the method by Floquet & Barbot [62] would still be not applicable.

The FDI literature based on unknown input observers (UIOs) is also not applicable here because assumptions G1 and G2 are typically required by Saif & Guan [158], Chen *et al.* [17, 18] and Darouach [33].

Notice that all faults and disturbances appear in states 2, 3, 4 and 6. For the method by Davila *et al.* [36] to be applicable, the integral of the states 2, 3, 4 and 6 would need to be measurable, which means that the yaw and roll angles need to be measurable, together with the integrals of the sideslip angle and rudder deflection. In this system, of the four states, only the sideslip angle is measurable. The rest are not measurable and hence the method in Davila *et al.* [36] is not applicable for this system. Also notice that $\tilde{C}\tilde{M} = 0 \Rightarrow r = 0 < q$, and hence the existing sliding mode methods shown in Edwards *et al.* [55, 177] cannot be used to reconstruct the fault.

7.4.1 Observers Design

It can be easily verified that conditions H1 and H2 are satisfied. Hence, the method proposed in this chaper can be used.

The disturbance $\tilde{\xi}$ is assumed to have a frequency $\omega < 10\ rad/s$, and therefore the filter (7.3) will have the Bode plot as shown in Figure 7.2, resulting in $A_\Omega = -10I_3, B_\Omega = 10I_3$.

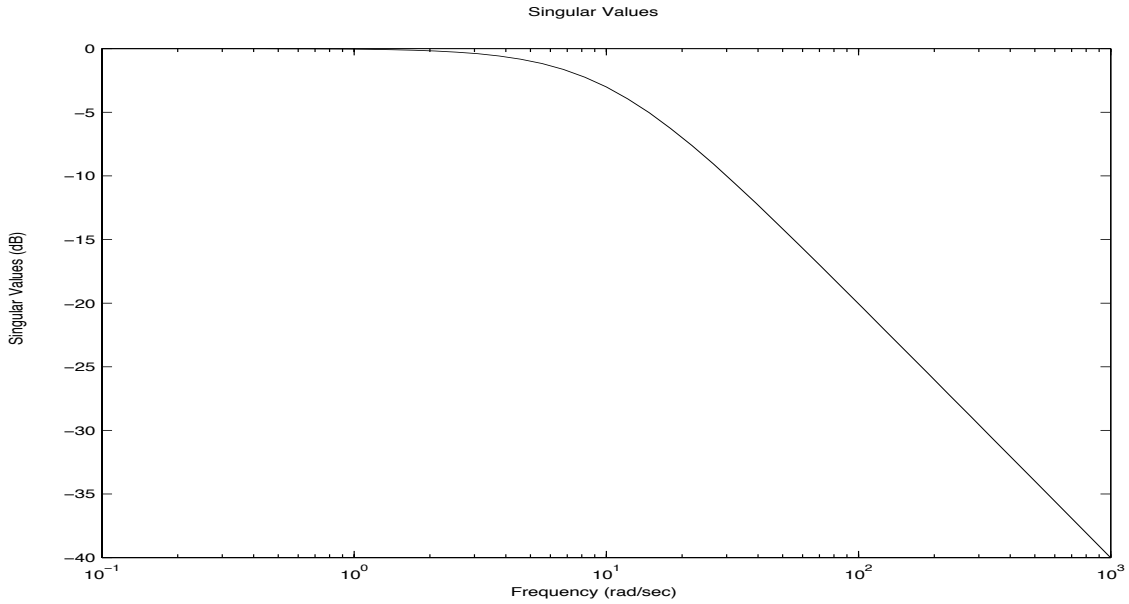

Figure 7.2: The gain plot of the filter (7.3).

Performing the coordinate transformation in Lemma 7.1 yields the following matrices

$$T_1 = \begin{bmatrix} 0 & 0 & 0 & 0 & 0 & 0 & 1 \\ 0 & 0 & 1 & 0 & 0 & 0 & 0 \\ 0 & 0 & 0 & 0 & 1 & 0 & 0 \\ 0 & 0 & 0 & 0 & 0 & -1 & 0 \\ 0 & 0 & 0 & 1 & 0 & 0 & 0 \\ 0 & 1 & 0 & 0 & 0 & 0 & 0 \\ 1 & 0 & 0 & 0 & 0 & 0 & 0 \end{bmatrix},\ T_2 = 1,\ \tilde{T} = \begin{bmatrix} 0 & 0 & 1 \\ 0 & 1 & 0 \\ 1 & 0 & 0 \end{bmatrix}$$

$$M_{11} = -20,\ M_{22} = \emptyset \text{ (empty matrix)}$$

with

$$\tilde{A} = \left[\begin{array}{rrrr|rrr} -25.0000 & 0 & 0 & 0 & 0 & 0 & 0 \\ -1.1200 & -1.0000 & 0 & -0.3370 & -5.2000 & 0.2490 & 0 \\ 0 & 0 & -4.0000 & 0 & 0 & 0.5000 & 0 \\ 0 & 0 & 0 & -20.0000 & 0 & 0 & 0 \\ \hline 0 & -0.0003 & 0 & -0.0200 & -2.1170 & -0.9960 & 0.0386 \\ -0.0320 & -0.0042 & 0 & 0.7440 & 1.5400 & -0.1540 & 0 \\ 0 & 1.0000 & 0 & 0 & 0 & 0 & 0 \end{array}\right]$$

and the distribution matrix for the disturbance $\tilde{\xi}$ can be written as

$$\tilde{Q} = \left[\begin{array}{ccc} 0 & 0 & 0 \\ 0 & 1 & 0 \\ 0 & 0 & 0 \\ 0 & 0 & 0 \\ 0 & 0 & 1 \\ 1 & 0 & 0 \\ 0 & 0 & 0 \end{array}\right]$$

which shows that $\tilde{A}_{32}$ is full rank, and Condition C3 is fulfilled. Furthermore, it can be seen that $rank \left[\begin{array}{ccc} \tilde{Q}_{21} & \tilde{A}_{31} & \tilde{A}_{32} \end{array}\right] = 3$, which means that $\bar{p} = 3$.

Augmenting the system as in (7.7) - (7.8) yields a 10th order system. Performing the coor-

dinate transformation in Lemma 7.4 gives

$$T_5 = \begin{bmatrix} 1.33 & 0.61 & -0.04 & -0.04 & 0 & 0 & 0 & 0 & 0 & 0 \\ 0 & 0 & 0 & 0 & 0 & 1.00 & 0 & 0 & 0 & 0 \\ -1.02 & 0.79 & 0.03 & 0 & 0 & 0 & 0 & 0 & 0 & 0 \\ 0 & 0.03 & 0 & 1 & 0 & 0 & 0 & 0 & 0 & 0 \\ -0.02 & 0 & -0.69 & 0 & -0.73 & 0 & 0 & 0 & 0 & 0 \\ 0.02 & 0 & 0.72 & 0 & -0.70 & 0 & 0 & 0 & 0 & 0 \\ 0.80 & 0 & -0.02 & -0.03 & -0.02 & 0 & -0.60 & 0 & 0 & 0 \\ 0 & 0 & 0 & 0 & 0 & 0 & 0 & -0.69 & -0.02 & -0.72 \\ 0 & 0 & 0 & 0 & 0 & 0 & 0 & 0.72 & 0.01 & -0.69 \\ 0 & 0 & 0 & 0 & 0 & 0 & 0 & -0.03 & 1.00 & -0.01 \end{bmatrix}$$

$$\begin{bmatrix} A_{42}^o & A_{43}^o \end{bmatrix} = \begin{bmatrix} 0.9999 & -0.0065 & -0.0067 \\ -0.0065 & 1.0003 & -0.0065 \\ -0.0084 & -0.0081 & 1.2472 \end{bmatrix}$$

The method in [172] has been implemented to design the primary observer. In designing the primary observer, the weights $V_1 = 100I_{10}, V_2 = I_3$ were chosen (where V_1 and V_2 are the Linear Quadratic Gaussian weights associated with the performance and noise amplification respectively. See [172] for details). The following gain matrices were obtained

$$P_o = \begin{bmatrix} 0.0906 & 0.0108 & -0.0007 \\ 0.0108 & 0.0816 & 0.0007 \\ -0.0007 & 0.0007 & 0.0884 \end{bmatrix}$$

as well as

$$G_l = \begin{bmatrix} 0.0217 & 0.0432 & 0.0095 \\ 0.2704 & -0.0373 & 0.0523 \\ -0.0473 & 0.0457 & 0.3365 \\ -0.0501 & 0.0030 & -0.0079 \\ 4.5408 & -0.3371 & -3.3790 \\ 0.0091 & 0.4141 & -0.0320 \\ 0.0277 & -0.1853 & 0.0191 \\ -0.5032 & 0.2387 & 10.8365 \\ 0.4417 & 13.3802 & 0.2387 \\ 10.7666 & 0.4417 & -0.5032 \end{bmatrix}, G_n = \begin{bmatrix} 0.0170 & 0.0363 & 0.0100 \\ 0.2929 & -0.0854 & 0.0721 \\ -0.0356 & 0.0380 & 0.3482 \\ -0.0536 & 0.0121 & -0.0113 \\ 4.6128 & -0.9944 & -3.2558 \\ -0.0534 & 0.3879 & -0.0451 \\ 0.0576 & -0.1794 & 0.0271 \\ 0.1060 & -0.1145 & 11.3096 \\ -1.4913 & 12.4549 & -0.1145 \\ 11.2189 & -1.4913 & 0.1060 \end{bmatrix}$$

The secondary observer was designed using the second algorithm in Section 7.3.2. The user-defined matrices were specified to be $\bar{D}_1 = 10I_3, \bar{\gamma}_o = 100$ and the following gains were obtained

$$\bar{G}_l = \begin{bmatrix} 0.0738 & 0.0690 & -0.0923 \\ -0.0001 & -0.0001 & 0.0002 \\ -0.0998 & -0.0932 & 0.1248 \\ -0.0008 & -0.0008 & 0.0011 \\ -0.1066 & -0.0303 & 0.0869 \\ -0.0304 & -0.1025 & 0.0877 \\ 0.0840 & 0.0842 & -2.9137 \end{bmatrix}, \bar{G}_n = \begin{bmatrix} 0.0741 & 0.0692 & -0.0369 \\ -0.0001 & -0.0001 & 0.0001 \\ -0.1001 & -0.0936 & 0.0498 \\ -0.0008 & -0.0008 & 0.0004 \\ -0.1060 & -0.0315 & 0.0343 \\ -0.0316 & -0.1017 & 0.0354 \\ 0.0329 & 0.0336 & -1.2027 \end{bmatrix}$$

$$\bar{P}_o = \begin{bmatrix} 10.4279 & -3.1027 & 0.2040 \\ -3.1027 & 10.8762 & 0.2246 \\ 0.2040 & 0.2246 & 0.6786 \end{bmatrix}$$

$$\bar{W}\bar{T}^{-1}\bar{P}_o^{-1} = \begin{bmatrix} -0.0415 & -0.0392 & -0.0786 \end{bmatrix}$$

The gains above provide an $\mathcal{L}_2$ bound of $\bar{\gamma} = 1.2238$.

7.4.2 Simulation Results

In the simulations that follow, the parameters associated with ν for the primary observer were chosen as $\rho = 100, \delta = 10^{-3}$ while for the secondary observer they were chosen as $\bar{\rho} = 100, \bar{\delta} = 10^{-3}$. A fault was induced in the first actuator. Figure 7.3 shows the fault and its reconstruction, where the left subfigure is the fault and the right subfigure is the reconstruction. Figure 7.4 shows the states that will affect $\tilde{\xi}$, i.e. the 2nd, 4th, 6th and 7th states. It can be clearly seen that the reconstruction signal $\hat{f}$ provides a good estimate of the fault f, despite the parameter variation $\triangle\tilde{A}$ that causes a disturbance that could corrupt the reconstruction. The design algorithm has calculated the observer gains such that the reconstruction is least affected by the disturbances in an $\mathcal{L}_2$ sense.

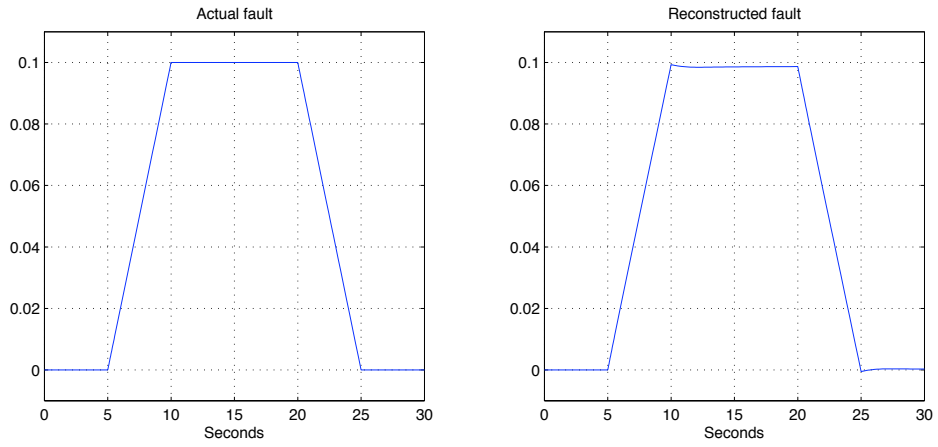

Figure 7.3: The left subfigure is the fault, the right subfigure is its reconstruction.

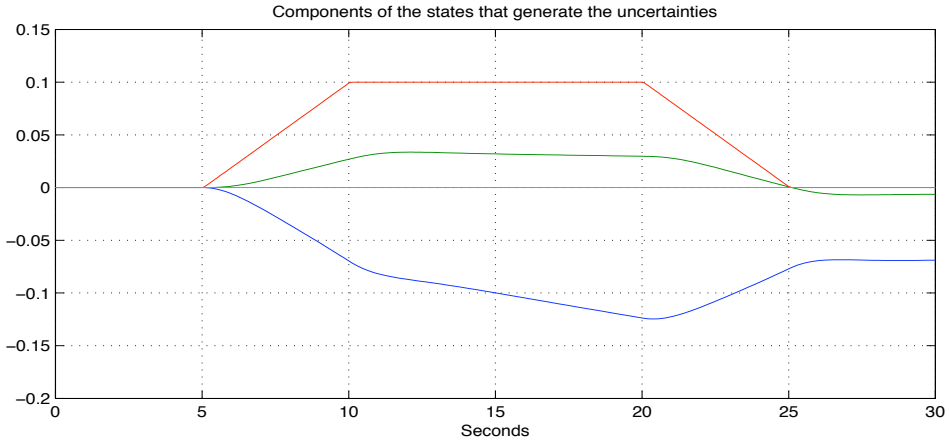

Figure 7.4: The components of $\tilde{x}$ that generate $\tilde{\xi}$, namely the 2nd, 4th, 6th and 7th components of $\tilde{x}$.

7.5 Conclusion

This chapter has proposed a new scheme for robust fault reconstruction in uncertain systems which is applicable to a wider class of systems than existing work. Early results were applicable only to the case where the first Markov parameter of the system is full rank and minimum phase with respect to the effect of faults on the measured outputs. Recent work has relaxed these conditions by either considering a specific class of nonlinear systems (relative degree two plants arising from models of mechanical systems), or by considering linear systems subject to a class of unknown inputs, which could be an aggregation of the faults and the uncertainty.

The method proposed in this chapter uses two sliding mode observers in cascade; the equivalent output error injection term of the first observer is processed to form the measurable output of a fictitious system. Then a secondary observer is implemented for the fictitious system such that the fault can be reconstructed using existing methods. An aircraft model has demonstrated the validity of the proposed scheme.

Chapter 8

Conclusion and Recommendations for Future Research

8.1 Conclusions

This thesis has presented advancements in robust fault reconstruction using sliding mode observers.

Chapter 2 has outlined the various techniques to perform FDI on engineering control systems. The various methods discussed include hardware redundancy as well as analytical redundancy. It was found that the hardware redundancy method, though being used popularly in the industry , contributes to a higher cost for both system operation and maintenance, a larger space required for the hardware sensors and equipment as well as a shorter lifespan due to the potential failure and wear and tear of the hardware set up. Given the conditions and constraints of critical systems such as aircrafts, power systems and chemical plants where the size, space required, performance and safety are of the utmost importance, the use of analytical method will be a much preferred approach for FDI.

Chapter 3 has presented on the concept of using the sliding mode observer for robust fault reconstruction. The chapter has explained on the development of the sliding mode observer throughout the years, starting from its introduction by Utkin [188] which utilises a nonlinear discontinuous term in the design of the observer and the estimate outputs converge to the actual system outputs in finite time. It was found that the performance of the sliding mode observer is not affected by the presence of disturbances and therefore, it can be extended and used for fault reconstruction. Since then, the sliding mode observer has been developed and enhanced for the purpose of FDI. Edwards *et al.* [52, 55] presented a method to design

the sliding mode observer that differs from other sliding mode observer schemes in that the sliding motion is maintained at all time, even when there are faults in the system. However, their work did not consider robustness towards uncertainties. Tan & Edwards [177] then presented a method to design the Edwards-Spurgeon observer [52] such that the $\mathcal{L}_2$ gain from the disturbance to the fault reconstruction is minimised so that the fault reconstruction is robust towards the uncertainties. This chapter described the method used by Tan & Edwards [177] to design the sliding mode observer using LMI and was demonstrated with a crane model. The design method discussed was used as the basis for the rest of the work in this thesis.

In Chapter 4, the work by Edwards & Tan [56] was extended and its main contribution was to investigate the conditions that guarantee the feasibility of disturbance decoupled fault reconstruction. Previous work by Edwards *et al.* [55] presented a design algorithm to minimise the $\mathcal{L}_2$ gain from the disturbances onto the fault reconstruction, but this method does not guarantee complete decoupling from the disturbances. Saif & Guan [158] then demonstrated a method whereby the disturbance could be completely decoupled by combining the fault with the disturbances, thus forming a new 'fault' vector which would then be reconstructed. However, this method requires very stringent conditions to be fulfilled and is conservative as the disturbances do not need to be reconstructed in order to achieve disturbance decoupled fault reconstruction, as pointed out by Edwards & Tan [56], though the conditions to do so was not investigated. It was found in this chapter that the conditions are less stringent than those presented by Saif & Guan [158], which ultimately proved that it is not necessary to reconstruct the disturbances in order to achieve disturbance decoupled fault reconstruction. Furthermore, the conditions in this chapter can be easily tested onto the original system matrices and this enables to immediately know whether disturbance decoupled fault reconstruction is feasible for that system. The work in this chapter was then verified using an aircraft system.

Chapter 5 extended the work in Chapter 4 such that the disturbance decoupled fault reconstruction could be implemented for sensor faults as well. The technique shown by Tan & Edwards [175] was adopted so that sensor faults were formulated as actuator faults of which

the method presented in Chapter 4 could then be used to reconstruct the faults. It has been shown by Tan *et al.* [57, 179, 184] that a good sensor fault reconstruction scheme can be used to perform fault tolerant control. As a result, it can be seen that should the sensor fault reconstruction scheme be completely robust towards the disturbances, a fault tolerant control scheme could then be designed such that the effects of the disturbances on the fault reconstruction are rejected and decoupled and hence, the system is able to continue operating as efficiently as it being in a fault-free scenario. The work in this chapter was validated using a double inverted pendulum system.

In Chapter 6 it addressed the case when disturbance decoupled fault reconstruction cannot be guaranteed and therefore it presented a scheme to make it feasible using cascaded observers. even though Condition C3 in Chapter 4 is not satisfied. It was shown that the signals from an observer are the output of a 'fictitious' system that is driven by faults and disturbances. This signals are then fed into the next observer arranged in cascade and the process is repeated until disturbance decoupled fault reconstruction can be achieved. It was found that the scheme proposed in this chapter can be applied to a wider class of systems compared to single observer schemes. This chapter has outlined a systematic algorithm to check for the feasibility of disturbance decoupled fault reconstruction and also the number of observers needed. The work in this chapter was verified using a rotational system.

Chapter 7 presented a robust fault reconstruction method for a class of systems with relative degree higher than one, thus relaxing the condition required by Edwards *et al.* [55, 54, 177]. The method demonstrated in this chapter uses two sliding mode observers in cascade which are designed based on the method shown in Edwards & Spurgeon [52]. Suitable processing of the equivalent output error injection in the first observer yields the measurable output of a 'fictitious' system where the first Markov parameter is full rank. This shows that the robust fault reconstruction method by Tan & Edwards [177] can be applied to the fictitious system and a second observer is designed for the fictitious system to generate a reconstruction of the fault that is robust to the disturbances. This approach is applicable to a wider class of systems compared to the methods by Edwards *et al.* [54, 55, 177]. In addition to that, this chapter considered robustness against disturbances, as opposed to the work by Floquet &

Barbot [62], and the scheme may be feasible for systems for which the method by Davila *et al.* [36] is not applicable. The method proposed in this chapter was validated using an aircraft model.

8.2 Recommendations for Future Work

The work presented in this thesis has the potential to generate some future work that will further improve the research results in the area of robust fault reconstruction. This section presents the outline of some of the potential future research and enhancement that can be carried out on (but not limited to) the following areas.

In Chapter 6, Section 6.2.1 has presented a systematic algorithm to design the multiple observers disturbance decoupled fault reconstruction scheme. However, the rank conditions analysis that satisfy A_{123}^{m-1} being full rank (in terms of the original system matrices) for the scheme was not explicitly presented and this could be further explored in the future.

Another area that could be explored would be on the use of higher sliding mode observers [163, 70, 162, 51, 71, 69] on the work in Chapter 6. With the implementation of higher order sliding mode observers, higher accuracy can be obtained as the equivalent output error injection is already smooth and no approximations are required to extract it.

In addition to that, the structure of the observer can be improved to cater for better robustness and higher accuracy in the fault reconstruction. A new structure for the observer could be proposed such that the robustness is enhanced or the existence conditions are relaxed. A possible research area that could be studied is the combination of the sliding mode observer with the adaptive observer [197]. Research work in this area seeks to produce possible results which could perform better robustness with disturbance having less effect on the fault reconstruction and/or perhaps even more relaxed conditions to achieve complete robustness.

And lastly, there could be a possibility that the work in Chapter 4 can be combined with the work in Chapter 7 such that a disturbance decoupled fault reconstruction scheme can be applied to a wider class of systems. This is so because it can be seen that although the work presented in Chapter 4 is able to achieve disturbance decoupled fault reconstruction,

its applicability is still inferior compared to the work presented in Chapter 7. Therefore, it is desired that the advantages discussed in these two chapters to be combined to form a new work which will produce better results.

References

[1] K. Adjallah, D. Maquin, and J. Ragot. Non-linear observer-based fault detection. *Proceedings of 3rd IEEE Conference on Control Applications*, 2:1115–1120, 1994.

[2] A. Akhenak, M. Chadli, D. Maquin, and J. Ragot. Sliding mode multiple observer for fault detection and isolation. *42nd IEEE International Conference on Decision and Control*, 1:953–958, 2003.

[3] E. Alcorta-Garcia and P. M. Frank. Deterministic nonlinear observer-based approaches to fault diagnosis: A survey. *Control Engineering Practice*, 5:663–670, 1997.

[4] S.A. Ashton, D.N. Shields, and S. Daley. Fault detection in pipelines using nonlinear observers. *UKACC International Conference on Control*, 1:135–140, 1998.

[5] J.P. Barbot, T. Boukhobza, and M. Djemai. Sliding mode observer for triangular input form. *Proceedings of IEEE Conference on Decision and Control*, pages 1489–1490, 1996.

[6] M. Basseville and I. Nikiforov. Fault isolation for diagnosis: Nuisance rejection and multiple hypotheses testing. *Annual Reviews in Control*, 26:189–202, 2002.

[7] G. Bastin and M.R. Gevers. Stable adaptive observers for nonlinear time-varying systems. *IEEE Transactions on Automatic Control*, 33(7):650–658, July 1988.

[8] R.V. Beard. *Failure accommodation in linear systems through self - reorganisation*. PhD thesis, M.I.T., Cambridge, 1971.

[9] S.P. Bhattacharyya, H. Chappellat, and L.H. Keel. *Robust Control: The Parametric Approach*. Prentice Hall PTR: Upper Saddle River, NJ, 1995.

[10] S. Bogh. Multiple hypothesis-testing approach to fdi for the industrial actuator benchmark. *Control Engineering Practice*, 3(12):1763–1768, 1995.

[11] N. Boudaoud and M. Masson. Detection of incipient fault using fuzzy agglomerative clustering algorithm. *18th International Conference of the North American Fuzzy Information*, pages 233–237, 1999.

[12] T. Boukhobza, M. Djemai, and J.P. Barbot. Nonlinear sliding observer for systems in output and output derivative injection form. *IFAC World Congress*, E:299–305, 1996.

[13] S.P. Boyd, L. El-Ghaoui, E. Feron, and V. Balakrishnan. *Linear Matrix Inequalities in Systems and Control Theory*. SIAM: Philadelphia, 1994.

[14] R.L. Carroll and D.P. Lindorff. An adaptive observer for single-input single-output linear systems. *IEEE Transactions on Automatic Control*, AC-18(5):428–435, October 1973.

[15] L.W. Chang. A mimo sliding control with a first-order plus integral sliding condition. *Automatica*, 27(5):853–858, 1991.

[16] J. Chen and R.J. Patton. Robust model-based fault diagnosis for dynamic systems. *Kluwer Academic Publishers*, 1999.

[17] J. Chen, R.J. Patton, and H.Z. Zhang. Design of unknown input observers and robust fault detection filters. *International Journal of Control*, 63:85–105, 1996.

[18] J. Chen and H. Zhang. Robust detection of faulty actuators via unknown input observers. *International Journal of Systems Science*, 22:1829–1839, 1991.

[19] R. H. Chen, D.L. Mingori, and J.L. Speyer. Optimal stochastic fault detection filter. *Automatica*, 39(3):377–390, 2002.

[20] R. H. Chen, H.K. Ng, J.L. Speyer, and D.L. Mingori. Fault detection, identification and reconstruction for ground vehicles. *Proceedings of the 2001 IEEE Conference on Intelligent Transportation Systems*, pages 924–929, August 2001.

[21] R. H. Chen and J.L. Speyer. Fault reconstruction from sensor and actuator failures. *Proceedings of the 40th IEEE Conference on Decision and Control*, pages 2277–2282, December 2001.

[22] W. Chen and J. Jiang. Fault-tolerant control against stuck actuator faults. *Proceedings of the IEE Control Theory and Applications*, 152(2):138–146, 2005.

[23] W. Chen and M. Saif. Robust fault detection in uncertain nonlinear systems via a second order sliding mode observer. *Proceedings of the 40th IEEE Conference on Decision and Control*, 1:573–578, 2001.

[24] W. Chen, M. Saif, and Y.C. Soh. A variable structure adaptive observer approach for actuator fault detection and diagnosis in uncertain nonlinear systems. *Proceedings of the American Control Conference*, 4:2674–2678, June 2000.

[25] M. Chilali and P. Gahinet. $\langle_\infty$ design with pole placement constraints: an lmi approach. *IEEE Transactions on Automatic Control*, 4:358–367, 1996.

[26] J.W. Choi. A simultaneous assignment methodology of righ/left eigenstructures. *IEEE Transactions on Aerospace and Electronic Systems*, 34(2):625–634, 1998.

[27] J.W. Choi, J.G. Lee, and Y. Kim. Design of an effective controller via disturbance accommodating left eigenstructure assignment. *Journal of Guidance, Control and Dynamics*, 18(2):347–354, 1995.

[28] E.Y. Chow and A.S. Willsky. Analytical redundancy and the design of robust failure detection systems. *IEEE Transactions on Automatic Control*, 29:603–614, 1984.

[29] M.Y. Chow and P.V. Goode. Adaptation of a neural/fuzzy fault detection system. *Proceedings of the 32nd Conference on Decision and Control*, 2:1733–1738, 1993.

[30] F.M. Chowdhury. Fault detection in multi-output stochastic system: statistical and neural approaches. *Proceedings of 30th Southeastern Symposium on System Theory*, pages 525–529, 1998.

[31] C. Cristalli, N. Paone, and R.M. Rodriguez. Mechanical fault detection of electric motors by laser vibrometer and accelerometer measurements. *Mechanical Systems and Signal Processing*, 20(6):1350–1361, August 2006.

[32] T. Curry, E.G. Collins Jr, and M. Selekwa. Robust fault detection using robust l_1 estimation and fuzzy logic. *Proceedings of the American Control Conference*, 2:1753–1758, 2001.

[33] M. Darouach, M. Zasadzinski, and S.J. Xu. Full order observers for linear systems with unknown inputs. *IEEE Transactions on Automatic Control*, 39:606–609, 1994.

[34] S. Dash, R. Rengaswamy, and V. Venkatasubramanian. Fuzzy-logic based trend classification for fault diagnosis of chemical processes. *Computers and Chemical Engineering*, 27(3):347–362, 15 March 2003.

[35] S.K. Dassanayake and G.J. Balas. Using unknown input observers to detect and isolate sensor faults in a turbofan engine. *Proceedings of the AIAA/IEEE Digital Avionics Systems Conference*, 2:6.E.5–1 – 6.E.5–7, 2000.

[36] J Davila, L. Fridman, and A. Levant. Second-order sliding mode observer for mechanical systems. *IEEE Transactions on Automatic Control*, 50:1785–1789, 2005.

[37] L.J. de Miquel and L.F. Blazquez. Fuzzy logic-based decision-making for fault diagnosis in a dc motor. *Engineering Applications of Artificial Intelligence*, 18:423–450, 2005.

[38] L.J. de Miquel, M. Mediavilla, and J.R. Peran. Fault diagnosis system based on sensitivity analysis and fuzzy logic. *Proceedings of the 26th International Symposium on Multiple-Valued Logic*, pages 50–55, 1996.

[39] J.C. Deckert and J.J. Deyst. F-8 dfbw sensor failure identification using analytic redundancy. *IEEE Transactions on Automatic Control*, 22(5):795–803, October 1977.

[40] G. Delmaire, J.P. Cassar, and M. Staroswiecki. Comparison of identification and par-

ity space approaches for failure detection in single input single output systems. *Proceedings of the 3rd IEEE Conference on Control Applications*, 2(2):865–870, 1994.

[41] G.H. Deng and R.H. Tang. An automatic diagnosis system with fuzzy diagnostic approach for linear analog circuits. *AUTOTESTCON '90. IEEE Systems Readiness Technology Conference*, pages 161–165, 1990.

[42] Y. Deng and Y. He. On the application of artificial neural networks to fault diagnosis in analog circuits with tolerances. *Proceedings of the 5th International Conference on Signal Processing*, 3:1639–1642, 2000.

[43] Y. Diao and K.M. Passino. Intelligent fault tolerant control using adaptive schemes and multiple models. *Proceedings of the American Control Conference*, 4:2854–2859, 2001.

[44] X. Ding and P.M. Frank. Fault detection via factorization approach. *Systems and Control Letters*, 14:431–436, 1990.

[45] X. Ding, P.M. Frank, and L. Guo. Fault detection via adaptive observers based on orthogonal functions. *Selected Papers from the IFAC/IMACS/IFORS Symposium (AIPAC '89)*, pages 95–100, 1990.

[46] X. Ding, L. Guo, and T. Jeinsch. Parameterization of linear observers and its application to observer design. *IEEE Transactions on Automatic Control*, 39(8):1648–1652, August 1994.

[47] X. Ding, L. Guo, and T. Jeinsch. A frequency domain approach to fault detection of uncertain dynamic systems. *Proceedings of the 32nd Conference on Decision and Control*, 2:1722–1727, December 1993.

[48] X. Ding, L. Guo, and T. Jeinsch. A characterization of parity space and its application to robust fault detection. *IEEE Transactions on Automatic Control*, 44(2):337–343, February 1999.

[49] R.K. Douglas and J.L. Speyer. Robust fault detection filter design. *Proceedings of the American Control Conference*, 1:91–96, 1995.

[50] C. Edwards. A comparison of sliding mode and unknown input observers for fault reconstruction. *Proceedings of the 43rd IEEE Conference on Decision and Control*, 5:5279–5284, 2004.

[51] C. Edwards, L. Fridman, and M.W.L. Thein. Fault reconstruction in a leader/follower spacecraft system using higher order sliding mode observers. *Proceedings of the American Control Conference*, pages 408–413, 2007.

[52] C. Edwards and S.K. Spurgeon. On the development of discontinuous observers. *International Journal of Control*, 59:1211–1229, 1994.

[53] C. Edwards and S.K. Spurgeon. *Sliding Mode Control: Theory and Applications*. Taylor & Francis Ltd, 1998.

[54] C. Edwards and S.K. Spurgeon. A sliding mode observer based FDI scheme for the ship benchmark. *European Journal of Control*, 6:341–356, 2000.

[55] C. Edwards, S.K. Spurgeon, and R.J. Patton. Sliding mode observers for fault detection and isolation. *Automatica*, 36(4):541–553, April 2000.

[56] C. Edwards and C.P. Tan. A comparison of sliding mode and unknown input observers for fault reconstruction. *European Journal of Control*, 12:245–260, 2006.

[57] C. Edwards and C.P. Tan. Fault tolerant control using sliding mode observers. *Control Engineering Practice*, 14:897–908, 2006.

[58] C. Edwards and C.P. Tan. Sensor fault tolerant control using sliding mode observers. *Control Engineering Practice*, 14(8):897–908, 2006.

[59] H. Elmali and N. Olgac. Robust output tracking of nonlinear mimo systems via sliding mode technique. *Automatica*, 28(1):145–151, 1992.

[60] E. Eryurek and B.R. Upadhyaya. Fault-tolerant control and diagnostics for large-scale systems. *IEEE Control Systems Magazine*, 15(5):34–42, 1995.

[61] C. Fantuzzi, S. Simani, and S. Beghelli. Robust fault diagnosis of dynamic processes using parametric identification with eigenstructure assignment approach. *Proceedings of the 40th IEEE Conference on Decision and Control*, 1:155–160, 2001.

[62] T. Floquet and J.P. Barbot. An observability form for linear systems with unknown inputs. *International Journal of Control*, 79:132–139, 2006.

[63] T. Floquet, J.P. Barbot, W. Perruquetti, and M. Djemai. On the robust fault detection via a sliding mode disturbance observer. *International Journal of Control*, 77(7):622–629, 2004.

[64] M. Fouladirad and I. Nikiforov. Optimal statistical fault detection with nuisance parameters. *Proceedings of the American Control Conference*, 4:2997–3002, 4-6 June 2003.

[65] P.M. Frank. Fault diagnosis in dynamic systems using analytical and knowledge-based redundancy - a survey and some new results. *Automatica*, 26(3):459–474, May 1990.

[66] P.M. Frank and X. Ding. A frequency domain based approach to fault identification. *Proceedigns of the IEEE International Symposium on Industrial Electronics*, 2:570–574, 1992.

[67] P.M. Frank and X. Ding. Frequency domain approach to optimally robust residual generation and evaluation for model-based fault diagnosis. *Automatica*, 30(5):789–804, 1994.

[68] P.M. Frank and X. Ding. Survey of robust residual generation and evaluation methods in observer-based fault detection systems. *Journal of Process and Control*, 7(6):403–424, 1997.

[69] L. Fridman. Higher order sliding modes observation, identification, and fault detection. *AIP Conference Proceedings*, 1019:573, 2008.

[70] L. Fridman, Y. Shtessel, C. Edwards, and X.G. Yan. State estimation and input reconstruction in nonlinear systems via higher order sliding mode observer. *Proceedings of the American Control Conference*, pages 3807–3812, 2007.

[71] L. Fridman, Y. Shtessel, C. Edwards, and X.G. Yan. Higher-order sliding-mode observer for state estimation and input reconstruction in nonlinear systems. *International Journal of Robust and Nonlinear Control*, 18(4–5):399–412, 2008.

[72] T. Furuhashi, S. Sangwongwanich, and S. Okuma. A position-and-velocity sensorless control for brushless dc motors using an adaptive sliding mode observer. *IEEE Transactions on Industrial Electronics*, 39(2):89–95, April 1992.

[73] B.O. Gaddouna and M. Ouladsine. Fault diagnosis in a hydraulic process using unknown input observers. *Proceedings of the 1997 IEEE International Conference on Control Applications*, pages 490–495, 5-7 October 1997.

[74] P. Gahinet, A. Nemirovski, A.J. Laub, and M. Chilali. *LMI Control Toolbox, Users Guide*. The MathWorks, Inc., 1995.

[75] E.A. Garcia and P.M. Frank. Multiplicative fault isolation in linear systems. *Proceedings of the 38th Conference on Decision and Control*, pages 3114–3115, 1999.

[76] E.A. Garcia, R. Seliger, and P.M. Frank. Nonlinear decoupling approach to fault isolation in linear systems. *Proceedings of the American Control Conference*, pages 2867–2871, 1998.

[77] J.J. Gertler. Survey of model-based failure detection and isolation in complex plants. *IEEE Control Systems Magazine*, 8(6):3–11, December 1988.

[78] K.B. Goh, S.K. Spurgeon, and N.B. Jones. Fault diagnostics using sliding mode techniques. *Control Engineering Practice*, 10(2):207–217, 2002.

[79] M.R. Gomez, J.E. Ventosa, and G.A. Aramendia. Expert system hardware for fault detection. *Applied Intelligence*, 9:245–262, 1998.

[80] Y. Guan and M. Saif. A novel approach to the design of unknown input observers. *IEEE Transactions on Automatic Control*, 36(5):632–635, May 1991.

[81] F. Hamelin and D. Sauter. Robust fault detection in uncertain dynamic systems. *Automatica*, 36, 2000.

[82] F. Hamelin, D. Sauter, and D. Theilliol. Some extensions to the parity space for fdi using alternated projected subspaces. *Proceedings of the 34th Conference on Decision and Control*, 3:2407–2412, December 1995.

[83] M. Hayar, M. Zasadzinski, and M. Darouach. A frequential approach to the unknown input observer design. *Proceedings of the 34th Conference on Decision and Control*, 4:3594–3595, December 1995.

[84] Y.G. He, Y.H. Tan, and Y. Sun. A neural network approach for fault diagnosis of large-scale analogue circuits. *IEEE International Symposium on Circuits and Systems*, 1, 2002.

[85] B.S. Heck, S.V. Yallapragada, and M.K.H. Fan. Numerical methods to design the reaching phase of output feedback variable structure control. *Automatica*, 31:275–279, 1995.

[86] D. Hengy and P.M. Frank. Component failure detection using local second-order observers. *Proceedings of the 2nd European Workshop on Fault Diagnostics, Reliability and Related Knowledge Based Approaches*, pages 147–154, 1987.

[87] J.M. Hereford. Fault-tolerant sensor systems using evolvable hardware. *IEEE Transactions on Instrumentation and Measurement*, 55(3):846–853, June 2006.

[88] F.J.J. Hermans and M.B. Zarrop. Sliding mode observers for robust sensor monitoring. *Proceedings of the 13th IFAC World Congress*, pages 211–216, 1996.

[89] M. Hou and P.C. Muller. Design of observers for linear systems with unknown inputs. *IEEE Transactions on Automatic Control*, 37:871–875, 1992.

[90] Y.C. Huang, H.T. Yang, and C.L. Huang. Design of robust transformer fault diagnosis system using evolutionary fuzzy logic. *IEEE International Symposium on Circuits and Systems*, 1:613–616, 1996.

[91] I. Husain, S. Sodhi, and M. Ehsani. A sliding mode observer based controller for switched reluctance motor drives. *Conference Record of the 1997 IEEE Industry Applications Conference Thirty-Second IAS Annual Meeting*, 1:525–532, 1997.

[92] H. Jamouli, D. Sauter, and J.Y. Keller. Fault tolerant control using augmented fault detection filter. *IEEE International Symposium on Industrial Electronics*, 1:109–114, 2004.

[93] B. Jiang and M. Staroswiecki. Adaptive observer design for robust fault estimation. *International Journal of Systems Science*, 33(9):767–775, 11 July 2002.

[94] B. Jiang, M. Staroswiecki, and V. Cocquempot. Fault diagnosis based on adaptive observer for a class of non-linear systems with unknown parameters. *International Journal of Control*, 77(4):415–426, 10 March 2004.

[95] I. Jikuya, N. Suzuki, and M. Suzuki. A constructive method for designing fault detection filter with application to a three-wheeled vehicle. *8th IEEE International Workshop on Advanced Motion Control*, pages 589–594, 2004.

[96] H.L. Jones. *Failure detection in linear systems*. PhD thesis, M.I.T., Cambridge, MA, 1973.

[97] M. F. Jorge-Zavala and E. Alcorta-Garcia. Detection of internal faults in transformers using non linear observers. *Proceedings of IEEE Conference on Control Applications*, 1:195–199, 2003.

[98] R.B. Jorgensen, R.J. Patton, and J. Chen. An eigenstructure assignment approach

to fdi for the industrial actuator benchmark test. *Control Engineering Practice*, 12:1751–1756, 1995.

[99] J. Jung, C.C. Liu, and M. Hong. Multiple hypotheses and their credibility in on-line fault diagnosis. *IEEE Transactions on Power Delivery*, 16(2):225–230, 2001.

[100] P. Kabore, M. Staroswiecki, and H. Wang. On parity space and observer-based approaches for fdi in state affine systems. *Proceedings of the 38th Conference on Decision and Control*, 3:2910–2911, December 1999.

[101] C.S. Kallesoe, P. Vadstrup, H. Rasmussen, and R. Izadi-Zamanabadi. Estimation of stator winding faults in induction motors using an adaptive observer scheme. *IEEE Industry Applications Society 2004*, 2:1225–1232, 2004.

[102] S.J. Katzberg, R.A. Walker, J.H. Roles, T. Lynch, and P.G. Black. First gps signals reflected from the interior of a tropical storm: Preliminary results from hurricane michael. *Geophysical Research Letters*, 28(10):1981–1984, May 2001.

[103] S. Kawaji and K. Sawada. Observer design for linear descriptor systems with unknown inputs. *Proceedings of the IECON '91*, 3:2285–2288, 1991.

[104] P.S. Kim and E.H. Lee. A new parity space approach to fault detection for general systems. *Proceedings of the 1st International Conference on High Performance Computing and Communications*, 3726:535–540, 2005.

[105] Y.W. Kim, G. Rizzoni, and V.I. Utkin. Developing a fault tolerant power-train control system by integrating design of control and diagnostics. *International Journal of Robust and Nonlinear Control*, 11(11):1095–1114, September 2001.

[106] D. Koenig and S. Mammar. Design of a class of reduced order unknown inputs nonlinear observer for fault diagnosis. *Proceedings of the American Control Conference*, 3:2143–2147, 25-27 June 2001.

[107] A.J. Koshkouei and A.S.I Zinober. Sliding mode controller-observer design for multivariable linear systems with unmatched uncertainty. *Kybernetika*, 36:95–115, 2000.

[108] F. Kratz, W. Nuninger, and S. Ploix. Fault detection for time-delay systems: a parity space approach. *Proceedings of the American Control Conference*, 4:2009–2011, 1998.

[109] V. Krishnaswami and G. Rizzoni. Model based health monitoring of vehicle steering system using sliding mode observers. *Proceedings of the American Control Conference*, 3:1652–1656, June 1995.

[110] V. Krishnaswami, C. Siviero, F. Carbognani, G. Rizzoni, and V. Utkin. Application of sliding mode observers to automobile powertrain diagnostics. *Proceedings of the IEEE International Conference on Control Applications*, pages 355–360, 1996.

[111] P. Kudva, N. Viswanadham, and A. Ramakrishna. Observer for linear systems with unknown inputs. *IEEE Transactions on Automatic Control*, 25(1):113–115, 1980.

[112] E.C. Larson, B.E. Parker Jr, and B.R. Clark. Model-based sensor and actuator fault detection and isolation. *Proceedings of the American Control Conference*, 5:4215–4219, 8-10 May 2002.

[113] H.M. Laurence and J.L. Speyer. Fault-tolerant gps/ins navigation system with application to unmanned aerial vehicle. *Journal of the Institute of Navigation*, 25(1):35–44, 2002.

[114] S. K. Lee and P. R. White. Higher-order time-frequency analysis and its application to fault detection in rotating machinery. *Mechanical Systems and Signal Processing*, 11(4):637–650, 1997.

[115] P. Li and V. Kadirkamanathan. Particle filtering based likelihood ratio approach to fault diagnosis in nonlinear stochastic systems. *IEEE Transactions on Systems, Man and Cybernetics - Part C: Applications and Reviews*, 31(3):337–343, 2001.

[116] P. Li and V. Kadirkamanathan. Fault detection and isolation in non-linear stochastic systems - a combined adaptive monte carlo filtering and likelihood ration approach. *International Journal of Control*, 77(12):1101–1114, 2004.

[117] S. Liberatore, J.L. Speyer, and A.C. Hsu. Application of a fault detection filter to structural health monitoring. *Automatica*, 42(7):1199–1209, July 2006.

[118] S.P. Linder. Behavior-based robust fuzzy control. *Proceedings of the 1998 IEEE ISIC/CIRA/ISAS Joint Conference*, pages 233–238, 1998.

[119] D.A. Linkens and J.S. Shieh. Self-organising fuzzy modeling for nonlinear system control. *IEEE International Symposium on Intelligent Control*, pages 210–215, 1992.

[120] B. Litkouhi and N.M. Boustany. On-board sensor failure detection of an active suspension system using the generalized likelihood ratio approach. *Proceedings of the 27th Conference on Decision and Control*, pages 2358–2363, December 1988.

[121] X.C. Lou, A.S. Willsky, and G.C. Verghese. Optimally robust redundancy relations for failure detection in uncertain systems. *Automatica*, 22:333–344, 1986.

[122] G. Luders and K.S. Narendra. A new canonical form for an adaptive observer. *IEEE Transactions on Automatic Control*, AC-19(2):117–119, April 1974.

[123] G. Luders and K.S. Narendra. Stable adaptive schemes for state estimation and identification of linear systems. *IEEE Transactions on Automatic Control*, 19(6):841–847, December 1974.

[124] G. Luders and K.S. Narendra. An adaptive observer and identifier for a linear system. *IEEE Transactions on Automatic Control*, AC-18(5):496–499, October 1973.

[125] D.G. Luenberger. An introduction to observers. *IEEE Transactions on Automatic Control*, 16:596–602, 1971.

[126] L. Ma, Y. Yang, F. Wang, and N. Lu. A sliding mode observer approach for fault detection and diagnosis in uncertain nonlinear systems. *Proceedings of the 4th World Congress on Intelligent Control and Automation*, 4(4):2714–2717, 2002.

[127] S.M. Magrabi and P.W. Gibbens. Decentralized fault detection and diagnosis using combined parity space and filter innovations based methods. *Proceedings of the IEEE National Aerospace and Electronics Conference*, page 602, 2000.

[128] H.J. Marquez and C.P. Diduch. Sensitivity-robustness in failure detection: A frequency domain approach. *Proceedings of the 29th Conference on Decision and Control*, 3:1389–1390, 1990.

[129] R. Martinez-Guerra, R. Garrido, and A. Osorio-Miron. The fault detection problem in nonlinear systems. *Proceedings of the American Control Conference*, 6:5686–5691, 2004.

[130] B. Marx, D. Koenig, and D. Georges. Robust fault-tolerant control for descriptor systems. *IEEE Transactions on Automatic Control*, 49(10):1869–1876, 2004.

[131] M.A. Massoumnia. A geometric approach to the synthesis of failure detection filters. *IEEE Transactions on Automatic Control*, 31(9):839–846, September 1986.

[132] M.A. Massoumnia and W.E. Vander Velde. Generating parity relations for detecting and identifying control system component failures. *AIAA Journal of Guidance, Control and Dynamics*, 11(1):60–65, 1988.

[133] E.W. McGookin. Reconfigurable sliding mode control for submarine manoeuvring. *Proceedings of the MTS/IEEE Conference Oceans 2001*, pages 1775–1782, 2001.

[134] L.F. Mendonca, J.M Sousa, and J.M.G Sa da Costa. Fuzzy model-based fault detection and isolation. *Proceedings of the IEEE Conference on Emerging Technologies and Factory Automation*, pages 768–774, 2003.

[135] J.A. Molnar. Summary and applicability of analog fault detection/isolation techniques. *Proceedings of AUTOTESTCON '97*, pages 383–389, 1997.

[136] G. Muscato, D. Caltabiano, S. Guccione, D. Longo, M. Coltelli, A. Cristaldi, E. Pecora, V. Sacco, P. Sim, G.S. Virk, P. Briole, A. Semerano, and T. White. Robovolc: a robot for volcano exploration result of first test campaign. *Industrial Robot*, 30(3):231–242, 2003.

[137] K.Y. Ng and C.P. Tan. New results in disturbance decoupled fault reconstruction in linear uncertain systems using two sliding mode observers in cascade,. *7th IFAC*

Symposium on Fault Detection, Supervision and Safety of Technical Processes, SAFEPROCESS, 2009.

[138] K.Y. Ng, C.P. Tan, R. Akmeliawati, and C. Edwards. Disturbance decoupled fault reconstruction using sliding mode observers. *Asian Journal of Control (under review)*, 2008.

[139] K.Y. Ng, C.P. Tan, R. Akmeliawati, and C. Edwards. Disturbance decoupled fault reconstruction using sliding mode observers. *Proceedings of International Federation of Automatic Control*, 17:7215–7220, 2008.

[140] K.Y. Ng, C.P. Tan, C. Edwards, and Y.C. Kuang. New results in robust actuator fault reconstruction for linear uncertain systems using sliding mode observers. *International Journal of Robust and Nonlinear Control*, 17:1294–1319, 2007.

[141] K.Y. Ng, C.P. Tan, Y.C. Kuang, and C. Edwards. New result in robust actuator fault reconstruction with application to an aircraft. *16th IEEE International Conference on Control Applications. Part of IEEE Multi-Conference on Systems and Control*, pages 801–806, 2007.

[142] K.Y. Ng, C.P. Tan, Z. Man, and R. Akmeliawati. New results in disturbance decoupled fault reconstruction in linear uncertain systems using two sliding mode observers in cascade. *International Journal of Control, Automation and Systems (under review)*, 2008.

[143] D. Noura, F. Hamelin, and D. Theilliol. Fault-tolerant control in dynamic systems: Application to a winding machine. *IEEE Control Systems Magazine*, 20(1):33–49, February 2000.

[144] T. Ono. Some studies on fault diagnosis of dynamic systems. *Proceedings of the IECON '91*, 3:2157–2162, 1991.

[145] J. Park and G. Rizzoni. An eigenstructure assignment algorithm for the design of fault detection filters. *IEEE Transactions on Automatic Control*, 39(7):1521–1524, July 1994.

[146] R.J. Patton and J. Chen. A review of parity space approaches to fault diagnosis. *Proceedings of the 1st IFAC-IMACS Symposium, SAFEPROCESS*, pages 239–255, 1991.

[147] R.J. Patton and J. Chen. A robust parity space approach to fault diagnosis based on optimal eigenstructure assignment. *International Conference on Control*, 2:1056–1061, 1991.

[148] R.J. Patton and J. Chen. Optimal unknown input distribution matrix selection in robust fault diagnosis. *Automatica*, 29(4):837–841, 1993.

[149] R.J. Patton and J. Chen. Observer-based fault detection and isolation: Robustness and applications. *Control Engineering Practice*, 5(5):671–682, 1997.

[150] R.J. Patton and J. Chen. On eigenstructure assignment for robust fault diagnosis. *International Journal of Robust and Nonlinear Control*, 10:1193–1208, 2000.

[151] R.J. Patton and J. Chen. Robust fault detection using eigenstructure assignment: A tutorial consideration and some new results. *Proceedings of the 30th Conference on Decision and Control*, 3:2242–2247, December 1991.

[152] R.J. Patton, S.W. Willcox, and S.J. Winter. Parameter-insensitive technique for aircraft sensor fault analysis. *AIAA Journal of Guidance, Control and Dynamics*, 10(4):359–367, 1987.

[153] G. Puglisi, A. Bonaccorso, M. Mattia, M. Aloisi, A. Bonforte, O. Campisi, M. Cantarero, G. Falzone, B. Puglisi, and M. Rossi. New integrated geodetic monitoring system at stromboli volcano. *Engineering Geology*, 79:13–31, 2005.

[154] V. Puig and J. Quevedo. Passive robust fault detection using fuzzy parity equations. *Mathematics and Computers in Simulation*, pages 193–207, 2002.

[155] S. Rajaraman, J. Hahn, and M.S. Mannan. A methodology for fault detection, isolation, and identification for nonlinear processes with parametric uncertainties. *Industrial and Engineering Chemistry Research*, 43:6774–6786, 2004.

[156] A.R. Reibman and L.W. Nolte. Optimal fault-tolerant signal detection. *IEEE Transactions on Acoustics, Speech and Signal Processing*, 38(1):179–180, 1990.

[157] H.H. Rosenbrock. *State space and multivariable theory*. John-Wiley, NY, 1970.

[158] M. Saif and Y. Guan. A new approach to robust fault detection and identification. *IEEE Transactions on Aerospace and Electronic Systems*, 29:685–695, 1993.

[159] D. Sauter and F. Hamelin. Frequency-domain optimization for robust fault detection and isolation in dynamic systems. *IEEE Transactions on Automatic Control*, 44, 1999.

[160] D. Sauter, H. Jamouli, J.-Y. Keller, and J.-C. Ponsart. Actuator fault compensation for a winding machine. *Control Engineering Practice*, 13(10):1307–1314, 2005.

[161] L.C. Shen, S.K. Chang, and P.L. Hsu. Robust fault detection and isolation with unstructured uncertainty using eigenstructure assignment. *Journal of Guidance, Control and Dynamics*, 21(1):50–57, 1998.

[162] Y. Shtessel, L. Fridman, and A. Zinober. Higher order sliding modes. *International Journal of Robust and Nonlinear Control*, 18(4–5):381–384, 2008.

[163] Y. Shtessel, S.K. Spurgeon, and L. Fridman. Editorial 1: Higher order sliding mode observers. *International Journal of Systems Science, Advances in Sliding Mode Observation and Estimation (Part One)*, 38(10):771–772, 2007.

[164] S. Simani, C. Fantuzzi, and S. Beghelli. Diagnosis techniques for sensor faults of industrial processes. *IEEE Transactions on Control System Technology*, 8(5):848–855, 2000.

[165] J.J.E. Slotine, J.K. Hedrick, and E.A. Misawa. On sliding observers for nonlinear systems. *ASME Journal of Dynamic Systems, Measurement and Control*, 109:245–252, 1987.

[166] E.S. Sogomonyan and M. Gossel. Concurrently self-testing embedded checkers for ultra-reliable fault-tolerant systems. *Proceedings of 14th VLSI Test Symposium*, pages 138–144, 1996.

[167] Q. Song and L. Yin. Robust adaptive fault accommodation for a robot system using a radial basis function neural network. *International Journal of Systems Science*, 32(2):195–204, 2001.

[168] B. Sreedhar, B. Fernández, and G.Y. Masada. Robust fault detection in nonlinear systems using sliding mode observers. *2nd IEEE Conference on Control Applications*, 2:715–721, 1993.

[169] M. Staroswiecki and B. Jiang. Fault identification for a class of linear systems based on adaptive observer. *Proceedings of the 40th IEEE Conference on Decision and Control*, 3:2283–2288, 2001.

[170] C.E. Stroud and Jr J.K. Tannehill. Applying built-in self-test to majority voting fault tolerant circuits. *Proceedings of the 16th IEEE VLSI Test Symposium*, pages 303–308, 1998.

[171] M. Takahashi, T. Narukawa, and K. Yoshida. Robustness and fault-tolerance of cubic neural network intelligent control method - comparison with sliding mode control. *Proceedings of the IEEE/ASME International Conference on Advanced Intelligent Mechatronics*, 1:17–22, 2003.

[172] C.P. Tan and C. Edwards. An LMI approach for designing sliding mode observers. *International Journal of Control*, 74:1559–1568, 2001.

[173] C.P. Tan and C. Edwards. Reconstruction of sensor faults using a secondary sliding mode observer. *Proceedings of the 40th IEEE Conference on Decision and Control*, 1:579–584, 2001.

[174] C.P. Tan and C. Edwards. A robust sensor fault reconstruction scheme using sliding mode observers applied to a nonlinear aero-engine model. *Proceedings of the American Control Conference*, pages 5086–5091, 2002.

[175] C.P. Tan and C. Edwards. Sliding mode observers for detection and reconstruction of sensor faults. *Automatica*, 38:1815–1821, 2002.

[176] C.P. Tan and C. Edwards. Sliding mode observers for reconstruction of simultaneous actuator and sensor faults. *Proceedings of the 42nd IEEE Conference on Decision and Control*, 2:1455–1460, 2003.

[177] C.P. Tan and C. Edwards. Sliding mode observers for robust detection and reconstruction of actuator and sensor faults. *International Journal of Robust and Nonlinear Control*, 13(3):443–463, 2003.

[178] C.P. Tan and C. Edwards. Multiplicative fault reconstruction using sliding mode observers. *5th Asian Control Conference*, pages 957–962, 2004.

[179] C.P. Tan and C. Edwards. A robust sensor fault tolerant control scheme implemented on a crane. *Asian Journal of Control*, 9:340–344, 2007.

[180] C.P. Tan, C. Edwards, and Y.C. Kuang. Robust sensor fault reconstruction using a reduced order linear observer. *9th International Conference on Control, Automation, Robotics and Vision*, pages 1040–1045, 2006.

[181] C.P. Tan, C. Edwards, and Y.C. Kuang. Robust sensor fault reconstruction using right eigenstructure assignment. *Proceedings of IEEE International Workshop on Electronic Design, Test and Applications, Kuala Lumpur, Malaysia*, pages 435–440, 2006.

[182] C.P. Tan and M.K. Habib. Implementation of a sensor fault reconstruction scheme on an inverted pendulum. *5th Asian Control Conference*, pages 1423–1428, 2004.

[183] C.P. Tan and M.K. Habib. Robust sensor fault reconstruction for an inverted pendulum using right eigenstructure assignment. *Proceedings of the 2004 IEEE International Conference on Control Applications*, 2(2):1236–1241, 2004.

[184] C.P. Tan and M.K. Habib. The development of fault tolerant control and its application on a flexible arm robot. *Advanced Robotics*, 21:887–904, 2007.

[185] C.P. Tan and M.K. Habib. Robust sensor fault reconstruction applied in real-time to an inverted pendulum. *Mechatronics*, 17:368–380, 2007.

[186] M.W.L. Thein and E.A. Misawa. Comparison of the sliding observer to several state estimators using a rotational inverted pendulum. *Proceedings of the 34th Conference on Decision and Control*, 4:3385–3390, 1995.

[187] C.C. Tsui. A new design approach to unknown input observers. *IEEE Transactions on Automatic Control*, 41(3):464–468, March 1996.

[188] V.I. Utkin. *Sliding Modes in Control Optimization*. Springer-Verlag, Berlin, 1992.

[189] E. Vazquez, H.J. Altuve, and O.L. Chacon. Neural network approach to fault detection in electric power systems. *IEEE International Conference on Neural Networks*, 4:2090–2095, 1996.

[190] G. Venkataramanan. A sliding mode observer for the induction motor. *IEEE Annual Power Electronics Specialists Conference*, pages 1151–1157, 1993.

[191] V. Venkatasubramaniam, R. Rengaswamy, K. Yin, and S.N. Kavuri. A review of process fault detection and diagnosis part i: Quantitative model-based methods. *Computers and Chemical Engineering*, 27:393–311, 2003.

[192] M.L. Visinsky, J.R. Callavaro, and I.D. Walker. Robotic fault detection and fault tolerance: A survey. *Reliability Engineering and System Safety*, 46(2):139–158, 1994.

[193] N. Viswanadham, J.H. Taylor, and E.C. Luce. A frequency domain approach to failure detection and isolation with application. *Control-theory and Advanced Technology*, 3:45–72, 1987.

[194] B.L. Walcott and S.H. Zak. State observation of nonlinear uncertain dynamical systems. *IEEE Transactions on Automatic Control*, 32:166–170, 1987.

[195] B.L. Walcott and S.H. Zak. Combined observer-controller synthesis for uncertain dynamical systems with applications. *IEEE Transactions on Systems, Man and Cybernetics*, 18:88–104, 1988.

[196] H. Wang and S. Daley. Actuator fault diagnosis: An adaptive observer-based technique. *IEEE Transactions on Automatic Control*, 41(7):1073–1078, July 1996.

[197] H. Wang and L. Shen. Fault detection and estimation for nonlinear systems with linear output structure. *International Journal of Adaptive Control and Signal Processing*, 19:267–279, 2005.

[198] H. Wang and Y. Wang. Neural-network-based fault-tolerant control of unknown nonlinear systems. *IEE Proceedings on Control Theory and Applications*, 146(5):389–398, September 1999.

[199] J. Wang, J. Zhao, and L. Ma. A robust fault detection and isolation method via sliding mode observer. *5th World Congress on Intelligent Control and Automation*, 2(2):1727–1730, 2004.

[200] K. Watanabe and D.M. Himmelblau. Instrument fault detection in system with uncertainties. *International Journal of Systems Science*, 13(2):137–158, 1982.

[201] J.E. White and J.L. Speyer. Detection filter design: spectral theory and algorithms. *IEEE Transactions on Automatic Control*, 32:593–603, 1987.

[202] A.S. Willsky. A survey of design methods for failure detection in dynamic systems. *Automatica*, 12:601–611, 1976.

[203] A.S. Willsky and H.L. Jones. A generalized likelihood ratio approach to the detection and estimation of jumps in linear systems. *IEEE Transactions on Automatic Control*, AC-21(1):108–112, February 1976.

[204] Q. Wu and M. Saif. Neural adaptive observer based fault detection and identification for satellite attitude control systems. *2005 American Control Conference*, 2:1054–1059, 2005.

[205] Y. Xiong and M. Saif. Robust fault isolation observer design. *Proceedings of the American Control Conference*, 3:2077–2081, 1999.

[206] Y. Xiong and M. Saif. Robust fault detection and isolation via a diagnostic observer. *International Journal of Robust and Nonlinear Control*, 10:1175–1192, 2000.

[207] Y. Xiong and M. Saif. Robust and nonlinear fault diagnosis using sliding mode observers. *Proceedings of the IEEE Conference on Decision and Control*, 1(1):567–572, 2001.

[208] P. Xu and A.K. Chan. Fast and robust neural network based wheel bearing fault detection with optimal wavelet features. *Proceedings of the 2002 International Joint Conference on Neural Networks*, 3:2076–2080, 2002.

[209] F. Yang and R.W. Wilde. Observers for linear systems with unknown inputs. *IEEE Transactions on Automatic Control*, 33(7):677–681, July 1988.

[210] H. Yang and M. Saif. Fault detection in a class of nonlinear systems via adaptive sliding observer. *1995 IEEE International Conference on Systems, Man and Cybernetics*, 3:2199–2204, 1995.

[211] H. Yang and M. Saif. Fault detection and isolation for a class of nonlinear systems using an adaptive observer. *Proceedings of the American Control Conference*, pages 463–467, 1997.

[212] Z.R. Yang, M. Zwolinski, C.D. Chalk, and A.C. Williams. Applying a robust heteroscedastic probabilistic neural network to analog fault detection and classification. *IEEE Transactions on Computer-Aided Design of Integrated Circuits and Systems*, 19(1):142–151, January 2000.

[213] H. Ye, G. Wang, and X. Ding. New parity space approach for fault detection based on stationary wavelet transform. *IEEE Transactions on Automatic Control*, 49(2):281–287, February 2004.

[214] S.O. Yee and M. Chow. Robustness of an induction motor incipient fault detector neural network subject to small input perturbations. *IEEE Proceedings of Southeastcon '91*, 1:365–369, 1991.

[215] G.G. Yen and L.W. Ho. Intelligent fault tolerant control using artificial neural networks. *Proceedings of the IEEE-INNS-ENNS International Joint Conference on Neural Networks*, 1:256–271, 2000.

[216] T.K. Yeu and S. Kawaji. Fault detection and isolation for descriptor systems using sliding mode observer. *Proceedings of the 40th IEEE Conference on Decision and Control*, 1:596–597, 2001.

[217] T.K. Yeu and S. Kawaji. Sliding mode observer based fault detection and isolation in descriptor systems. *Proceedings of the 2002 American Control Conference*, 6(6):4543–4548, 2002.

[218] S.S. Young and W.C. Jae. Continuous-time deadbeat fault detection and isolation filter design. *Proceedings of the 38th IEEE Conference on Decision and Control*, 3:3130–3131, 1999.

[219] D.L. Yu, T.K. Chang, and D.W. Yu. Fault tolerant control of multivariable processes using auto-tuning pid controller. *IEEE Transactions on Systems, Man and Cybernetics - Part B*, 35:32–43, February 2005.

[220] B. Zhang, K. Xu, W. Liu, and J.X. Liu. Research on fault tolerant control of marine multi-phase permanent magnet synchronous motors propulsion systems. *Proceedings of the International Conference on Electrical Machines and Systems*, 3:2511–2514, 2005.

[221] C. Zhang, Z. Mao, and Q. Zhou. On-line incipient fault detection of induction motors using artificial neural networks. *Proceedings of the IEEE International Conference on Industrial Technology*, pages 458–462, 1994.

[222] H.Y. Zhang and R.J. Patton. Optimal design of robust analytical redundancy for uncertain systems. *IEEE TENCON'93*, 4:218–221, 1993.

[223] P. Zhang, H. Ye, S.X. Ding, G.Z.Wang, and D.H. Zhou. On the relationship between parity space and $\mathcal{H}_2$ approaches to fault detection. *Systems and Control Letters*, 55(2):94–100, February 2006.

[224] Q. Zhang. Adaptive observer for multiple-input-multiple-output (mimo) linear time-varying systems. *IEEE Transactions on Automatic Control*, 47(3):525–529, 2002.

[225] Q. Zhang, G.L. Slater, and R.J. Allemang. Suppresion of undesired inputs of linear systems by eigenspace assignment. *Journal of Guidance, Control and Dynamics*, 13(2):330–336, 1990.

[226] K. Zhou, J. Doyle, and K. Glover. *Robust and Optimal Control*. Englewood Cliffs, N.J. : Prentice Hall, 1995.

[227] F. Zidani, M.E.H. Benbouzid, D. Diallo, and A. Benchaib. Active fault-tolerant control of induction motor drives in ev and hev against sensor failures using a fuzzy decision system. *IEEE International Conference on Electric Machines and Drives*, 2:677–683, June 2003.

Appendix A

Guide To Attached CD-R

A.1 Sliding Mode Observers for Robust Fault Reconstruction

The files in this section of the CD-R can be found in the directory *∼/SMO/* and are used to simulate the crane system example shown in Section 3.5.

The file *crane.mat* is where the system matrices are stored and *smo.m* is the main root simulation file. The *outfor.m* file is used to perform the necessary coordinate transformation such that the canonical form of the system in Section 3.2.1 can be obtained and *abcchk.m* is used within *outfor.m* to check for the consistency of the system matrices and also to ensure that the system is controllable before the design process commences. The sliding mode observer is then designed using the LMI method via the file *HINFOBS_mod.m*. The Simulink model file *sliding.mdl* will then be simulated and the results are plotted.

The link between the notation used in the thesis and the variables in Matlab is given in the Table A.1.

A.2 Disturbance Decoupled Fault Reconstruction

The files in this section of the CD-R can be found in the directory *∼/DDFR/Actuator/* and are used to simulate the aircraft system example shown in Section 4.4.

The file *aircraft.mat* stores the system matrices data. The file *ddfr.m* is the main root simulation file for this example. The coordinate transformation discussed in Proposition 4.1 is carried out by *ddfr.m* and the observer design procedure in discussed Section 4.2.1 is com-

puted using *obsdesign.m*. The Simulink model file *sliding.mdl* (different system setup as the one used in Section A.1) will then be simulated and the results are plotted.

The link between the notation used in the thesis and the variables in Matlab is given in Table A.1.

A.3 Disturbance Decoupled Sensor Fault Reconstruction

The files in this section of the CD-R can be found in the directory *∼/DDFR/Sensor/* and are used to simulate the double inverted pendulum system example shown in Section 5.4.

The system matrices of double inverted pendulum model is loaded through the file *dip.mat*. The file *sensor.m* is the main root simulation file in this example. The file *coordtrans.m* computes the transformation explained in Section 5.3 and the augmented system in (5.10) - (5.11) can be obtained through the file *augmented.m*. The feasibility of disturbance decoupled sensor fault reconstruction can then be determined using *ranktest.m*. The Simulink model file *invpend.mdl* will then be simulated and the results are plotted.

The link between the notation used in the thesis and the variables in Matlab is given in the table below.

Description of Parameter	**Thesis Notation**	**Matlab Variable**
Linear gain of observer	G_l	Gl
Nonlinear gain of observer	G_n	Gn
Matrix that scales the nonlinear gain of observer	P_o	Po

Table A.1: Description for key variables used in simulations

A.4 DDFR Using Multiple Sliding Mode Observers In Cascade

The files in this section of the CD-R can be found in the directory *∼/Multiple SMOs/* and are used to simulate the rotational system example shown in Section 6.4.

The system matrices for the rotational system used in the example are stored in the file *rotate.mat*. The main root file to run the simulation is *multiplesmo.m*. Firstly, the system is

transformed to the coordinates explained in Proposition 4.1 using the file *ddfrcoord.m*. Then, a test would be conducted to find out the number of observers that are needed in order to achieve disturbance decoupled fault reconstruction. This is done through the file *obstest.m*. Next, the file *ranktest.m* will be executed to to determine if the matrix A_{32}^i is full rank. If A_{32}^i is full rank, then a sliding mode observer can be designed and disturbance decoupled fault reconstruction can be achieved. The file *obs.m* will perform the necessary coordinate transformation as discussed under Step 2 of the Design Algorithm in Section 6.2.1 and from there the sliding mode observer will be designed using *obsdesign.m*. The Simulink model file *multiple.mdl* will then be simulated and the results are plotted.

The link between the notation used in the thesis and the variables in Matlab is given in the table below.

Description of Parameter	**Thesis Notation**	**Matlab Variable**
System matrices after the $\bar{T}_2^i$ transformation *Replace i with the observer count	A^i, M^i, C^i, Q^i	A$i$new,M$i$new, C$i$new,Q$i$new
Linear gain of observer 1	G_l^1	Gl1
Nonlinear gain of observer 1	G_n^1	Gn1
Matrix that scales nonlinear gain of observer 1	$\bar{P}_o^1$	Po1
Linear gain of observer 2	G_l^2	Gl2
Nonlinear gain of observer 2	G_n^2	Gn2
Matrix that scales nonlinear gain of observer 2	$\bar{P}_o^2$	Po2

Table A.2: Description for system simulated in ∼/Multiple SMOs/

A.5 New Results in Robust Fault Reconstruction

The files in this section of the CD-R can be found in the directory *∼/Robustness/* and are used to simulate the aircraft system example demonstrated in Section 7.4.

The system matrices of the aircraft model is loaded through the file *aircraft.mat*. The file *simu.m* is the main root simulation file in this example. The file *cotr1.m* serves to perform the coordinate changes as shown in Lemmas 7.1 and 7.4 to get the system matrices (A, M, C, Q)

into the desired structure. The final structure of the matrices will match with the ones shown in Equations (7.12) and (7.13). The design of the primary observer will then be designed via the file *LMI1.m*. Then the augmented system in (7.32) - (7.32) will then be computed with *cotr2.m* and *LMI2.m* will design the second observer for fault reconstruction. The Simulink model file *smo.mdl* will then be simulated and the results are plotted.

The link between the notation used in the thesis and the variables in Matlab is given in the table below.

Description of Parameter	**Thesis Notation**	**Matlab Variable**
Linear gain of observer 1	G_l	Gl
Nonlinear gain of observer 1	G_n	Gn
Matrix that scales nonlinear gain of observer 1	$\bar{P}_o$	Po
Linear gain of observer 2	$\bar{G}_l$	Glbar
Nonlinear gain of observer 2	$\bar{G}_n$	Gnbar
Matrix that scales nonlinear gain of observer 2	$\bar{P}_o$	Pobar

Table A.3: Description for system simulated in ∼/Robustness/

Appendix B

Addenda: 1 Demo and Simulation CD-R (inside of back cover)